Homogeneous Catalysis

International Edition: DOI: 10.1002/anie.201503873
German Edition: DOI: 10.1002/ange.201503873

Metal–Ligand Cooperation

*Julia R. Khusnutdinova and David Milstein**

Keywords:
cooperating ligands · homogeneous catalysis · metal complexes

Angewandte International Edition Chemie

Metal–ligand cooperation (MLC) has become an important concept in catalysis by transition metal complexes both in synthetic and biological systems. MLC implies that both the metal and the ligand are directly involved in bond activation processes, by contrast to "classical" transition metal catalysis where the ligand (e.g. phosphine) acts as a spectator, while all key transformations occur at the metal center. In this Review, we will discuss examples of MLC in which 1) both the metal and the ligand are chemically modified during bond activation and 2) bond activation results in immediate changes in the 1st coordination sphere involving the cooperating ligand, even if the reactive center at the ligand is not directly bound to the metal (e.g. via tautomerization). The role of MLC in enabling effective catalysis as well as in catalyst deactivation reactions will be discussed.

From the Contents

1. Introduction

The use of transition metal catalysts expanded the scope of reactivity of organic compounds due to the ability of transition metals to participate in various reaction types, such as oxidative addition, reductive elimination and β-hydride elimination (Scheme 1 a,b). In many classical examples in homogeneous catalysis, such transformations occur at the metal center, while the ligands remain unchanged over the course of the reaction.

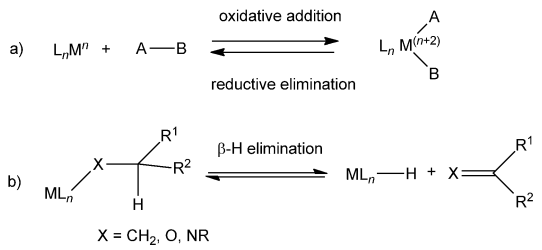

Scheme 1. a) Oxidative addition/reductive elimination and b) β-H elimination. Note that these processes might involve ligand dissociation/association steps.

However, bond activation in many enzymes occurs in a different manner and involves a finely adjusted ligand environment that acts in cooperation with the metal and participates in bond activation, leading to chemical modification of both the ligand and the metal center (Scheme 2). For example, H_2 activation in [FeFe], [NiFe], and [Fe]-only hydrogenases occurs through cooperation between the ligand and the metal leading to H_2 heterolytic splitting across the metal–ligand bond without an overall change of the metal's oxidation state. Discovery of such systems inspired new approaches to ligand design and expanded the scope of catalytic reactions, including the recent discoveries of several environmentally benign and energy-related reactions.

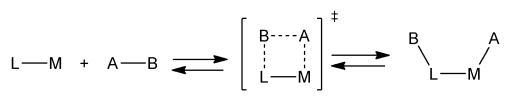

Scheme 2. Bond activation by metal–ligand cooperation.

This Review will discuss diverse modes of metal–ligand cooperation (MLC) in bond formation or bond cleavage reactions that affects the 1st coordination sphere of the metal (i.e. ligands that are directly bound to the metal are chemically modified as a result of bond breaking/bond formation processes). References up to February 2015 are covered. Selected examples that satisfy the following criteria will be covered:

1) Both the metal and the ligand participate in the bond cleavage or bond formation steps.
2) Both the metal and the ligand are chemically modified during bond activation.
3) The coordination mode of the cooperative ligand undergoes significant changes in the 1st coordination sphere as a result of bond activation.

In addition, we will focus predominantly on examples in which the ligand does not act as a permanent leaving group, which is an important prerequisite for catalytic applications. Mechanistic studies will be discussed that allow to confirm the involvement of MLC in the bond activation process. The structural changes that occur during MLC will also be demonstrated. At the same time, as it is not always possible to unambiguously rule out or confirm the mechanism, some controversial examples in which several mechanistic scenarios can be realized will also be discussed.

The following examples will not be covered in this Review:

[*] Prof. Dr. D. Milstein
Department of Organic Chemistry, Weizmann Institute of Science
Rehovot 76100 (Israel)
E-mail: david.milstein@weizmann.ac.il
Assist. Prof. Dr. J. R. Khusnutdinova
Coordination Chemistry and Catalysis Unit
Okinawa Institute of Science and Technology
1919-1 Tancha, Onna-son, Kunigami-gun, Okinawa, 904-0495
(Japan)

1) Systems with redox-non-innocent ligands, where the ligand participates only in transferring electrons to/from the metal, but not in bond cleavage/formation.
2) Hemilabile ligands whose main function is to create coordinative unsaturation at the metal center, while bond activation takes place primarily at the metal.
3) Examples in which MLC involves only the 2nd coordination sphere, but not the 1st coordination sphere (for example, ligands containing non-coordinated functional groups acting as internal Brønsted or Lewis bases; frustrated Lewis pair (FLP)-inspired activation).

Based on the last criterion, examples of ligands that mimic H_2 activation by [FeFe]-hydrogenase with a pendant amine group will not be discussed here, as the amine both in the starting material and the product of H_2 activation remains essentially in the 2nd coordination sphere of the metal. These examples were covered in several other articles and reviews.[1–3] At the same time, it is important to distinguish from examples where the ligand backbone modification (formally in the 2nd coordination sphere) leads to significant changes of the ligands in the 1st coordination sphere, which is particularly important for N-heterocyclic ligands that can exist as several tautomeric forms with different donor properties of the N-atoms (see Section 3).

This Review is divided into two main sections. Section 2 discusses bond activation directly across a metal–ligand bond as shown in Scheme 2. Section 3 is dedicated to systems in which bond activation by MLC leads to disruption/restoration of the conjugated system in the ligand.

2. Metal–Ligand Cooperation through M–L Bonds

Examples of bond cleavage/formation across M–L bonds (Scheme 2) with various donor atoms (N, O, S, B, and C) are covered in this section and some catalytic applications are discussed in the context of MLC.

2.1. Metal–Nitrogen Bond

H–H and H–heteroatom bond activation by metal amide/amine systems is among the most well studied and widely used in catalysis. Several types of bond activation processes that occur through MLC in amide/amine complexes will be discussed here using several selected examples of such systems. The goal of this section is not to cover all currently known systems, but to show common patterns of bond cleavage/formation and their mechanisms. The catalytic applications of metal amide/amine complexes and their mechanistic studies were discussed in detail in several recent reviews.[2–8]

In search for reactive Ru-based catalysts for ketone hydrogenation using H_2 gas or 2-propanol (in transfer hydrogenation), Noyori's group discovered that additives of diamines or ethanolamine containing at least one NH group have a tremendous effect on the reactivity of Ru catalysts for ketone hydrogenation.[4–6] In particular, $[RuCl_2(PPh_3)_3]$ in combination with ethylenediamine and KOH was found to be an effective catalyst for acetophenone hydrogenation, while the turnover frequency in the absence of either ethylenediamine or KOH was significantly lower.[5,9] Notably, at least one primary or secondary amine group should be present in the amine additive in these systems: for example, *N*,*N*,*N*′,*N*′-tetramethylethylenediamine (TMEDA) was not effective under analogous conditions.[5] Following these observations, a family of highly active catalysts for ketone hydrogenation were developed containing bisphosphine and 1,2-diamine ligands (Scheme 3).[4–6] Dichloro complexes such as **1** and **2** (in combination with a base: KOH, KO*t*Bu, NaO*i*Pr) or hydridoborohydrido complexes **3** and **4** with chiral BINAP and chiral diamine ligands (either under base-free conditions, or in the presence of a base), serve as pre-catalysts in highly efficient enantioselective ketone hydrogenation (Scheme 4).[10]

Mechanistic studies of ketone hydrogenation led to the proposed dual pathway shown in Scheme 5, with the contribution of cycles I and II dependent on the reaction conditions. Notably, ketone hydrogenation is proposed to occur through

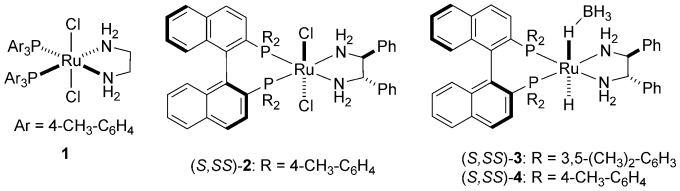

Scheme 3. Bisphosphine diamine bifunctional catalysts for ketone hydrogenation.

Julia Khusnutdinova received her Ph.D. degree from the University of Maryland. She then worked as a postdoctoral fellow at the Washington University in St. Louis. In 2012 she joined the group of Prof. Milstein at the Weizmann Institute as a Dean of Faculty fellow working on Ru-catalyzed amine transformations in water and CO_2 hydrogenation to MeOH. She is currently an Assistant Professor at Okinawa Institute of Science and Technology (OIST) leading the Coordination Chemistry and Catalysis Unit.

David Milstein is the Israel Matz Professor of Chemistry and the Director of the Kimmel Center of Molecular Design at the Weizmann Institute of Science. He received his Ph.D. degree with Prof. Blum at the Hebrew University in 1976 and performed postdoctoral research at Colorado State University with Prof. Stille. In 1979 he joined DuPont Company's CR&D where he became a Group Leader, and in 1986 he moved to the Weizmann Institute, where he headed the Department of Organic Chemistry in 1996–2005. He has received several awards, including the Israel Prize in 2012.

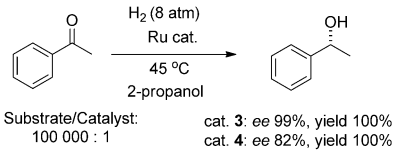

Scheme 4. Enantioselective hydrogenation of acetophenone.

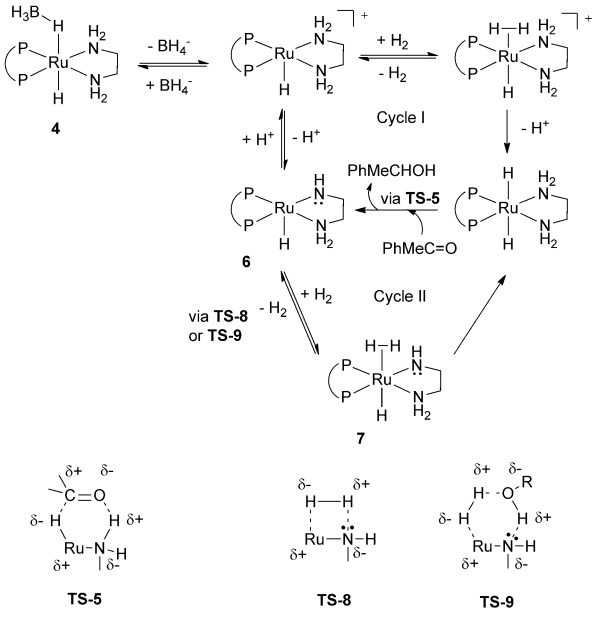

Scheme 5. Mechanism of hydrogenation of acetophenone catalyzed by **4**. The aryl groups of the diamine backbone and diphosphine are omitted for clarity.

an outer-sphere mechanism, via a six-member pericyclic transition state **TS-5** (Scheme 5).[10] In this mechanism, the proton from the amine ligand and the hydride from the metal are simultaneously transferred to a C=O group, to form a formally 16e⁻ amide complex **7**.[11] Bergens et al. later proposed that a partial Ru–O bond or a strong H-bond between NH and alkoxide could be present in the transition state based on the observed formation of alkoxide intermediates at low temperatures.[12]

Cooperative activation of H_2 by **7** in cycle II was proposed to occur either through a four-membered transition state **TS-8**,[13] or through an alcohol-assisted pathway via a six-membered **TS-9** (Scheme 5).[10]

Transfer hydrogenation is catalyzed by Ru-arene complexes [{$RuCl_2(\eta^6$-arene)}$_2$] developed by Noyori, Ikariya et al.[4,7,14] Similar to the phosphine-based system, a significant acceleration of the transfer hydrogenation of ketones was discovered when catalyzed by Ru-arene complexes in the presence of ethanolamine and other additives containing at least one primary or secondary amine ("NH effect").[4,14,15] The precatalysts **10** bearing chiral amine-sulfonylamide ligands catalyze in the presence of a base the enantioselective transfer hydrogenation of ketones. Similarly, hydrogen transfer to a ketone substrate in these systems was proposed to occur via a concerted pathway involving simultaneous transfer of a proton of the NH group and a hydride of the Ru–H group to a carbonyl group (**TS-11**) (Scheme 6).[4,16]

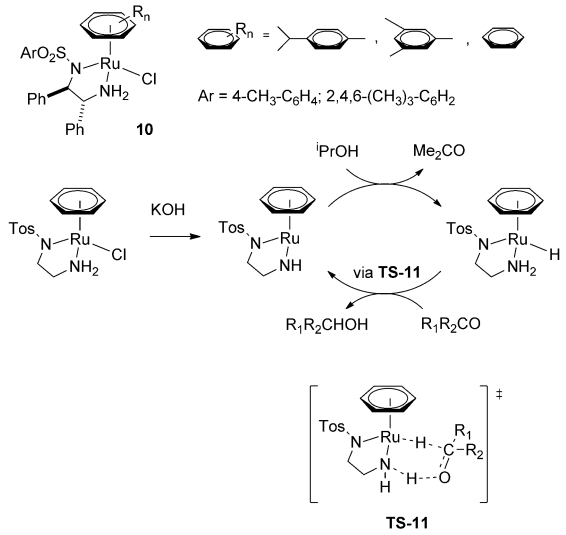

Scheme 6. (Arene)Ru-based bifunctional catalysts for enantioselective transfer hydrogenation of ketones and the proposed mechanism (Ph groups of diamine are omitted for clarity).

The outer-sphere mechanism was proposed in other Ru, Rh, and Ir systems and was studied extensively and supported by kinetic isotope effect (KIE) studies and calculations.[16–18] For example, kinetic isotope effects were measured for the reaction of [(*p*-cymene)Ru(HNCHPhCHPhNTs)] with isopropyl alcohol; the rates were measured for $(CD_3)_2CHOH$, $(CD_3)_2CDOH$, $(CD_3)_2CHOD$, and $(CD_3)_2CDOD$. The KIE for hydrogen transfer from OH to N was found to be 1.79, and the KIE for hydrogen transfer from CH to RuH was 2.86. The KIE for transfer of hydrogen from a doubly labeled substrate, $(CD_3)_2CDOD$, was found to be 4.88, which approximately corresponds to the product of two individual KIE's, consistent with the concerted transfer.[17]

The presence of the NH group as well as metal-hydride in a hydrogenation catalyst does not necessarily imply that an outer-sphere mechanism of C=O hydrogenation is operative. The hydricity of Ru–H and acidity of NH as well as hemilability of the ligands also play important roles in determining the reaction pathway. For example, Morris et al. studied the mechanisms of ketone hydrogenation with Ru complexes containing N-heterocyclic carbene (NHC) ligands with tethered primary amines (Scheme 7). Hydrogenation of ketones catalyzed by the pre-catalyst **12** was proposed to occur through an alcohol-assisted outer-sphere

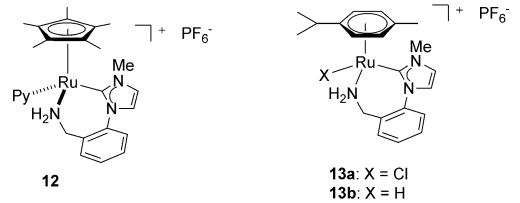

Scheme 7. Ru (pre)catalysts with NHC-tethered amines.

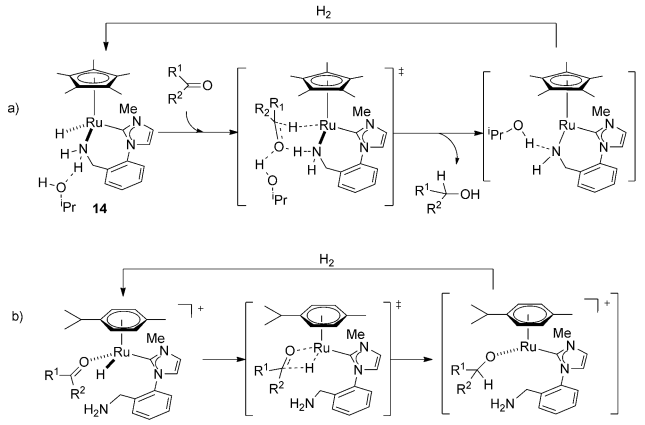

Scheme 8. Proposed outer-sphere (a) and inner-sphere (b) mechanisms of ketone hydrogenation catalyzed by **12** or **13**, respectively.

mechanism of hydrogen transfer from an in situ formed neutral Ru-hydride species **14** similar to that proposed for Noyori-type systems (Scheme 8, path a).[19] An outer-sphere mechanism was also suggested for ester hydrogenation catalyzed by **12**.[20] At the same time, experimental and computational studies imply that the analogous outer-sphere mechanism would be unfavored for complex **13b**, likely due to diminished nucleophilicity of the cationic hydride species.[21] Based on kinetic and isotopic effect studies, an inner-sphere mechanism was proposed (Scheme 8, path b), and supported by a computational investigation.[21]

Grützmacher et al. developed diolefin amide ligands that assist in facile concerted heterolytic cleavage of H_2 across the metal–amide bond (Scheme 9). In particular, the Rh complex

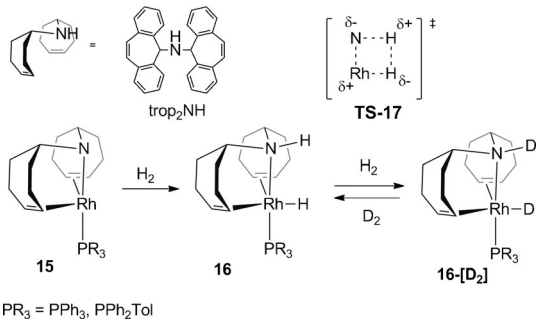

Scheme 9. Heterolytic H_2 activation by diolefin amide Rh complexes.

15 heterolytically activates H_2 (1 atm) even at −78 °C to give the hydrido amine complex **16**.[22] Unlike in the "classical" oxidative addition, the oxidation state of the metal (Rh^I) remains unchanged during the concerted H_2 heterolysis. This reaction is reversible and selective H/D exchange occurs upon exposure of **16** to D_2 to give **16-[D_2]**. The reverse reaction of **16-[D_2]** with H_2 was also observed and was monitored by NMR spectroscopy, which indicated that the exchange occurs simultaneously in both Rh–H and NH positions.[22] These studies suggest that a concerted heterolytic H_2 splitting via a four-membered transition state **TS-17** is a plausible mechanism. The feasibility of this metal–ligand cooperative mechanism was further confirmed by DFT studies, which also showed that the "classical" oxidative addition of H_2 to a Rh^I center in **15** to form Rh^{III} dihydride is an unfavorable endothermic process.[22] The diolefin amide complexes of this type were shown to be active catalysts for a wide variety of direct hydrogenation, transfer hydrogenation and dehydrogenation reactions, including hydrogenation of ketones and imines as well as dehydrogenative coupling of alcohols with MeOH, amines, water to form esters, amides and carboxylates, respectively.[23]

An outer-sphere mechanism was also proposed for hydrogenation of nitriles catalyzed by the Ru complex **18** with a tetradentate PNNP ligand, including sequential hydrogenation of the CN triple bond of the nitrile and the CN double bond of the imine (Scheme 10).[24]

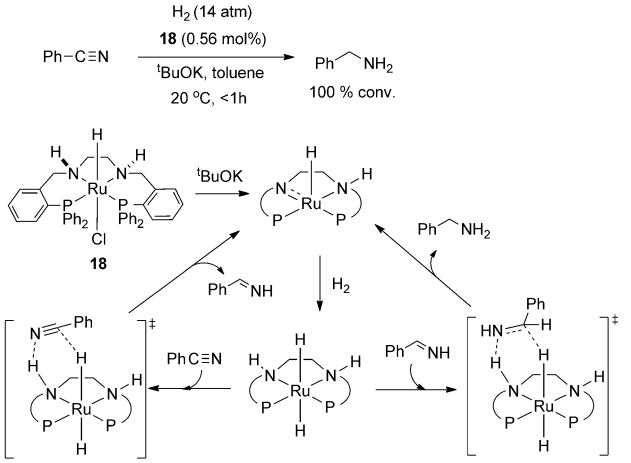

Scheme 10. Proposed mechanism of nitrile hydrogenation catalyzed by **18**.

Morris et al. also reported efficient asymmetric transfer hydrogenation of ketones catalyzed by Fe complexes supported by an aliphatic tetradentate PNNP ligand, and the mechanistic studies suggest that an outer-sphere mechanism could be operative.[25]

Application of aminophosphine Ru complexes for catalytic dehydrogenation of borane–amine adducts was reported by Fagnou et al.[26]

The aliphatic tridentate "pincer" ligands with a central amide/amine nitrogen donor offer a versatile platform for studying metal–ligand cooperativity in catalysis. The first examples of reversible heterolytic splitting of H_2, employing disilylamido PNP complexes of late transition metals, were reported by Fryzuk et al. starting from 1980s and catalytic alkene hydrogenation with such complexes was also studied.[27] Numerous examples of catalytic applications of Ru, Ir, Os, and Fe complexes (Scheme 11) supported by aliphatic PNP and PNN complexes in hydrogenation and transfer hydrogenation reactions were recently reported.[28–30] For example, Ir complexes **19** and **20** (Scheme 11) are catalysts for direct hydrogenation and transfer hydrogenation of ketones, imines, and hydrogenation of CO_2 to formate.[31] Ru complexes **21**, **22** and **23** were used for transfer hydrogenation of

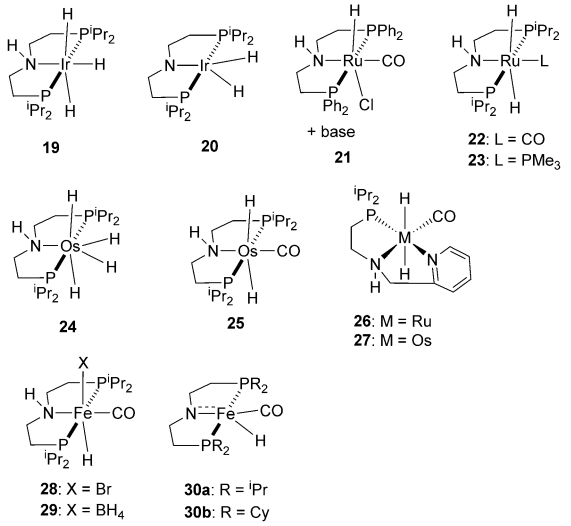

Scheme 11. Complexes with aliphatic PNP pincer ligands used for catalytic hydrogenation, transfer hydrogenation and dehydrogenation.

ketones,[32] hydrogenation of esters[33] and azides,[34] and dehydrogenation of alcohols[35] and amine–borane adducts.[36] Experimental and computational studies of these reactions suggest that MLC through a metal–amide/metal–amine bond may play an important role in these reactions. A mechanism was proposed for the Ir-catalyzed transfer hydrogenation of ketones through an outer-sphere hydrogen transfer to carbonyl from Ir–H/N–H, similar to Noyori–Morris-type mechanism (Scheme 12).[37] For PNN complexes **26** and **27**, both

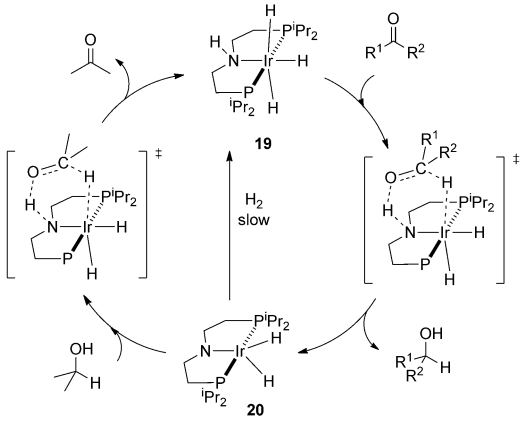

Scheme 12. Proposed mechanism for (PNP)Ir-catalyzed ketone hydrogenation.

inner-sphere and outer-sphere mechanisms were considered as plausible because of the presence of a potentially hemilabile pyridine arm.[38]

Interestingly, complexes with aliphatic PNP ligands may also show a different mode of H_2 elimination through participation of the ligand backbone. For example, complex **23** undergoes double H_2 elimination to form **33** with an unsaturated ligand backbone (Scheme 13). Mechanistic studies suggest that the first H_2 elimination occurs by transfer of the NH proton to the metal hydride (step (*i*) in Scheme 13; see also Scheme 14).[39] The resulting amide species **31** undergoes β-hydride elimination to form an unstable imine intermediate **32** (step (*ii*)), which further eliminates H_2 by proton transfer from a C–H group in the ligand backbone to the hydride ligand (step (*iii*) in Scheme 13, via **TS-34**). This reactivity resembles the H_2 elimination from aromatic PNP Ru complexes discussed in Section 3.1.

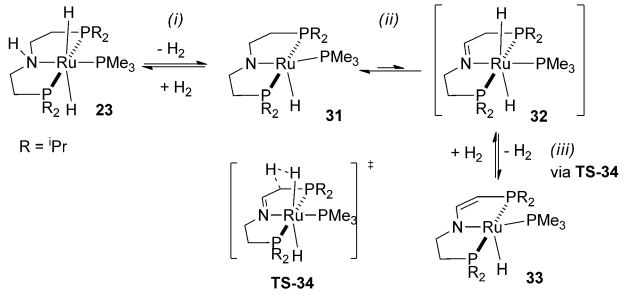

Scheme 13. Double H_2 elimination from **23**.

The H_2 elimination in step (*i*) (Scheme 13) could involve the direct coupling of the NH proton with a Ru–H via a four-membered transition state **TS-35** in the absence of protic solvents, similar to the amide complexes discussed above (Scheme 14, path a). At the same time, an alternative

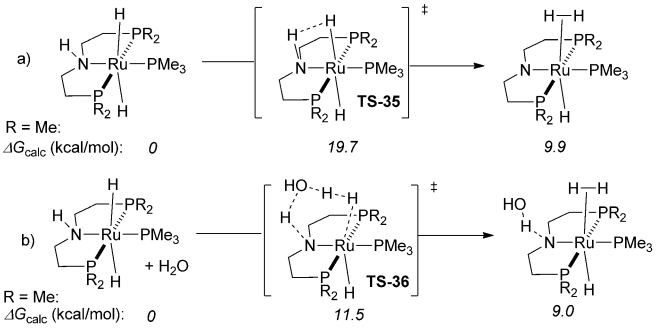

Scheme 14. Proposed pathways for H_2 elimination from **23** and calculated free energies (kcal mol^{-1}).

mechanism becomes feasible in the presence of water, which can act as a proton shuttle between NH and a hydride. According to the DFT study of the model system (R = Me in Scheme 14), the reaction barrier for a water-catalyzed pathway (b) via **TS-36** lowers $\Delta G^{\neq}$ by about 8 kcal mol^{-1} compared to path (a).[28,39] Proton exchange NMR studies also revealed a stereoselective exchange between water and Ru–H that is *syn*-coplanar with N–H, consistent with the water-assisted pathway (b). The importance of protic solvents acting as proton shuttles between the ligand and the metal was proposed not only for metal–amide/amine–type cooperation, but also for many other ligand frameworks that participate in bond activation systems via MLC (see Section 3).

Fe complexes **29** and **30a** with aliphatic PNP ligand were found to be catalytically active in acceptorless alcohol

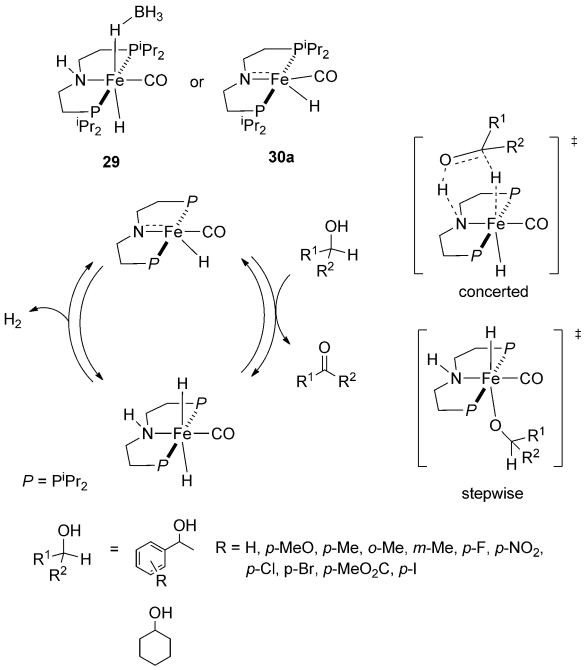

Scheme 15. Proposed mechanisms for Fe-catalyzed acceptorless dehydrogenation of alcohols.

dehydrogenation under base-free conditions.[40] Both concerted (via MLC) and stepwise mechanisms were considered and could not be distinguished based on the experimental data (Scheme 15).

An outer-sphere (concerted) mechanism was proposed for hydrogenation of esters to alcohols catalyzed by **29** based on the DFT studies and supported by NMR experiments.[30]

Beller et al. reported that the iron complex **29** is also catalytically active in MeOH dehydrogenation in the presence of KOH.[41] It was recently found that Fe complexes **30a,b** and **37a,b** operate under base-free conditions, in the presence of $LiBF_4$ as a Lewis acid co-catalyst (Scheme 16).[42] Mechanistic studies of the reaction and DFT analysis suggest that metal–ligand cooperation likely plays a role and a concerted, outer-sphere mechanism is operative.

By contrast to aliphatic PNP ligands, the amide nitrogen in diarylamide PNP complexes is significantly less basic and

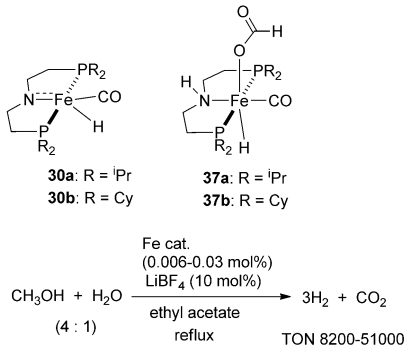

Scheme 16. Fe-catalyzed MeOH dehydrogenation in the presence of Lewis acid co-catalyst. TON = turnover number.

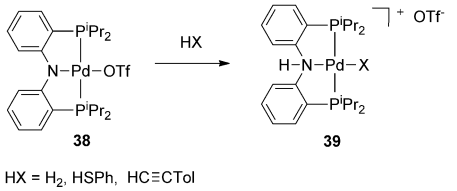

Scheme 17. HX heterolytic splitting by the Pd diarylamide complex.

MLC is unlikely to play an important role in such systems. For example, as reported by Ozerov et al., the palladium complex **38** with diarylamide PNP ligand heterolytically splits H–X bonds (HX = H_2, terminal alkyne, thiol) to give **39** (Scheme 17).[43] Although these reactions eventually lead to a net addition of H_2 bond across the Pd–amide bond, direct transfer of a proton from H_2 to the amide nitrogen was considered unlikely. The mechanism proposed for H_2 activation involves initial coordination of H_2 to the Pd center to give $[(PNP)Pd(H_2)]^+$ followed by an intermolecular proton transfer from coordinated H_2 to the amide nitrogen assisted by an external Brønsted base (triflate or solvent). Activation of B–B and B–H bonds with (PNP)Pd complexes with weakly coordinating anions was also reported and the possibility of oxidative addition to form a Pd^{IV} intermediate was proposed, but no conclusive experimental evidence was obtained yet in favor of Pd^{IV} intermediates in this reaction.[44]

Apart from amide/amine ligands, cooperative bond activation in mononuclear imide complexes is widely known. However, the application of such systems in catalysis is more problematic, largely because of the irreversibility of bond activation by highly reactive metal imides (Scheme 18 a,b).

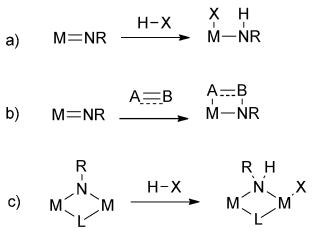

Scheme 18. MLC in mononuclear imido and binuclear imido-bridged complexes.

Mononuclear imido complexes of early transition metals are known to cleave C–H bonds of hydrocarbons through a 1,2-addition pathway (Scheme 18 a) and undergo cycloaddition of substrates containing C–C and C–heteroatom double and triple bonds across the M–imide bond (Scheme 18 b).[45,46] For example, zirconium(IV) imido complexes cleave the C–H bond of benzene to give a phenyl amido complex (Scheme 19).[45] However, the catalytic application of such reactivity is quite challenging due to stability of the resulting products and their inability to undergo further functionalization (in particular, reductive elimination does not occur as a d^0 metal center is present).

Bridged binuclear imido complexes can serve as bifunctional Lewis acid–Lewis base platforms for heterolytic split-

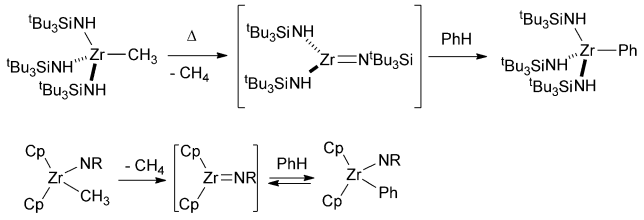

Scheme 19. C–H bond activation by Zr imido complexes.

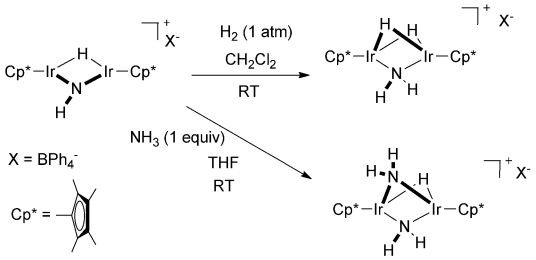

Scheme 20. H–H and N–H bond cleavage by imido-bridged diiridium complex.

ting of H–H and H–X bonds (Scheme 18c).[47] For example, heterolytic splitting of H_2 and NH_3 was reported by Ikariya, Kuwata et al. (Scheme 20) and it may be potentially relevant to N_2 fixation chemistry with binuclear late transition metal complexes.[48]

The binuclear bis(tosylimido)-bridged Rh^{III} complex **40** heterolytically splits H_2 to give bis(amido)bridged Rh^{II} complex **41** (Scheme 21a).[49] A DFT study of the reaction

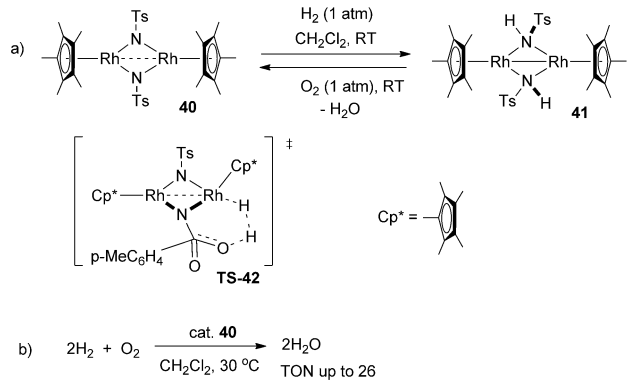

Scheme 21. H_2 activation by binuclear Rh tosylimido complex.

mechanism shows that a plausible mechanism involves sulfonyl-mediated H_2 heterolytic splitting (**TS-42** in Scheme 21) followed by proton transfer from the sulfonyl oxygen atom to the imide nitrogen, and then proton migration from Rh–H to another imide. Experimental evidence for Rh-hydride intermediates was obtained. Interestingly, the starting material can be regenerated by the reaction with O_2, which enables catalytic oxidation of H_2 with O_2 to water in the presence of **40** (Scheme 21b).[49]

2.2. Metal–Oxygen Bond

Compared to metal amide/amine complexes, the involvement of MLC in bond activation is less common for metal alkoxide/alcohol complexes due to the lower basicity of coordinated alkoxides and greater lability of coordinated alcohol in late transition metal complexes.

Gelman et al. reported a well-defined iridium pincer complex **33** with a dibenzobarrelene-based PCP pincer ligand that catalyzes the acceptorless dehydrogenation of alcohols to ketones and esters. Attempted crystallization of **43** leads to the release of H_2 gas, likely through an intramolecular interaction of Ir–H with dangling OH proton, and results in the formation of **44** with a coordinated alkoxide arm (Scheme 22). Such a H_2 release step was proposed to be involved in the catalytic dehydrogenation of alcohols. In contrast to Noyori-type systems, the alcohol dehydrogenation step was proposed to occur through an inner-sphere mechanism, via coordination and β-hydride elimination of the alkoxide (Scheme 23).[50]

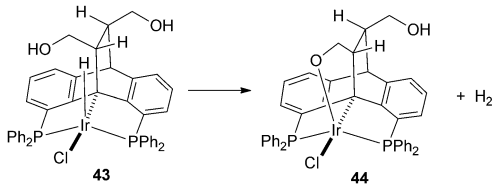

Scheme 22. H_2 extrusion from [(PCP)IrH(Cl)] complex **43** with dangling OH arm.

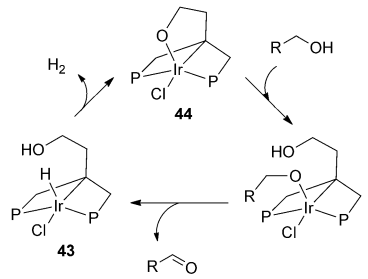

Scheme 23. Proposed mechanism of alcohol dehydrogenation to ketones catalyzed by **33** or **34**.

A Ru complex with an analogous dibenzobarrelene PCP ligand was shown to be a catalyst for the acceptorless dehydrogenation of alcohols and the acceptorless dehydrogenative coupling of alcohols with amines to form imines. The liberation of H_2 was proposed to occur through a similar pathway involving Ru–H/OH interactions.[51]

A similar pathway for H_2 elimination could be operative in the dehydrogenative coupling of amines with alcohols to form imines catalyzed by the binuclear complex **45** in the presence of a base, although the mechanism of H_2 elimination was not studied (Scheme 24).[52]

The iridium complex **46** with an NHC-tethered alcohol catalyzed the alkylation of amines with alcohols (Scheme 25).

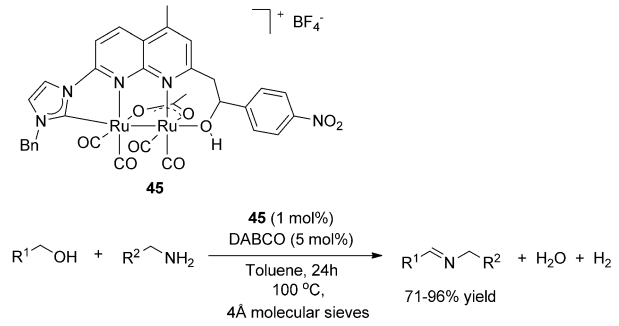

Scheme 24. Dehydrogenative coupling of amines with alcohols catalyzed by a binuclear Ru complex. DABCO = 1,4-diazabicyclo-[2.2.2]octane.

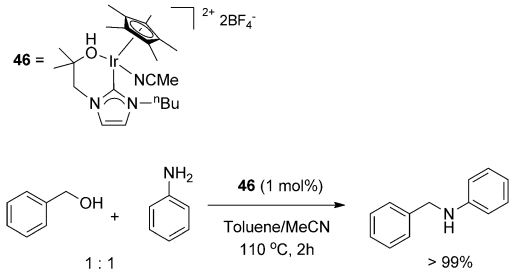

Scheme 25. Alkylation of aniline with benzyl alcohol catalyzed by **46**.

However, the mechanism was not investigated and both inner-sphere and outer-sphere mechanisms were considered to be plausible in this system.[53] Cooperative Si–H bond splitting by a diphosphine-dialkoxide Fe^{II} complex accompanied by the silylation of one of the alkoxide ligands was recently reported by Rauchfuss et al.[54]

Overall, due to the greater lability of alcohol ligands compared to amines, an inner-sphere mechanism through β-hydride elimination from alkoxide intermediates is often a viable pathway that may compete with an outer-sphere hydrogen transfer in hydrogenation or transfer hydrogenation reactions of carbonyl compounds.

2.3. Metal–Sulfur Bond

Activation of H_2 through M–S bond cooperation is highly relevant to the mechanism of H_2 oxidation to H^+ in [NiFe]-hydrogenase, where H_2 bond splitting assisted by the coordinated S atom of cysteine across the Ni–S bond was proposed based on experimental and computational studies (Scheme 26).

This inspired investigations of metal–sulfur cooperation for activation of H_2 and H–X bonds. Heterolytic H_2 and H–X bond splitting is known for metal complexes containing various types of S-donor ligands, including terminal and bridging sulfides and thiolate complexes.

The titanium sulfide complex **48** reported by Bergman, Andersen et al. was shown to activate H_2 reversibly (Scheme 27a).[55] Based on detailed isotopic and NMR studies,

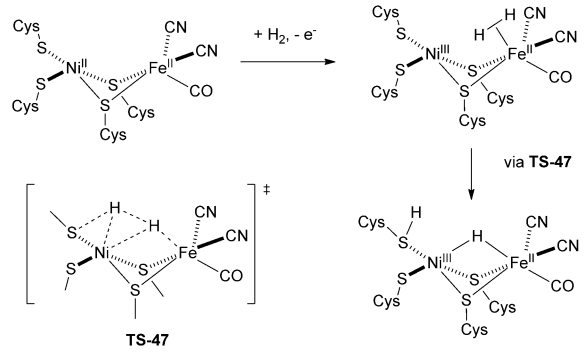

Scheme 26. Proposed mechanism of H_2 splitting in [NiFe]-hydrogenase.

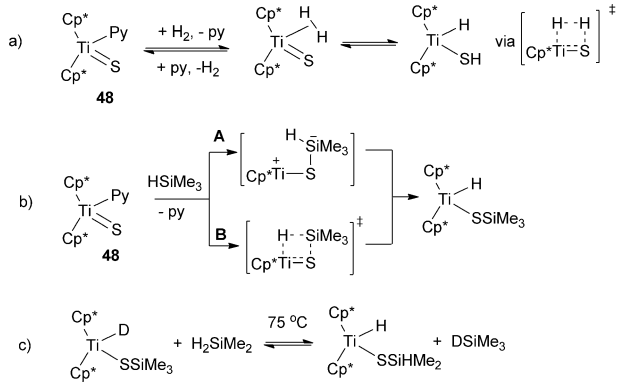

Scheme 27. H–H and Si–H bond activation by a Ti sulfide complex: a) proposed H_2 activation and proposed mechanism. b) Considered mechanisms for Si–H activation. c) Reversible Si–H/Si–D activation.

a concerted mechanism via a polarized four-membered transition state was proposed (Scheme 25a). Consistent with this mechanism, when $[(Cp^*)_2Ti(py)(S)]$ reacted with HD, an equilibrium mixture of $[(Cp^*)_2Ti(H)(SD)]$ and $[(Cp^*)_2Ti(D)(SD)]$ was formed, and no H_2 or D_2 was detected. In addition, ^1H NMR EXSY experiments showed that the rates of exchange of H_2 with Ti–H and SH positions were identical, consistent with a concerted pathway.[55]

The same complex **48** was shown to activate Si–H bonds (Scheme 27b,c). Two possible mechanisms were considered for Si–H activation: path **A** via a pentacoordinate silicon intermediate, and path **B** via a four-membered transition state (Scheme 27b).[55] Based on observation of a normal kinetic isotope effect for silane activation, the authors concluded that path **B** is more likely as the Si–H bond is expected to be significantly weakened in the transition state, while an inverse isotope effect could be expected for path **A** based on previous studies of Si–H addition in metal–imide complexes.[56] The Si–H activation is reversible: when $[(Cp^*)TiD(SSiMe_3)]$ was heated in the presence of H_2SiMe_2, a mixture of starting materials, $[(Cp^*)_2TiH(SSiHMe_2)]$, and $DSiMe_3$ was present, but no H/D scrambled products were detected (Scheme 27c). This is consistent with an intramolecular 1,2-elimination of Si–H bonds that occurs in a strictly pairwise manner.

The binuclear Ir complex **49** with bridging sulfides reported by Rauchfuss et al. features two modes of H_2 activation: first, homolytic H_2 activation leading to the formation of the dihydride complex **50**, followed by heterolytic activation of another equivalent of H_2 to generate **51** with bridging hydride and hydrosulfide ligands (Scheme 28).[57] The unstable complex **51** observed by NMR spectroscopy at low temperature eventually isomerizes to **52**.

Heterolytic splitting of 2 equivalents of H_2 was also observed with the binuclear sulfide-bridged Rh complex with a triphos ligand (Scheme 29).[58]

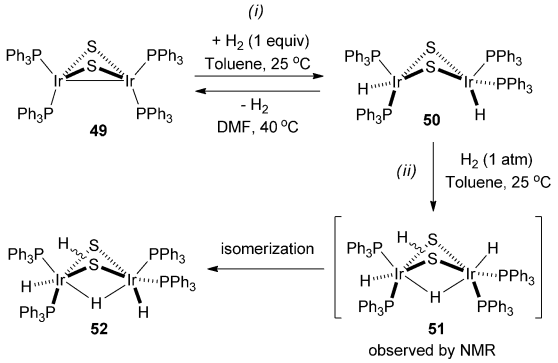

Scheme 28. H_2 activation by binuclear bis(sulfide)-bridged Ir complex: i) homolytic activation; ii) heterolytic activation.

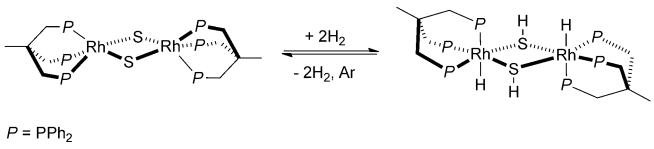

Scheme 29. Heterolytic H_2 splitting by binuclear triphos Rh complex.

The reversible activation of Si–H bonds by the cationic Ir complex **53** supported by a P,S-ligand was reported by Stradiotto et al. and resulted in a net addition of Si–H across the Ir–S bond (Scheme 30). However, no detailed mechanistic studies were carried out and it remains to be seen whether this reactivity involves MLC.[59] Although complex **53** could be regenerated by the reaction with a ketone, it was not an effective catalyst for ketone hydrosilylation.[59]

The reactivity of coordinatively unsaturated Ir, Rh and Ru complexes with bulky thiolate ligands was studied by the

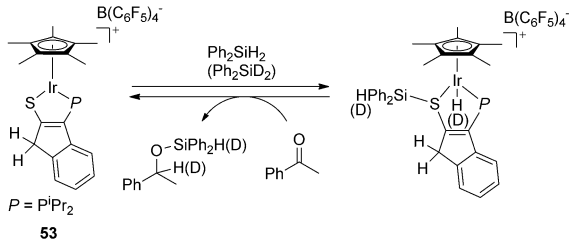

Scheme 30. Si–H activation by cationic Ir complex **53**.

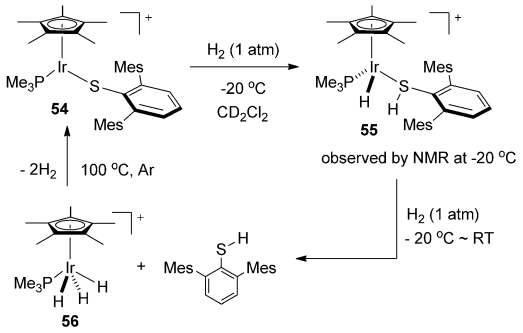

Scheme 31. Reversible H_2 activation by Ir thiolate compelx.

groups of Ohki, Tatsumi, and Oestreich. Reversible heterolysis of H_2 by the Ir complex **54** occurs at low temperatures, giving rise to complex **55** as the major product, characterized by NMR spectroscopy at low temperatures (Scheme 31).[60] This is a rare example of H_2 heterolysis by a metal thiolate complex under mild conditions and it functionally resembles the reactivity of [NiFe]-hydrogenase described above (Scheme 26). The measured kinetic isotope effect suggests that H–H bond cleavage is involved in the rate-limiting step.[60] Warming up in the presence of H_2 eventually results in the loss of free thiol and formation of the Ir^V trihydride **56**. Interestingly, the starting material can be regenerated in 81% yield by heating **56** in the presence of free thiol.[60]

The reaction with the analogous Rh complex was less selective and led to more significant degradation.[60,61] The lability of a protonated thiol ligand and its irreversible loss is an important issue for Ir and Rh complexes and it is likely responsible for the lack of catalytic reactivity of the Ir complex in C=O and imine hydrogenation, while the analogous Rh complex was active in aldehyde, ketone and imine hydrogenation at −50 °C.[61]

Based on a computational study of this reactivity, Li et al. suggested that H_2 activation by the Ir complex **54** occurs through initial oxidative addition of H_2 to give an Ir^V dihydride followed by S–H reductive elimination.[62] At the same time, DFT studies suggest that the analogous Rh complex operates through metal–ligand cooperative heterolytic splitting of H_2.[62]

The metal-thiolate-mediated H_2 activation could be operative in hydrogenation of ketones catalyzed by a Ru complex **57** bearing a tethered thiol as reported by Ohki, Tatsumi et al. (Scheme 32a).[63] The authors also proposed a concerted outer-sphere hydrogen transfer to the carbonyl similar to the Noyori-type mechanism.[63] However, given the lability of a protonated thiol ligand, inner-sphere mechanisms cannot be unambiguously ruled out without further studies.

Furthermore, the Ru thiolate complex **57** was found to be an active catalyst for the electrophilic borylation of indoles.[64] Cooperative activation of B–H by the metal thiolate was proposed and an activated borane complex **61** was characterized by NMR spectroscopy and X-ray crystallography (Scheme 33).[64]

The same complex **57** is active in C–H silylation of indoles (Scheme 34a).[65] Low-temperature NMR studies of the

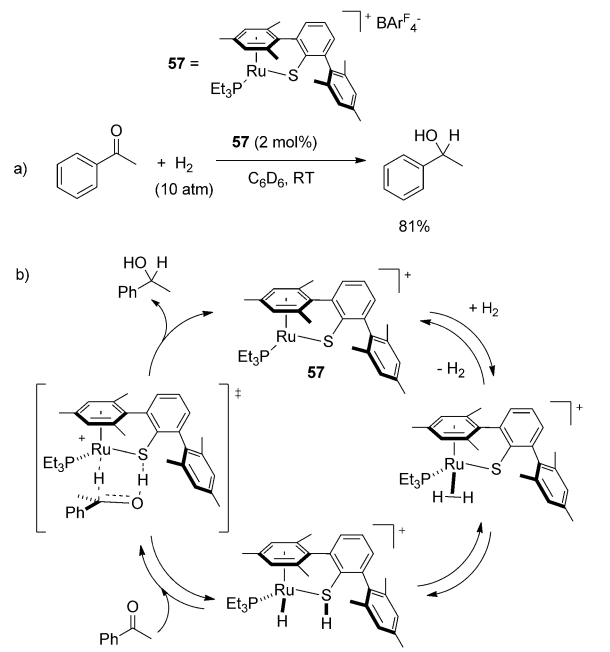

Scheme 32. Ketone hydrogenation catalyzed by a) Ru thiolate complex **57**; b) proposed mechanism.

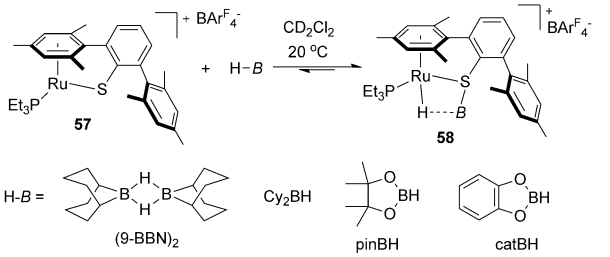

Scheme 33. Borane activation by the Ru thiolate complex **57**.

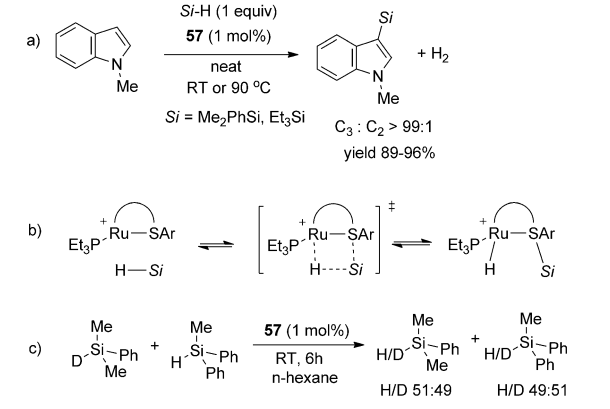

Scheme 34. a) Silylation of indoles catalyzed by **57**. b) Proposed cooperative Si–H bond activation. c) Catalytic Si–H/Si–D scrambling.

reaction between **57** and excess silane allowed to detect a metal–hydride species, with the hydride signal showing splitting from the phosphine ligand, but no detectable $^1J_{Si\text{-}H}$ satellites. By analogy with H_2 activation, a cooperative Si–H activation was proposed (Scheme 34b), however, alternative mechanistic scenarios were not considered.[65] Interestingly, complete H/D scrambling between Ph_2MeSiH and $PhMe_2SiD$ was observed at room temperature in the presence of catalytic **57** to give a mixture of $Ph_2MeSi(H/D)$ and $PhMe_2Si(H/D)$ (H/D ca. 50:50) suggesting that Si–H bond formation does not occur in a pairwise fashion and the mode of Si–H activation may be more complicated than that shown in Scheme 34b.[65]

Overall, while thiolato complexes of late transition metals show interesting potential in catalysis, the extent of metal–ligand cooperation in H–H and H–X bond activation needs to be further elucidated through mechanistic studies. The hemilability of a protonated thiolate ligand as well as alternative metal-only or ligand-only mediated pathways should be taken into account when considering possible reaction mechanisms.

2.4. Metal–Boron Bond

Although there are only a few examples so far of H_2 activation by metal–borane complexes and their application in catalysis, this topic attracts significant attention in the context of metal-mediated borohydride regeneration using H_2 for catalytic hydrogenation reactions. Compared to previously discussed metal amide, alkoxides, or thiolate complexes, the mode of H_2 activation by metal–borane complexes is different as the borane ligand acts as a Lewis acid site in H–H bond activation resulting in the formation of a borohydride and a metal hydride.[66]

Reversible addition of H_2 to $[(^tBu_3SiO)_3Ta(BH_3)]$ to form $[(^tBu_3SiO)_3TaH(\eta^3\text{-}BH_4)]$ was studied recently by Wolczanski et al.[67] Complex **59** reported by Owen et al. undergoes hydride migration from the borohydride to the coordinated norbornadiene followed by its rearrangement to give an alkyl complex **60** (Scheme 35).[68] Subsequent activation of 2 equivalents of H_2 with **60** leads to elimination of the alkane product (tricyclo[2.2.1.0^{2,6}]heptane) and the formation of the borohydride complex **61**. Alkene hydrogenation catalyzed by **60** was also accomplished.[68]

Peters et al. reported on the reversible oxidative addition of H_2 to the nickel-borane complex **62** resulting in the

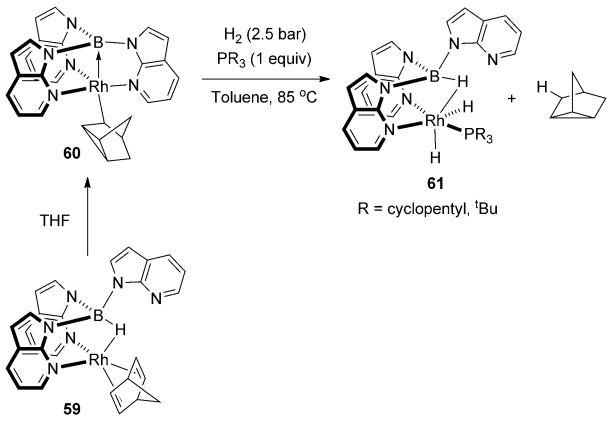

Scheme 35. Double H_2 addition to the Rh-borane complex **60**.

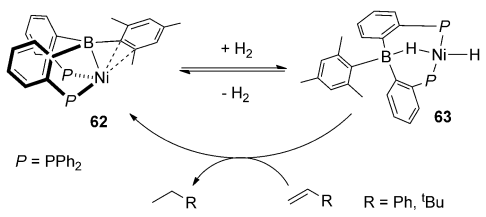

Scheme 36. H_2 activation by Ni borane complex **65**.

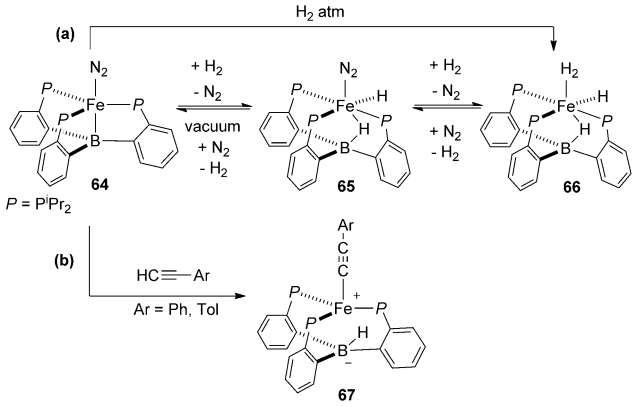

Scheme 37. a) H_2 and b) alkyne activation by **64**.

formation of the borohydrido-hydrido Ni^{II} complex **63**, which serves as a catalyst for alkene hydrogenation (Scheme 36).[69]

Similar reactivity was reported for the Fe-boratrane complex **64** that can activate H_2 to generate complex **65** or, with excess H_2, **66** (Scheme 37 a).[70] Stoichiometric reaction of **65** with styrene under N_2 atmosphere generates ethylbenzene and **64**, thus demonstrating that the bridging hydride in **65** is competent in hydrogen transfer to alkenes under stoichiometric conditions. Catalytic alkene hydrogenation was also achieved with complex **64** as a catalyst. Complex **64** was also shown to activate C–H bonds of terminal alkynes to give alkynyl-borohydride complexes **67** (Scheme 37 b).[70] As noted by the authors, the possible contribution of metal–borane cooperation in H_2 splitting in such systems needs to be addressed through more detailed mechanistic investigations.

Borane-assisted bond activation reactions were recently reported for the three-coordinate Pt complex supported by a small bite-angle bidentate (boryl)iminomethane ligand.[71] Reversible activation of H_2 by complex **68** bearing a wide bite-angle bis(phosphine)borane ligand (Scheme 38) results in the formation of Pt hydride borohydride complex **69**.[72] Interestingly, phenylacetylene activation by **68** eventually leads to the formation of vinylborane complex **70**, resulting from migration of the Ph group from B to the acetylide carbon.

A boryl-assisted pathway was recently proposed for the hydrogenolysis of Ni-Me PBP pincer complex based on a DFT study.[73]

To conclude, while borane and boryl ligands represent an interesting platform for bond activation studies, one of the potential drawbacks is alkyl or aryl group migration from

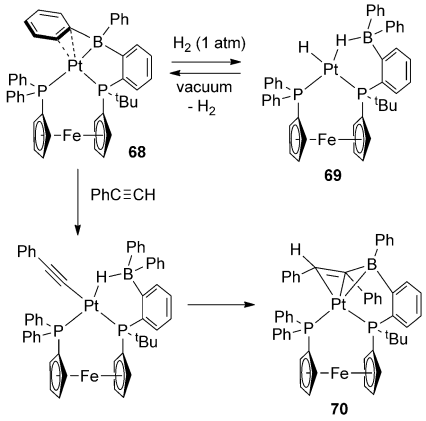

Scheme 38. H_2 and terminal alkyne activation by a borane Pt complex.

boron to other substrates leading to irreversible ligand modification. Moreover, even if the borane ligand is chemically modified as a result of bond activation, cooperation between metal and boron needs further proof through experimental and theoretical studies For example, some of the reactions shown in Scheme 38 could involve "classical" oxidative addition to a low-coordinate reactive Pt center followed by binding to a Lewis-acidic borane. In addition, borane and boryl ligands significantly affect the reactivity of transition metal complexes due to their unique electronic properties, regardless of metal–ligand cooperative pathways in bond activation.[66]

2.5. Metal–Carbon Bond

The studies of the ability of aliphatic PCP pincer complexes to reversibly lose H_2 were pioneered by Shaw et al. and this reactivity was later explored by other groups.[74,75] The reversible elimination of H_2 from the cyclometalated osmium complex **71** with agostic α-CH interactions was reported by Gusev et al., leading to the formation of the hydrido carbene **72** (Scheme 39), however,

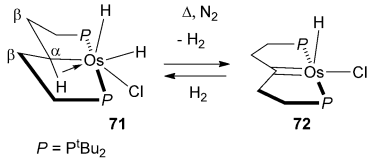

Scheme 39. Reversible H_2 elimination from a cyclometalated Os complex.

the mechanism was not discussed in detail. Treatment of the hydrido carbene **72** with D_2 gave a partially deuterated **71** with deuterium incorporated in both Os–H positions (64% D), α-CH (85%) and β-CH_2 positions (14%).[76] The analogous Ru carbene complex could not be obtained in a pure form due to competing β-hydride elimination.[76]

In order to avoid β-hydride elimination from the aliphatic backbone of the PCP ligand, the reactivity of iridium carbene

complexes with diarylphosphine arms was studied by Piers et al. Single C–H bond activation of a free bis(2-(diarylphosphino)phenyl)methane leads to the formation of **73**, while the reaction at elevated temperature produces the product of a double C–H bond activation, the carbene complex **74**, in high yield (Scheme 40).[77] The authors

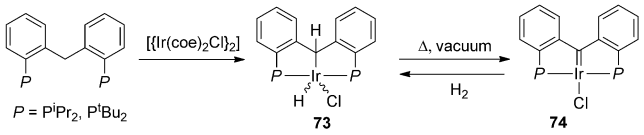

Scheme 40. Formation of carbene complex **74** and H_2 activation.

suggested that the central carbon in **74** behaves essentially as a Fischer carbene, thus allowing to assign a formal oxidation state +1 for the Ir center. Facile addition of H_2 occurs upon exposure of **74** to H_2 to give **73**. The mechanism of this reaction is not clear and it could involve oxidative addition of H_2 to a formally Ir^I center.[77]

By contrast to the Ir complex **74**, the analogous ligand in the Ni complex **75** was assigned as a Schrock-type carbene bearing a formal −2 charge, supporting a Ni^{II} center (Scheme 41).[78] Unlike **74**, the Ni complex **75** undergoes

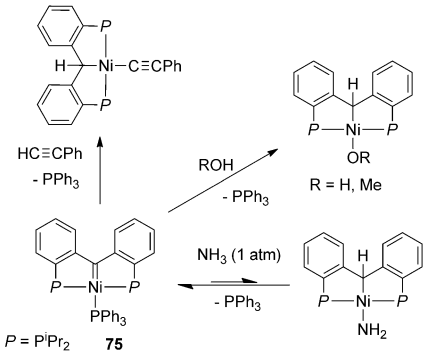

Scheme 41. H–X and H–H bond activation by (PCP)Ni carbene complex **75**.

rapid addition of polar C–H, N–H, and O–H bonds. Structural and DFT studies along with the observed reactivity also suggest a nucleophilic character of the central carbon atom in a similar Pd complex.[79]

Overall, although net activation of H–H and H–X bonds is observed for both complexes **74** and **75**, the mechanism of activation may be different, depending on the electronic nature of the carbene ligand and the metal atom.

Another type of carbene-based PCP ligand was shown by Piers et al. to participate in an oxygen transfer reaction from N_2O to the Ir complex **76** leading to formation of the iridaepoxide species **77** by addition of O across the Ir=C bond (Scheme 42).[80] Complex **77** was also identified as one of the possible products of the reaction of **76** with O_2 upon exposure to air, although its formation was less selective. Complex **77**

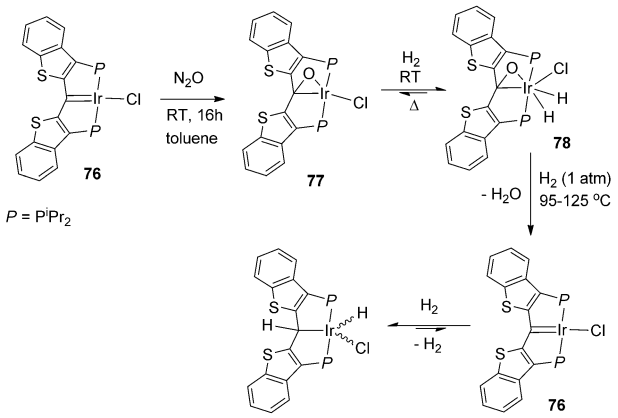

Scheme 42. N_2O hydrogenation mediated by Ir complex **76**.

reacts cleanly with H_2 via intermediate dihydride **78** to eventually give H_2O and regenerate **76**, although further reactivity with excess H_2 leads to its reversible addition across the Ir=C bond. Although this reactivity points out toward possible catalytic N_2O hydrogenation, an attempted catalytic reaction led to complex decomposition.[80]

The reactivity of complexes with a cycloheptatrienyl-based PCP pincer ligand developed by Kaska, Mayer, and co-workers[81] was covered in detail in a recent review, along with other examples of aliphatic PCP pincer complexes.[75]

3. Metal–Ligand Cooperation through Aromatization/Dearomatization

In this section, examples of MLC will be considered in which the ligand's aromatic system is disrupted or restored during the bond breaking/formation step.

3.1. Lutidine- and Picoline-based Ligands

A great number and variety of tridentate pincer ligands have been developed over the last decades (Scheme 43). The majority of the ligands discussed in this section are substituted lutidines or 2-picolines, with one or two CH_2 groups in the *ortho*-position(s) of a central pyridine unit, which upon deprotonation by strong bases undergo dearomatization of the heteroaromatic core, with formation of an exocyclic double bond, thus forming a reactive center for metal–ligand cooperation, as shown by our group (Scheme 44).[82]

Although deprotonation occurs at the methylene group located remotely from the metal center, it has a direct influence on the first coordination sphere of the metal, as the central pyridine ring loses its aromatic character and a central N-atom can be seen as an amide-donor. For example, the NMR spectrum of complex **89** obtained by deprotonation of the cationic complex **88** shows three pyridine protons that shift upfield and appear at 5.4, 6.35 and 6.43 ppm, consistent with dearomatization of the pyridine system (Scheme 45).[83] The X-ray structure of **89** reveals that the C6–C7 bond is significantly shorter than the C1–C2 bond (Figure 1).[83] At

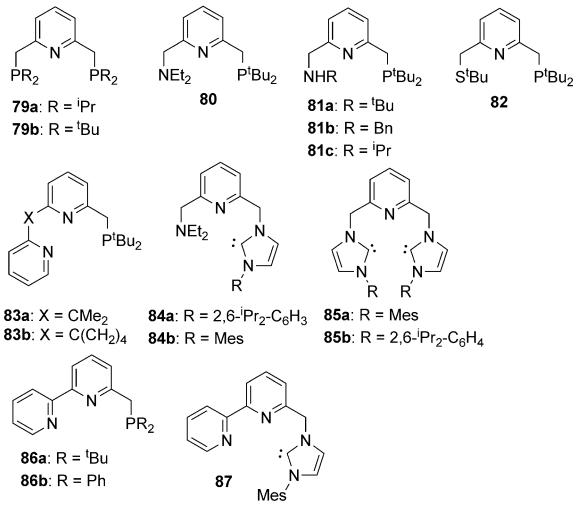

Scheme 43. Lutidine- and picoline-based pincer ligands.

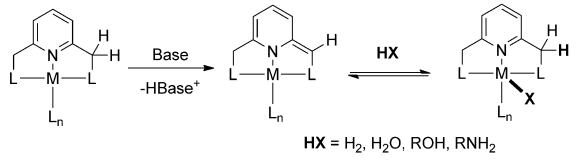

Scheme 44. Bond activation in complexes bearing lutidine-based pincer ligands.

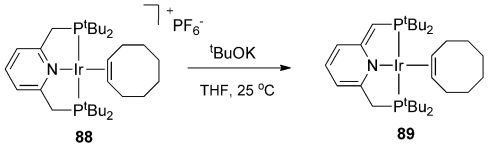

Scheme 45. Synthesis of complex **89**.

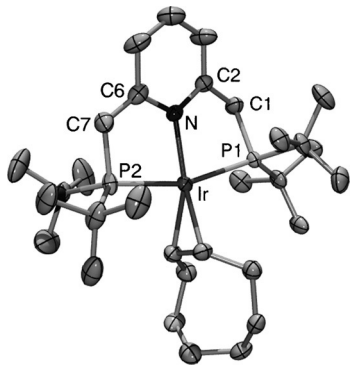

Figure 1. ORTEP representation of **89** (50% probability ellipsoids). Hydrogen atoms are omitted for clarity. Selected bond lengths (Å): C1–C2 1.506, C6–C7 1.351, C1–P1 1.830, C7–P2 1.784, Ir–N 2.089.

the same time, the C7–P2 bond is only slightly shorter than C1–P1 bond, showing that the phosphor-ylide resonance structure has a much lesser contribution.[82]

Lutidine-based ligands offer versatile platforms for studying MLC in activation of H–H, H–X (X = C, N, O, B) as well as C=O double bonds and C≡N triple bonds of nitriles as will be discussed below.

3.1.1. H_2 Activation in Complexes with Lutidine-based Ligands.

Iridium complexes with PNP ligands **79** were shown by our group to activate H_2 and C–H bonds.[82–84] For example, the reaction of the phenyl iridium(I) complex **90** with H_2 generated the *trans*-dihydride complex **92** as the product (Scheme 46).[83] Interestingly, a *cis*-dihydride complex was not

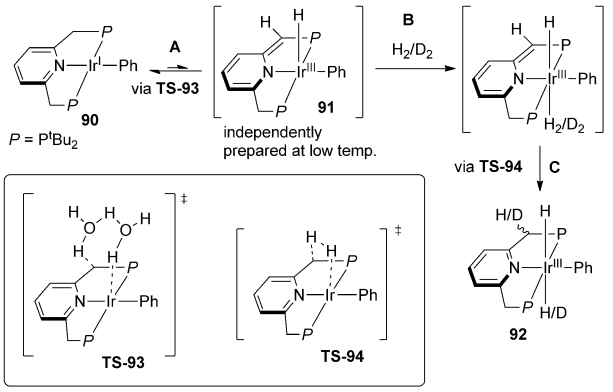

Scheme 46. H_2 activation by the Ir^I complex **90**.

detected in this reaction, suggesting that a mechanism different from oxidative addition to the Ir^I center is operative. Moreover, the reaction with D_2 leads to incorporation of one deuterium atom into the ligand's arm. A mechanism was proposed and studied both experimentally and computationally, which involves initial H-transfer from the methylene arm to the metal center to give a dearomatized Ir^{III} hydride (step **A** in Scheme 46), followed by H_2 coordination (step **B**) and heterolytic H_2 splitting through metal–ligand cooperation, with aromatization (step **C**).[83] Therefore, although the overall reaction leads to $2e^-$ oxidation of the Ir center, the H_2 activation step likely occurs at the oxidized, Ir^{III} center. Indeed the postulated dearomatized intermediate hydride **91** was independently prepared and fully characterized at low temperature, and shown to react with hydrogen to give the same *trans*-dihydride product

Later, computational studies of the H-transfer step **A** showed that the barrier for the direct transfer from the arm to the metal is high, not consistent with the mild reaction conditions.[85] As an alternative, a water-assisted proton shuttle mechanism was proposed, where one or two water molecules form a bridge between the arm and the metal, leading to significantly lower activation barriers (for example, **TS-93** in Scheme 46).[85] Accessible activation barriers were found for H_2 splitting at the Ir^{III} center in the MLC pathway (**TS-94**, Scheme 46).[86]

Catalytic applications of Ru and other transition metal complexes with pincer ligands were reviewed thoroughly in recent reviews, and bond activation by MLC was implicated in

many of these transformations.[87,88] Some selected examples of bond activation will be discussed here to illustrate the metal–ligand cooperation concept in lutidine-based systems.

As shown by our group, complexes **97** and **98**, formed by deprotonation of precursors **95** and **96**, heterolytically split H_2 in a reversible fashion (Scheme 47a). Both complexes **97** and **98** are catalysts for ester hydrogenation, however, the PNN complex **98** shows significantly higher activity.[89] The reverse

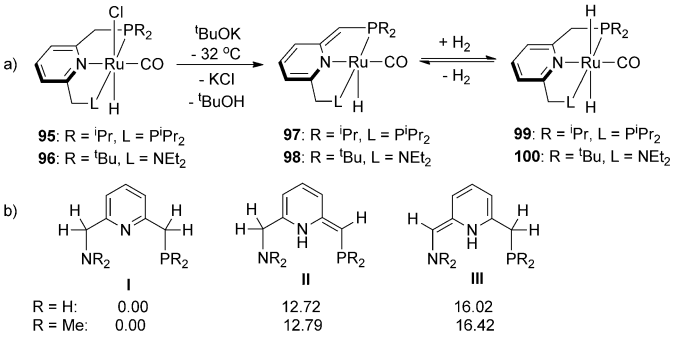

Scheme 47. a) Formation of dearomatized Ru complexes and H_2 activation and b) hypothetical tautomers of PNN pincer ligand and their calculated relative electronic energies (kcal mol^{-1}).

reaction, alcohol dehydrogenation, is also mediated by complexes **95** or **96** in the presence of a base, or in the absence of base by dearomatized species **98**.[90] Reversible H_2 activation was proposed as one of the key steps in several catalytic transformations that generate hydrogen or consume it catalyzed by **97**, including the new amide bond forming reaction, by acceptorless dehydrogenative coupling of alcohols and amines.[89,91]

Notably, deprotonation of the unsymmetrical PNN complex **96** generates a P-arm deprotonated species **98** selectively (Scheme 47a).[89] This correlates with theoretical studies by Yang and Hall who calculated relative energies of several tautomers of the simplified PNN ligands.[92] While the aromatized form **I** of the ligand was significantly more stable that both α-protic tautomeric forms **II** and **III**, the P-arm deprotonated form **II** was several kcal mol^{-1} more stable that the N-arm deprotonated isomer **III** (Scheme 47b).[92] However, as shown below, the reactivity at both P- and N-arms can be observed depending on the substrate and reaction conditions.

In the analogous Ru complex with an unsymmetrical NN(NHC) ligand, initial deprotonation generates a NHC-arm deprotonated species **101** and subsequent reaction with D_2 at low temperature leads to incorporation of the D label at the NHC arm (Scheme 48).[93] However, complete incorporation of D into both arms was observed upon warming up the reaction mixture in the presence of excess D_2, suggesting that deprotonation of the amine arm also takes place.

Metal–ligand cooperation was also proposed to play a role in H_2 elimination during water splitting mediated by complex **98** discovered by our group (Scheme 49).[94] First, the dearomatized complex **98** reacts with water to give the aromatized hydrido hydroxo complex **102**, which then thermally elimi-

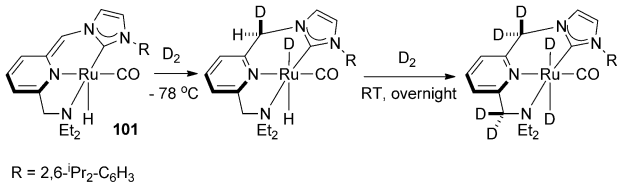

Scheme 48. D_2 activation by **101**.

nates H_2 to give the isolated dihydroxo complex **103**. The latter is capable of O_2 elimination upon irradiation of 320–420 nm light, presumably via H_2O_2 intermediacy, thus closing the net thermal/photochemical cycle for water splitting. DFT studies of the reaction mechanism suggest cooperative pathways for H_2 elimination, either directly or through proton shuttle mechanisms, although alternative pathways have also been considered.[92,95] This water splitting reactivity was described in more detail in recent reviews.[87,96] Activation of water by an NCN pincer complex containing a central NHC ligand and two pyridine arms was also reported by Morris et al. Dearomatization of one or both Py arms by a CH_2Py group deprotonation was observed in these systems.[97]

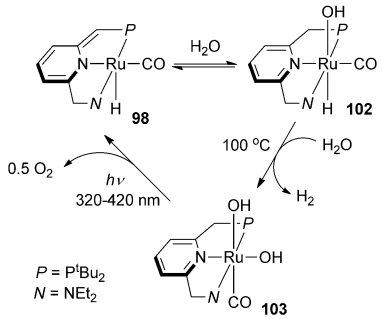

Scheme 49. Water splitting mediated by **98**.

Our group reported the first examples of hydrogenation of organic carbonates, carbamate esters[98] and ureas[99] to form methanol, alcohols and amines catalyzed by the bipyridyl-PNN Ru dearomatized pincer complex **104** (Scheme 50). Since these compounds can be formed from CO_2 or from CO, this provides a mild, two-step process for the hydrogenation of these gases to methanol. Indeed, this has led to the development of a 2-step procedure for CO_2 capture with aminoalcohols at low pressure and subsequent hydrogenation of the in situ formed oxazolidinone products to MeOH.[100]

Interestingly, the same complexes **104** and **105** show unprecendented reactivity in catalytic dehydrogenation of alcohols to carboxylic acid salts in refluxing water in the presence of an equivalent amount of NaOH.[101]

Interestingly, a dual mode of MLC can be enabled in the Ru complexes **106a**, **106b**, and **106c** with a secondary amine group, both through amide/amine and pyridine aromatiza-

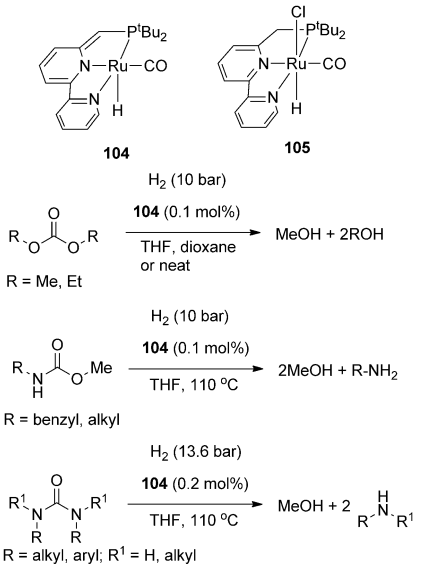

Scheme 50. Hydrogenation of organic carbonates, carbamates and ureas catalyzed by **104** and **105**.

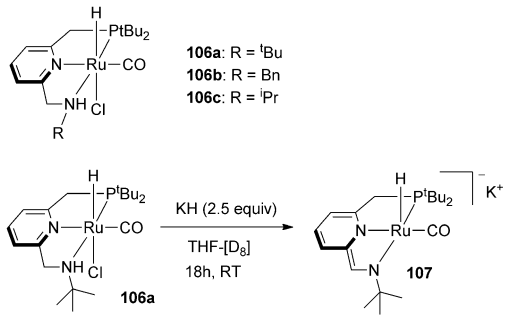

Scheme 51. a) (PNNH)Ru complexes and b) the formation of dearomatized enamido complex **107**.

tion/dearomatization transformations, as recently reported by our group (Scheme 51).[102] In particular, double deprotonation of **106a** generates the anionic enamido complex **107** characterized by X-ray crystallography. Complexes **106a**, **106b**, and **106c** in the presence of 2 equiv of base are active catalysts for ester hydrogenation at room temperature and 5 bar of H_2, which are the mildest conditions for ester hydrogenation reported so far. Moreover, they catalyze the acceptorless dehydrogenative coupling of alcohols to form esters at a temperature as low as 35 °C (boiling ether solvent).[102]

Hydrogen activation was also observed by our group with Re complexes supported by PNP ligands. The dearomatized complex **108** reacts with D_2 at room temperature to give **109-[D_2]** (Scheme 52).[103] The following observations support intramolecular D_2 activation through a MLC mechanism: 1) formation of Re–D occurs concomitantly with incorporation of only one D at the methylene arm; 2) D-incorporation on only one face on the ligand; and 3) no further H/D exchange was observed in the methylene arms under these conditions (1 atm, RT). Interestingly, when **109-[D_2]** was

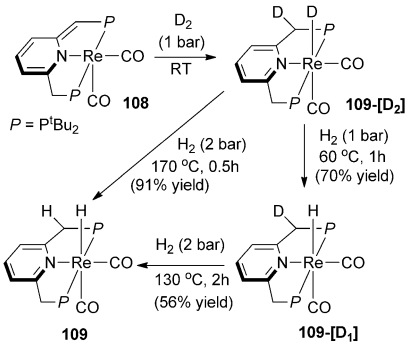

Scheme 52. Hydrogen activation by a (PNP)Re complex.

reacted with 1 bar H_2 at 60 °C, selective Re–D/Re–H exchange was observed at initial stages to form **109-[D_1]**, while the CHD arm remained intact (Scheme 52). This suggests that Re–H/Re–D exchange occurs by a non-MLC mechanism under these conditions. At higher reaction temperatures and 2 bar of H_2, H/D exchange at the methylene arm was also seen to give **109** (Scheme 52).[103]

3.1.2. N–H Bond Activation

As reported by our group, activation of the N–H bond of electron-poor arylamines by the dearomatized Ru complex **110** generates complexes **112** (Scheme 53).[104] For *p*-nitro-

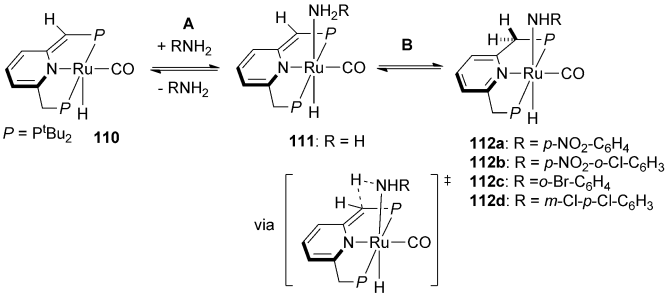

Scheme 53. N–H activation by (PNP)Ru complex.

substituted arylamines, complexes **112a** and **112b** were the only products present, while for halogen-substituted arylamines, an equilibrium mixture of **112c** or **112d** and **110** was formed. For ammonia, the most thermodynamically stable form in solution was the coordination complex **111**. However, evidence for N–H bond activation of ammonia was obtained in a reaction with excess ND_3 leading to stereoselective incorporation of a single D-label on only one face of the ligand, consistent with N–D activation by MLC (Scheme 54).[104] DFT studies of the reactions in Scheme 53 were in good agreement with experimental observations, and accessible activation barriers were found for N–H activation by MLC.[104]

Detailed mechanistic studies of N–H bond activation in square planar Rh^I complexes suggest an associative pathway (Scheme 55).[105]

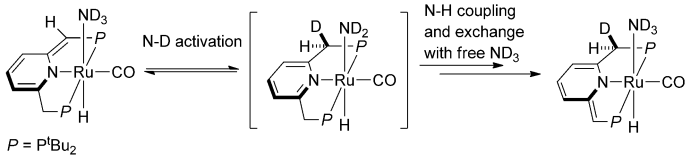

Scheme 54. D-label incorporation to methylene arm in a reaction with ND_3.

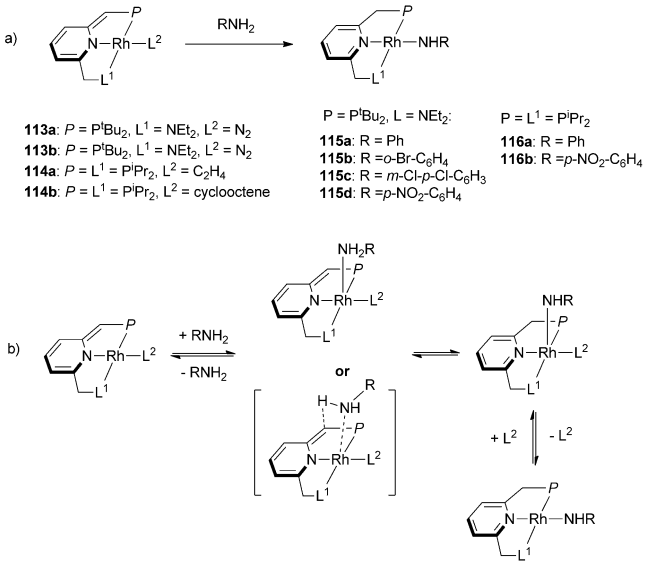

Scheme 55. a) N–H activation by Rh complexes and b) proposed associative mechanism.

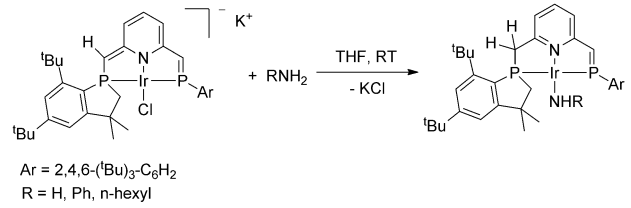

Scheme 56. N–H activation by Ir phosphaalkene complex.

Yoshizawa, Ozawa et al. reported N–H activation of amines and ammonia by an anionic Ir^I complex supported by the phosphaalkene ligand to give the corresponding amido complexes in quantitative yields (Scheme 56), and a similar associative mechanism was proposed.

3.1.3. ***Alcohol, Aldehyde and Ketone Activation***

Activation of these three types of substrates by Ru complexes is considered in this section, as Ru pincer complexes described here also act as effective dehydrogenation catalysts for alcohols.

Alcohol activation by the dearomatized (PNP)Ru complex **110** was studied by our group using low-temperature NMR spectroscopy, showing that the formation of an alkoxo complex **117** is reversible even at −80 °C (Scheme 57 a).[106] Upon warming up to −30 °C, alcohol dehydrogenation was observed, leading to formation of the dihydride **118** (Scheme 57 b). Notably, free aldehydes were not detected under these conditions, and the other product of this reaction was complex **119** that results from in situ trapping of aldehydes by **110**. Complex **110** was shown to react rapidly with free aldehydes even at −70 °C to give an adduct **119**, with formation of new Ru–O and C–

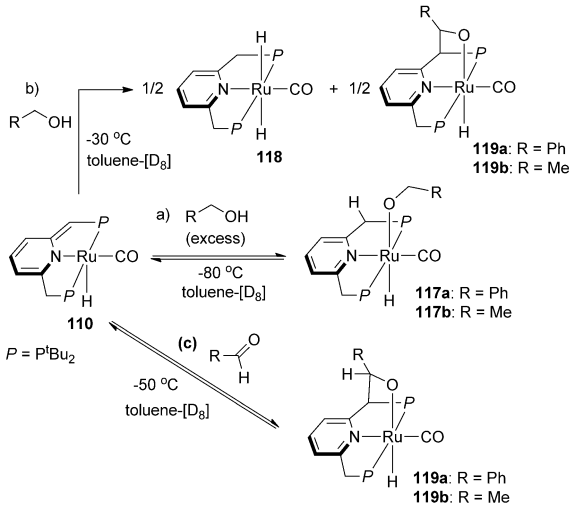

Scheme 57. Bond activation by MLC for complexes with lutidine-based ligand framework.

C bonds through C=O activation. This demonstrated for the first time a new mode of MLC for facile carbonyl group activation accompanied by a reversible C–C coupling with a ligand backbone (Scheme 57 c). Upon warming up to −50 °C, the reverse reaction, aldehyde elimination, takes place to give an equilibrium mixture of **119**, **110**, and free aldehyde. Reversibility of this reaction at −50 °C was also confirmed by spin saturation transfer (SST) NMR experiments. When complex **119 a** was warmed up to room temperature, a mixture of **110** and benzaldehyde was formed, while for complex **117 b** the reaction was less clean. In addition, facile alcohol dehydrogenation at −30 °C suggests that a mechanism different from the "classical" β-hydride elimination is operative, as coordinative unsaturation (for example, through P-arm dissociation) is unlikely at this temperature.[106]

Activation of carbonyl compounds (aldehydes, ketones, esters) with (PNN)Ru complex **98** was later studied in detail by Sanford et al. Benzaldehyde reacted at low temperature to initially give a P-arm adduct observed at low temperature, similar to complex **119 a**.[107] However, upon warming up to room temperature, the aldehyde migrated to the N-arm to generate adduct **120 a** (as a mixture of diastereomers) (Scheme 58). Reactions with formate esters and ketones at room temperature led to the formation of N-arm adducts **121 a**, **121 b** and **122** (Scheme 58). The equilibrium constants were shown to be sensitive to both steric and electronic properties of carbonyl compounds.[107] Except for benzaldehyde, most of these reactions were reversible and **98** could be

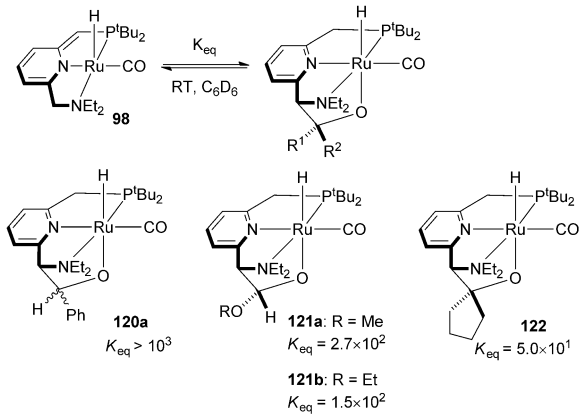

Scheme 58. C=O activation with **98**.

regenerated after removing volatiles under vacuum. No reaction was observed with *N*,*N*-dimethyl formamide and methyl acetate and only trace product formed with acetone.

3.1.4. CO_2 *Activation*

Reversible trapping of CO_2 with C–C bond formation at the ligand was observed by our group for the (PNP)Ru complex **110** (Scheme 59), and the reversibility of CO_2

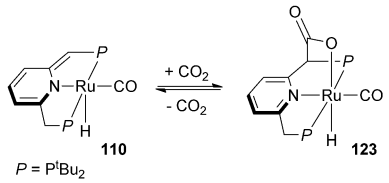

Scheme 59. CO_2 activation by the Ru complex **110**.

binding was confirmed by SST NMR studies.[108] DFT calculations revealed a low-barrier (8.1 kcal mol^{-1}) transition state for the concerted addition of CO_2 to **110**.[108]

The reactivity of the PNN complex **98** with CO_2 was studied by Sanford et al. and initial formation of a C–C bond at P-arm was observed to give **124** as a kinetic product in less than 5 min.[109] However, after reacting overnight at room temperature or heating at 70 °C, complex **125** was obtained as a thermodynamic product (Scheme 60). Conversion to **125** was irreversible at room temperature, but further studies showed that the reactivity at the N-arm becomes reversible at high temperatures, upon heating to 120 °C in anisol for several hours. Complex **98** catalyzes CO_2 hydrogenation to formate

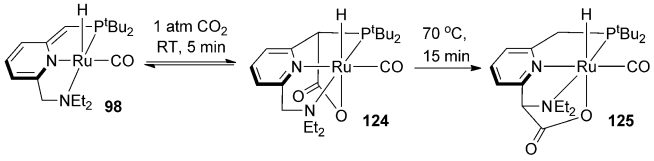

Scheme 60. CO_2 activation by **98**.

salts in the presence of K_2CO_3 or other bases. The proposed catalytic cycle involves heterolytic H_2 activation by **98**, CO_2 insertion into Ru dihydride **100**, and base-promoted formate release.

Although complex **125** is also catalytically active in CO_2 hydrogenation, this reactivity could be due to reversible CO_2 liberation, although an alternative catalytic cycle mediated by **125** was also considered.[109] However, even in this case, formate generation likely occurs through direct CO_2 insertion into Ru dihydride through a non-MLC pathway, and no evidence was obtained so far that adducts such as **124** or **125** can play a role as active intermediates in CO_2 hydrogenation.

The reversibility of CO_2 binding to the Re complex **108** to give adduct **126** at 90 °C was shown by our group by exchange experiment with labeled $^{13}CO_2$ (Scheme 61 a).[103] In addition,

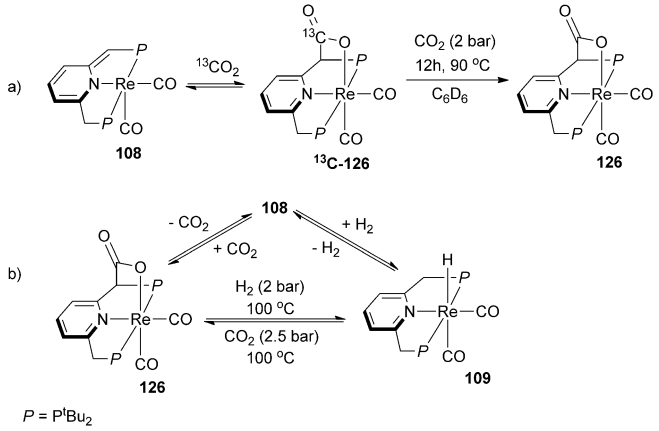

Scheme 61. a) Reversible CO_2 activation by (PNP)Re complexes.

reversible loss of CO_2 occurs upon heating **126** under H_2 to generate the Re hydride **109**, presumably via intermediate formation of **108** (Scheme 61 b).

The Re hydride **109** exhibits different types of reactivity depending on the reaction temperature: while the reaction at elevated temperature under CO_2 pressure leads to the release of H_2 and re-formation of **126** (Scheme 61 b), the reaction at room temperature produces the formate complex **127** by CO_2 insertion to Re–H bond (Scheme 62 a).[103]

Complex **127**, which was shown to liberate CO_2 and re-form **109** at elevated temperatures, was utilized as a catalyst

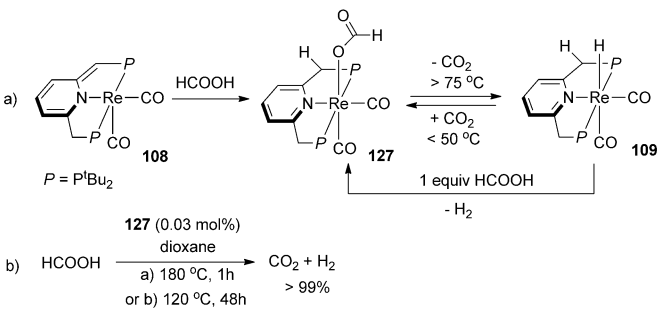

Scheme 62. a) Formation and reactivity of the formate complex **127**. b) Catalytic formic acid decomposition.

for selective formic acid decomposition to CO_2 and H_2 under base-free conditions at 120–180 °C (Scheme 62 b).[103]

3.1.4. Nitrile Activation

Cooperative activation of the CN triple bond of nitriles was first reported by our group, using the dearomatized Re complex **108** (Scheme 63).[110] Two types of nitrile adducts

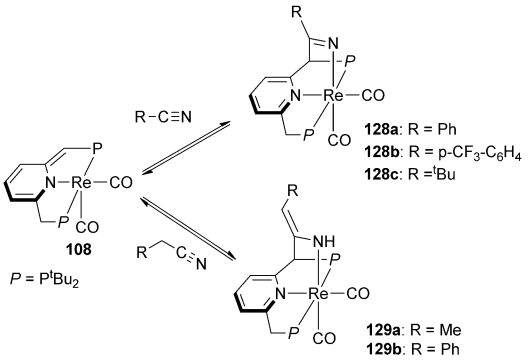

Scheme 63. Nitrile activation by dearomatized Re complex **108**.

were observed: ketimido complexes **128** formed when **108** reacted with nitriles lacking α-methylene groups, and enamido complexes **129** formed with aliphatic nitriles. In both cases, the reactions with nitriles were reversible as confirmed by exchange experiments. DFT studies suggest a stepwise mechanism via initial pre-coordination of a nitrile. The formation of enamido complexes could also proceed through initial formation of the ketimido complexes followed by their tautomerization to give enamido complexes **129**. The enamido complexes **129** readily undergo electrophilic attack at the enamide double bond. Based on these observations, a catalytic cycle was designed for facile conjugate addition of benzyl cyanide derivatives to α,β-unsaturated carbonyl compounds as electrophiles, with no added base, catalyzed by complexes **108** and **129 b** (Scheme 64).

Pidko et al. later reported nitrile activation by Ru pincer complexes with two NHC arms in the presence of a base. By contrast to Re complexes, the Ru adducts **130** are cationic complexes with a protonated ketimide nitrogen atom (Scheme 65).[111] Nitrile liberation takes place upon addition

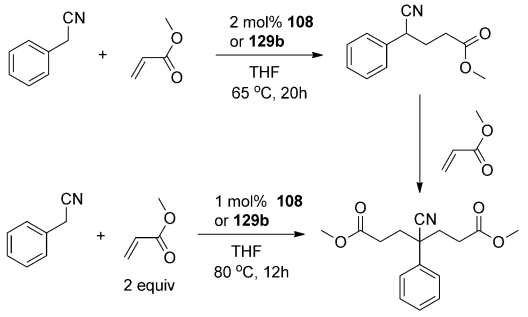

Scheme 64. Conjugate addition of nitriles catalyzed by **108** and **129 b**.

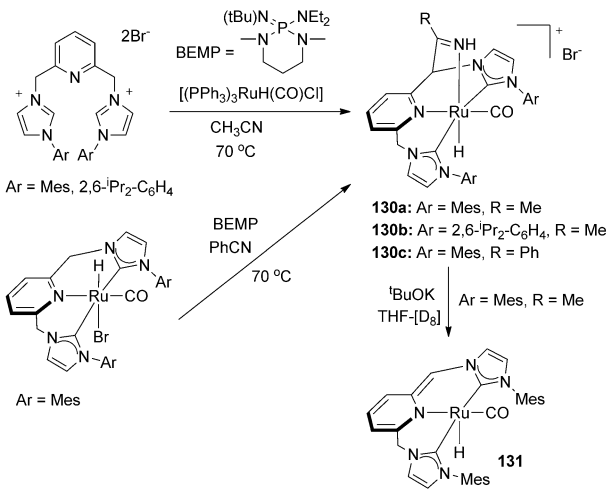

Scheme 65. Nitrile activation by bis(NHC)-based (CNC)Ru pincer complexes.

of a base to **130 a** to quantitatively generate dearomatized complex **131** which was characterized in situ.

The same dearomatized complex **131** was proposed as an intermediate in catalytic CO_2 hydrogenation to formate in the presence of a DBU base.[112] Interestingly, metal–ligand cooperation was proposed to be involved both in the formation of a catalytically active dihydride species **132** by cooperative H_2 activation, and in catalyst deactivation by formation of a stable CO_2 adduct **133** (Scheme 66). Increasing

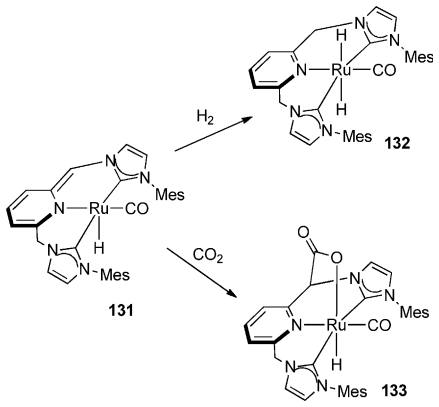

Scheme 66. H_2 and CO_2 activation by bis(NHC)-based (CNC)Ru pincer complexes.

the H_2:CO_2 ratio allowed to suppress the catalytic deactivation pathway; for example, stable catalytic performance was obtained at H_2:CO_2 39:1.[112]

The involvement of metal–ligand cooperative nitrile activation in catalytic reactions was also proposed recently by de Vries and Otten who demonstrated that the previously reported dearomatized complex **98**[90] catalyzed the oxa-Michael addition of alcohols to unsaturated nitriles in the absence of external base (Scheme 67).[113]

The catalytically active dieneamido complex **134** was isolated from the reaction of **98** with 3-pentenenitrile and 2-

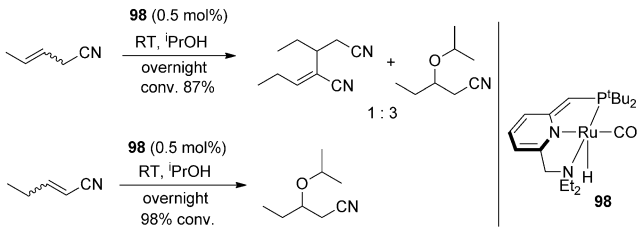

Scheme 67. Oxa-Michael addition to unsaturated nitriles catalyzed by **98**.

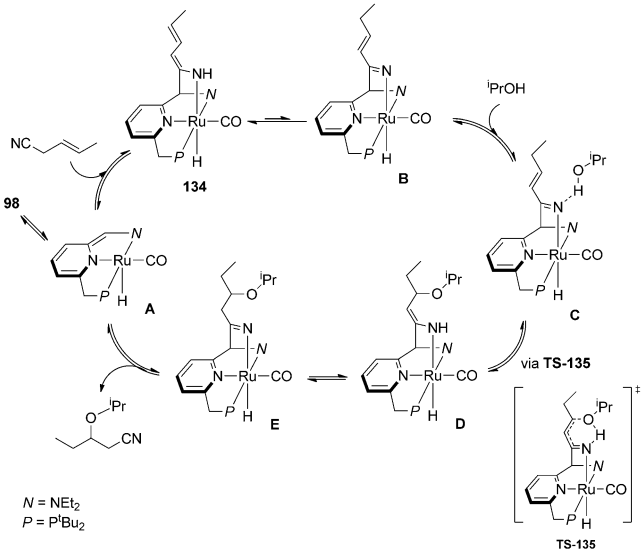

Scheme 68. Proposed mechanism of the oxa-Michael addition catalyzed by **98**.

pentenenitrile (complex **98** is also catalytically active in alkene double bond isomerization) (Scheme 68).[113] Notably, nitrile activation occurs at the N-arm, likely because of greater thermodynamic stability of the N-arm adduct compared to P-arm adduct, similar to CO_2 activation reactivity described above. The catalytic cycle for oxa-Michael addition to 3-pentenenitrile was proposed and studied by DFT that involves conversion of complex **134** to a less stable tautomer **B**, which activates alcohol through hydrogen bonding to a Brønsted-basic N-center. The oxa-Michael addition was then proposed to occur through a six-membered transition state **TS-135** in a concerted manner. The ketimido intermediates are proposed to play an important role as they increase nucleophilicity of the alcohol due to basicity of the ketimido nitrogen, so that the reaction occurs under mild conditions even in the absence of external base.[113]

3.1.5. B–H Bond Activation

By contrast to H–X activation where X is an oxygen or nitrogen atom (Scheme 44), activation of the B–H bond of catecholborane and pinacolborane leads to generation of a new B–C bond as shown by our group (Scheme 69).[114] A mixture of **136** and dihydride **118** are formed in a room

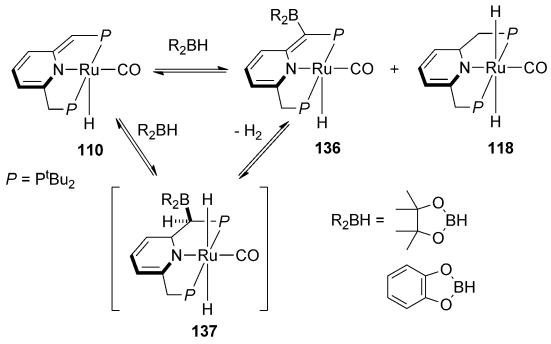

Scheme 69. B–H activation by **110**.

temperature reaction, while heating to 60 °C gives complete conversion to **136**. DFT studies suggest that the reaction might proceed via the unobserved intermediate **137** which then undergoes H_2 elimination to generate **136**.[114]

The dearomatized (PNN)Ru complex **98** reacted with the sterically demanding pinacolborane in a similar way to give the product of P-arm borylation, **138**, and the Ru dihydride **100** (Scheme 70).[114] In a reaction with the less bulky substrate

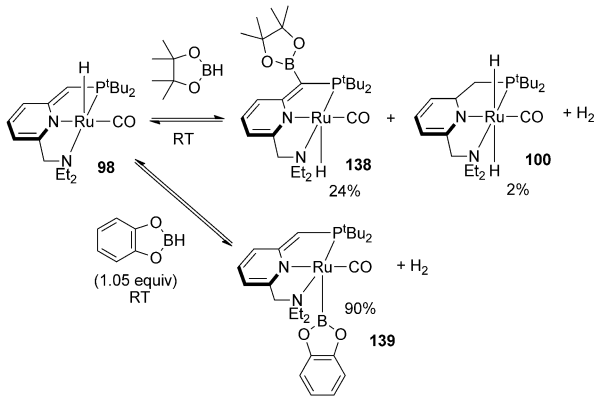

Scheme 70. B–H activation by **98**.

catecholborane, the major product of the reaction was assigned as the σ-boryl complex, which was characterized by NMR spectroscopy.

Attempted dehydrogenative coupling of borane catalyzed by **110** or **98** gave only low yields of diborane. Complex **98** catalyzed C–H borylation of benzene and toluene, however, the mechanism of this reaction was not studied.[114]

3.1.6. Reactivity with Dioxygen

Compared to MLC reactivity with HX and C–heteroatom multiple bond activation that does not involve change in the oxidation state of the metal, examples of reactivity under oxidative conditions remain relatively rare. Recently, our group reported the reactivity of the Ir^I phenyl complex that leads to the formation of Ir^{III} hydroxo phenyl dearomatized complex **141** as the final product (Scheme 71).[115] Both O-atoms of dioxygen were utilized in this reaction. The proposed

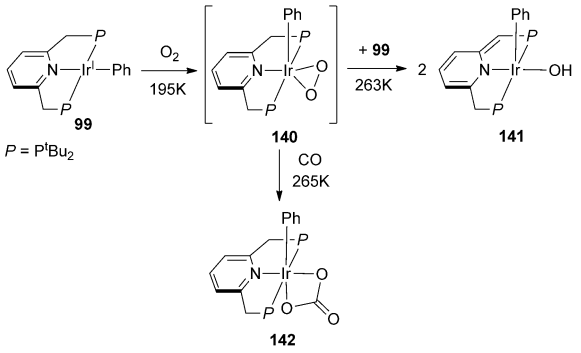

Scheme 71. O_2 activation by **90**.

mechanism involves formation of mononuclear Ir^{III} peroxo species and its subsequent conversion to **141**. The diamagnetic intermediate, observed by NMR spectroscopy, was formed in 50% yield, when the reaction with 0.5 equiv O_2 was performed at 195 K, which was tentatively assigned as a peroxo species **140**. Consistent with this assignment, addition of CO results in the formation of a carbonato complex **142**. Although the mechanism of formation of **141** remains unclear, an intermolecular reaction of **140** with another equivalent of **90** is likely operative leading to oxygen transfer, while the benzylic arm of the ligand acts as a source of a proton for the hydroxo group in aprotic solvents. This reactivity is a rare example of O_2 activation that is accompanied by dearomatization of a ligand backbone (see also Sections 3.5 and 3.6).

3.2. Aminopyridine-based Ligands

Representative examples of pincer ligands based on 2-aminopyridine and 2,6-diaminopyridine (structures **143**–**146**), as well as other diaminosubstituted N-heterocycles (**147**–**148**) are shown in Scheme 72.[116] By contrast to picoline- or lutidine-based ligands described above which bear a reactive CH_2 group, these ligands contain an NH spacer, which is generally more acidic than a CH_2 group. Deprotonation of the NH arm leads to dearomatization of the pyridine ring (Scheme 73), and the deprotonated species can participate

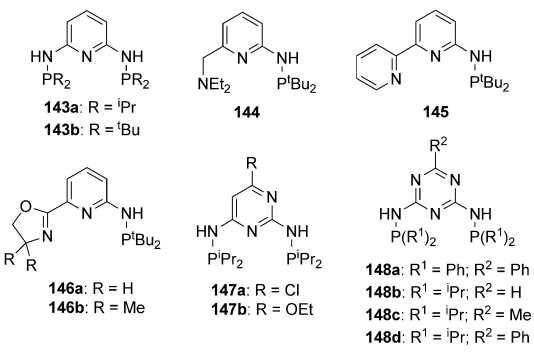

Scheme 72. Pincer ligands based on 2-aminopyridines (**143**–**146**), diamino-substituted pyrimidine (**147**) and triazine (**148**).

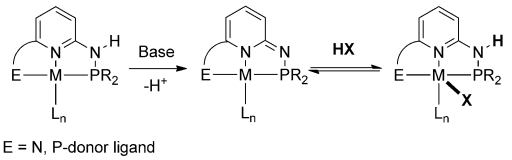

Scheme 73. Bond activation via MLC by complexes with 2-aminopyridine-based ligands.

in a range of bond activation processes through MLC that involves reversible aromatization/dearomatization of the 2-aminopyridine system.[116] The potential drawback of aminopyridine-based ligands is the hydrolysis of the aminophosphine bond that has been observed in some complexes.[117]

Heterolytic splitting of H_2 by Fe complexes was recently studied by Kirchner et al. who found that the Fe^{II} complex **149** reacts with Zn under H_2 atmosphere to give a hydride complex **151** (Scheme 74).[118] The analogous reaction with D_2

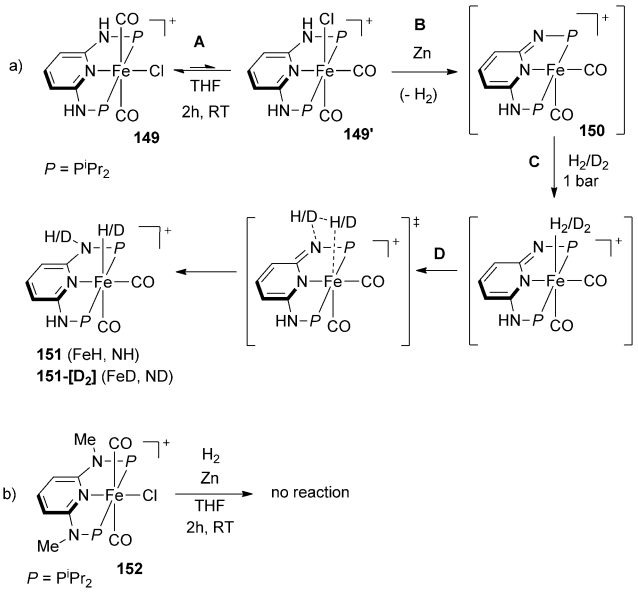

Scheme 74. Heterolytic H_2 activation by the Fe complex **149**.

affords **151-[D_2]**, in which D-labels are incorporated into Fe–D and the N–D group, according to ^2H NMR spectroscopic characterization. The authors noted that a slower reaction of **149** with D_2 compared to the reaction with H_2 could be due to a large KIE suggesting that H–H splitting is involved in the rate-limiting step. Notably, an NMe-substituted analog **152** did not react under analogous conditions (Scheme 7b). The proposed mechanism, supported by DFT calculations, involves partial isomerization of **149** to the *cis*-isomer **149′** (step **A**, Scheme 74a) followed by reduction of NH protons with Zn, resulting in the formation of H_2 and Zn^{2+} (step **B**). Zn^{2+} ions formed at this step abstract a Cl ligand to form a $16e^-$ complex **150**, which then coordinates (step **C**) and splits H_2 through MLC (step **D**). An accessible transition state was found by DFT for an intramolecular H_2 activation

($\Delta G^{TS} = 22.8$ kcal mol^{-1} for the rate-determining step **D**, Scheme 74a).[118]

The dicarbonyl complex **151** was not catalytically active in hydrogenation, while replacing one CO with a labile ligand L (L Br$^-$, MeCN, BH_4^-) led to a catalytically active species that hydrogenates ketones and aldehydes to alcohols under mild conditions.[119] Mechanistic studies of the catalytic reactivity suggest that the catalytic hydrogenation catalyzed by monocarbonyl complexes involves an inner-sphere mechanism without metal–ligand cooperation.

Dearomatization was observed upon reaction of Ru complexes [(L)RuH(CO)Cl] with a base to give the corresponding dearomatized species [(L*)RuH(CO)] (L = **143b**, **145**, **146a**, **146b**) (Scheme 75). Catalytic applications for both

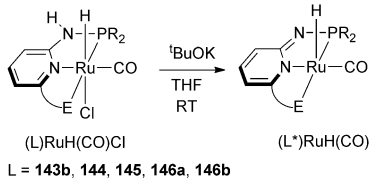

Scheme 75. Dearomatization of Ru complexes with aminopyridine-based pincer ligands via deprotonation.

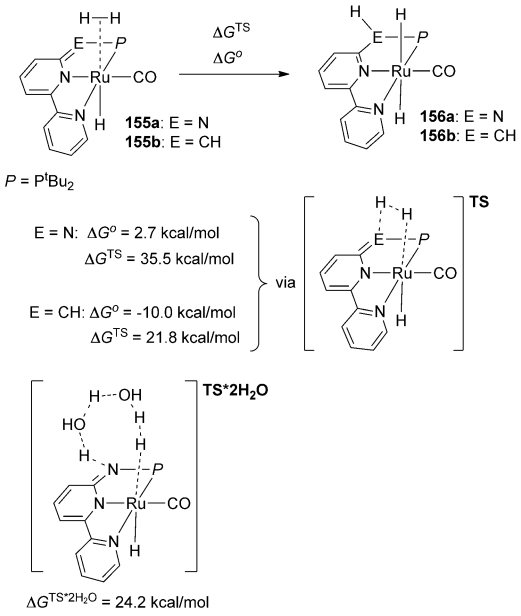

Scheme 77. Intramolecular H_2 activation to form Ru dihydride by direct splitting (**TS**) and water-assisted pathways (**TS-2H$_2$O** for complex **155a** and **TS-H$_2$O** for **155b**).

aromatized complexes [(L)RuH(CO)Cl] (L = **143b**, **145**, **146a**, **146b**) and the corresponding dearomatized complexes [(L*)RuH(CO)] were developed and covered recently in a review by Huang et al. and include 1) transfer hydrogenation, 2) alcohol dehydrogenation to esters, 3) dehydrogenation of amines to imines, 4) hydrogenation of esters to alcohols etc.[116]

The differences in the reactivity of aminopyridine-based versus picoline-based ligands were highlighted in a theoretical study of H_2 activation by dearomatized complexes **154a** and **154b**,[116,120,121] which can be generated by deprotonation of precursors **153a** and **153b**, respectively, with a strong base (Scheme 76). Both complexes **153a** and **153b** in combination

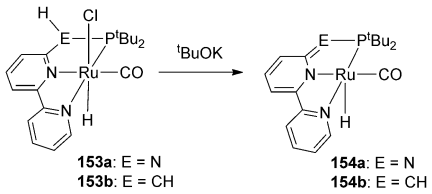

Scheme 76. Generation of dearomatized complexes **154a** and **154b**.

with catalytic amounts of base were reported to be efficient catalysts for ester hydrogenation.[87,116] The free energies and activation barriers were calculated for the intramolecular H_2 activation by complex **155a** or **155b**, which results from H_2 coordination to unsaturated species **154a** or **154b**, respectively.[120,121] The dihydride formation was found to be exergonic for CH-bridged complex **155b** by -10 kcal mol^{-1}, and endergonic for N-bridged complex **155a** by $+2.7$ kcal mol^{-1} (Scheme 77).[120,121] Interestingly, the activation barrier for direct H_2 splitting by complex **155a** was too high to be accessible under reaction conditions ($\Delta G^{TS} = 35.5$ kcal mol^{-1}), while the activation barrier for **155b** was considerably lower.[120,121] The authors suggested an alternative proton shuttle mechanism for H_2 activation by **155a** in which H-transfer is facilitated through bridging with two water molecules in a transition state **TS-2H$_2$O** (Scheme 77).[121]

Pyrrole synthesis by dehydrogenative coupling of β-aminoalcohols and secondary alcohols is catalyzed by the Ir complex **157**, as reported by Kemp et al., and also by the Ru complex **154b**, as reported by us (Scheme 78).[122] A DFT

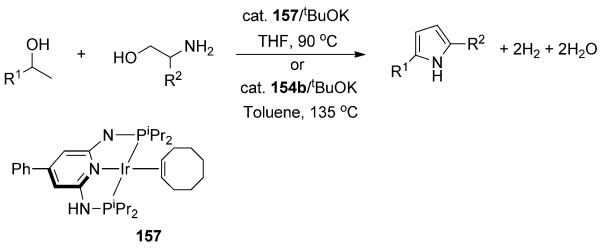

Scheme 78. Pyrrole synthesis from secondary alcohols and 2-amino-alcohols.

investigation of the reaction mechanisms by Wang et al. suggests that proton shuttle pathways for metal–ligand cooperation likely play an important role in the Ir-catalyzed reactions.[120]

3.3. Hydroxypyridine-based Ligands

The general mode of bond activation in metal complexes containing the 2-hydroxypyridine moiety can be represented by Scheme 79a. Although the OH/O^- group in these complexes is not coordinated to a metal, protonation/deprotonation and bond activation in these systems directly affect the 1st coordination sphere of the metal through significant contribution of a pyridonate resonance form, in which C–O bond has a significant double bond character (see below), and a formally negatively charged N-atom can act as a strong π-donor, by contrast to the pyridine nitrogen in a protonated 2-hydroxypyridine form (Scheme 79a). Interestingly, lactam–lactim tautomerism is also observed in free 2-hydroxypyridine, which exists in its 2-pyridone tautomeric form in the solid state, and the relative stability of the two tautomeric forms in solution depends on the solvent's properties (Scheme 79b).[123] This is in contrast to free 2-aminopyridine, in which the corresponding imine tautomer is not observed under typical conditions.

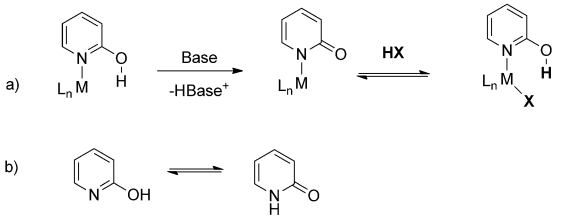

Scheme 79. a) Bond activation in hydroxypyridine complexes. b) 2-Hydroxypyridine–2-pyridone tautomerism.

The applications of the 2-hydroxypyridine ligand for hydrogen activation reactions were inspired by the discovery that this ligand motif is present at the active site of monoiron hydrogenase.[124,125] [Fe] hydrogenase is involved in one of the steps of methane generation from CO_2 and H_2 in methanogenic archae, and it catalyzes the reversible reduction of methenyltetrahydromethanopterin (methenyl-H_4MPT$^+$) with H_2 to form methylene-H_4MPT and a proton (Scheme 80).[124]

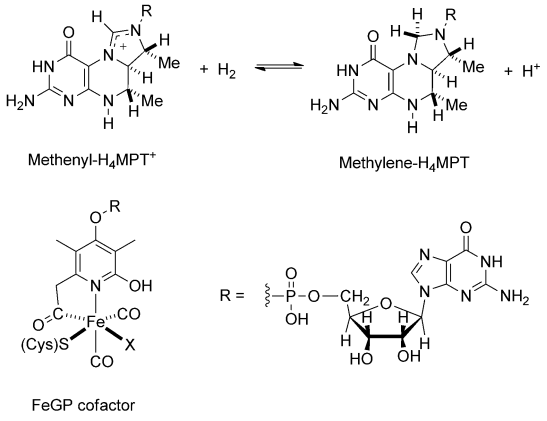

Scheme 80. [Fe] hydrogenase FeGP cofactor and catalytic reduction of methenyl-H_4MPT$^+$.

According to crystallographic studies by Shima et al., the enzyme contains a Fe-guanylylpyridinol cofactor (FeGP) in which a catalytically active Fe center is surrounded by guanylylpyridinol ligand, two carbonyls, a sulfur of cysteine, and an "unknown" ligand X (most likely water solvent).[126]

The nucleophilic O-atom of deprotonated 2-hydroxypyridine can be potentially involved in H_2 activation by FeGP by acting as an internal base. A theoretical study of H_2 activation pathways in a model system showed two energetically

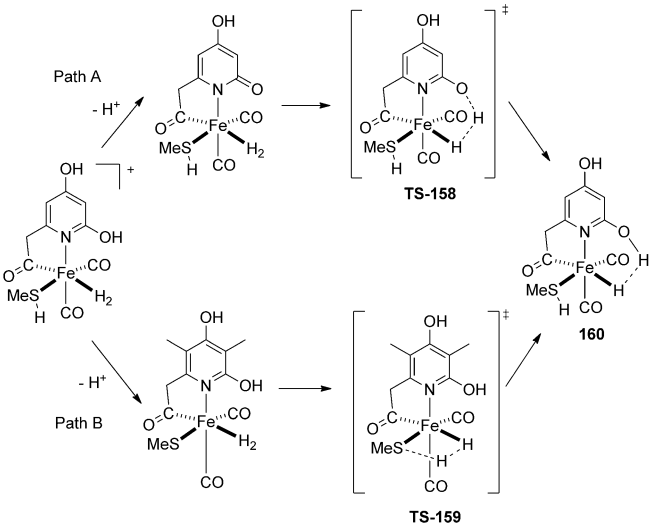

Scheme 81. Possible pathways of H_2 activation in [Fe] hydrogenase model system.

accessible mechanisms (Scheme 81): heterolytic H_2 activation assisted by the O-atom of pyridonate (path **A**, via **TS-158**) and S-assisted pathway (path **B**, via **TS-159**), in which the S-atom acts as an internal base. In addition, the OH group of 2-hydroxypyridine stabilizes product **160** by forming a dihydrogen FeH···HO bond (Scheme 81).[127]

The important role that the *ortho*-hydroxy group plays in [Fe] hydrogenase reactivity inspired numerous studies of the reactivity of transition metal complexes with 2-hydroxypyridine-based ligands in catalysis, especially in relevance to H_2 activation. Indeed, it was shown that the presence of an *ortho*-OH group in pyridine- or pyridimide-based ligands has a large effect on the catalytic activity in these systems.[125] A few selected examples will be discussed below to illustrate the role of the ligand and a solvent in such reactions in the context of MLC. For a more detailed discussion of the scope of such systems in energy-relevant catalysis, the reader can be referred to a recent review by Szymczak et al.[125]

Stoichiometric and catalytic hydrogen activation in Ir complexes containing the pyridonate ligand was studied by Rauchfuss et al. In particular, Ir complex **161** reacts with H_2 even at −30 °C to give unstable complex **162** which was characterized by NMR spectroscopy as the first observable hydride, along with binuclear species formed by 2-hydroxypyridine dissociation (Scheme 82). The species **162** can also be generated by the reaction of **161** with a transfer hydrogenation catalyst **163** (Scheme 82). This type of H_2 activation

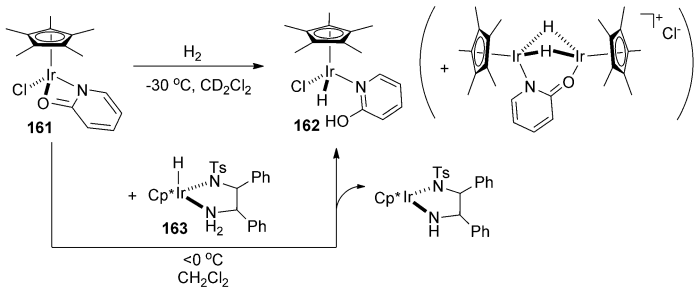

Scheme 82. H_2 activation by **161** and generation of **162**.

reactivity is likely involved in the acceptorless dehydrogenation of alcohols catalyzed by the monometallic complex **161**.[128] However, the lability of 2-hydroxypyridine may be a potential problem leading to catalyst decomposition and formation of catalytically inactive binuclear species in such systems.

Interestingly, heterolytic H_2 splitting was studied by Morris et al., using an Ir complex with S-coordinated 2-pyridylthiol ligand, in which H_2 activation occurs with participation of an uncoordinated pyridine N-atom, rather than S-atom of a coordinated thiol, as confirmed by H/D exchange experiments.[129]

Chelating bipyridyl or bipyrimidyl systems with *ortho*-OH groups can afford more stable and catalytically active systems for H_2 activation reactions. Efficient reversible hydrogenation of CO_2 to formate is catalyzed by the diiridium complex **164a,b** bearing a tetrahydroxybispyrimidine ligand (Scheme 83 and Table 1).[130] The catalytic activity can be turned on and off by varying the pH of the solution. Complex **164a** undergoes facile exchange of Cl^- ligands with H_2O in aqueous solutions to give **164b**, and the equilibria between protonated and deprotonated forms depend on the pH: a fully protonated form **164b** is predominant at pH < 2, while a neutral deprotonated species **164b′** is the predominant form at pH > 5 (Scheme 84). Notably, the catalyst **164b** containing hydroxy groups in *ortho*-positions showed superior catalytic activity in CO_2 hydrogenation to formic acid salts compared to its analogs lacking hydroxy groups (**165a**,**b**) and the monometallic complex with a *para*-substituted ligand (**166**) (Table 1). This effect was explained by the ability of an *ortho*-O^- to act as internal base facilitating H_2 heterolysis, as well as by electronic activation of the complex **164b′** supported by strongly π-donating deprotonated ligand. Upon lowering the pH, the same catalyst also catalyzes formic acid

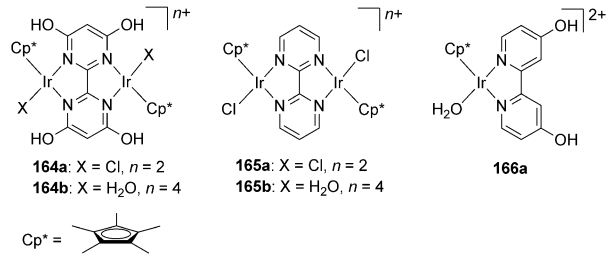

Scheme 83. Catalysts for reversible CO_2 hydrogenation.

Table 1: CO_2 hydrogenation to formate salt catalyzed by Ir complexes with bipyrimidyl- and bipyridyl-based ligands.

Catalyst[a]	TOF initial [h^{-1}]	TON[b]
164b′[a]	64	7200
165b[a]	0	0
166a[a]	7	92
164b′[b]	15 700	153 000

[a] $p = 0.1$ MPa (1:1 H_2/CO_2), 25 °C, 1 M $NaHCO_3$. [b] $p = 4$ MPa, 50 °C, 2 M $KHCO_3$.

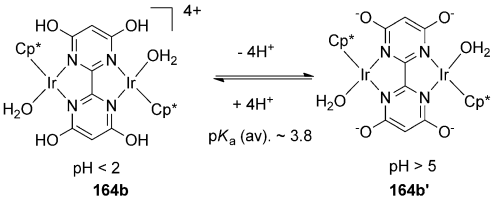

Scheme 84. pH-Dependent equilibria in solution of **164b**.

decomposition to CO_2 and H_2, thus enabling reversible H_2 storage using formic acid.[130]

Fujita, Himeda and co-workers also studied the positional effect of hydroxy groups on the reactivity of Ir complexes for a series of 6,6′-, 5,5′-, 4,4′-, and 3,3′-dihydroxy-substituted bipyridyl complexes (Scheme 85).[131,132] The protonated forms **166a** and **166b** and the corresponding doubly deprotonated forms **166a′** and **166b′** were characterized by X-ray crystallography.[131] While C–O bonds in the protonated forms **166a** and **166b** are within a normal range for a C–O single bond (1.329 Å for **166a**; 1.319 and 1.321 Å for **166b**), they shorten significantly upon deprotonation (1.295 Å for **166a′** and 1.272 Å for **166b′**). This is consistent with a C=O double bond character in these deprotonated complexes and signifi-

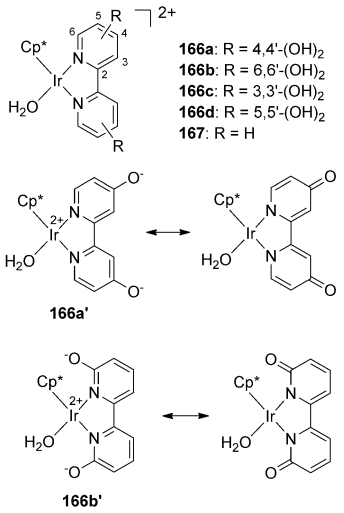

Scheme 85. Catalysts tested for CO_2 hydrogenation at pH 8.5.

cant contribution of a pyridonate resonance structure with a negative charge localized at the N-atom (Scheme 85). Complexes **166a** and **166b** exhibit much higher catalytic activity for CO_2 hydrogenation at pH 8.5 compared to **166c,d** and **167**, showing that the electronic effects and resonance stabilization of π-donating pyridonate ligand play an important role in the catalytic reactivity. At the same time, catalyst **166b** was more active than **166a**, due to the presence of *ortho*-OH groups that can act as internal bases in metal–ligand cooperative H_2 activation. Interestingly, KIE investigations revealed that water is involved in the rate-determining H_2 heterolysis in this system. Accordingly, a low activation barrier was found by DFT for a proton-relay pathway (via **TS-168**, Scheme 86), which was 3.42 kcal mol^{-1} lower than the

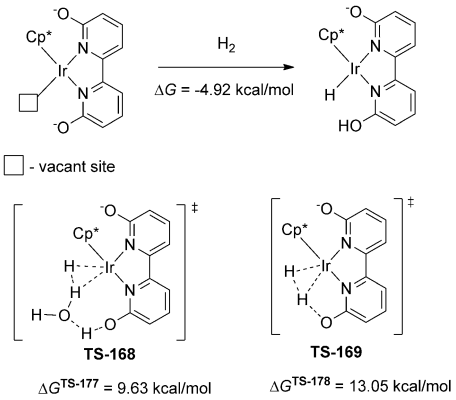

Scheme 86. Proposed pathways for H_2 activation by 2,2′-dihydroxybipyridyl Ir complex.

activation barrier of H_2 heterolysis directly with *ortho*-O^- acting as a pendant base (**TS-169**, Scheme 86).[132]

The mechanism of acceptorless alcohol dehydrogenation catalyzed by **166b′** was investigated by DFT, and the outer-sphere, concerted pathway for alcohol dehydrogenation was found to be more favorable than an inner-sphere, β-hydride elimination pathway.[133]

To summarize, the presence of an *ortho*-OH group in pyridine-based ligands leads to significant alternation of the reactivity of the derived metal complexes. First, deprotonation of an *ortho*-OH group changes the electronic properties of the ligand and generates strongly π-donating pyridonate systems. Second, the close proximity of an *ortho*-O^- acting as a pendant base in deprotonated species enables ligand-assisted pathways for heterolytic H_2 activation, however, proton shuttle mechanisms assisted by water or alcohol solvents are likely to play an important role in these systems. In addition, the *ortho*-OH group is capable of forming hydrogen bonds with the ligands in the first coordination sphere of the metal (i.e. hydride, halides) thus affecting their stability and reactivity.

3.4. Acridine-based Pincer Ligands

This section will focus on the acridine-based PNP pincer ligands, first developed in our group, that demonstrate non-innocent behavior in stoichiometric reactions with H_2, alcohols and amines. By sharp contrast to the previously described examples of MLC reactivity where a ligand acts as a Lewis-basic site, the acridine backbone acts as an acceptor of a hydride leading to the reduction of an acridine ring.

Ru complexes with an acridine-based PNP ligand (AcrPNP^{iPr}) show an unusual type of a long-range MLC in H_2 activation that involves participation of the C9 atom of the central acridine ring. Complex **170** reacts with H_2 in the presence of KOH in refluxing toluene to give dearomatized complex **171** with the reduced central acridine ring (Scheme 87).[134] The analogous reaction with D_2 leads to

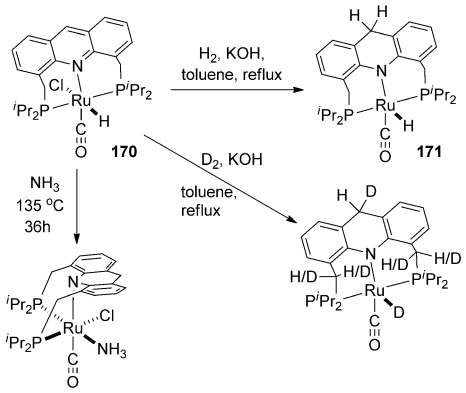

Scheme 87. Activation of H_2 and D_2 by **170**.

incorporation of one D-label in the central acridine ring (Scheme 87) and the formation of Ru–D. Partial H/D exchange was also observed in the CH_2 arms and ^{i}Pr groups. Hydride transfer from Ru to acridine was also induced by the reaction of **170** with NH_3 to generate a complex where the reduced flexible AcrPNP^{iPr} ligand coordinates to Ru in an unusual *fac*-fashion (Scheme 87).[134]

Based on DFT analysis of a model system (with P^{i}Pr$_2$ replaced by PMe_2), a mechanism was suggested for the reaction with H_2, which involves initial formation of Ru^0 monocarbonyl by Ru–H deprotonation by a strong base, followed by oxidative addition of H_2 to generate the Ru^{II} dihydride **II** (Scheme 88). One of the Ru hydrides is then transferred directly to the C9 carbon of central acridine ring (Scheme 88).[134]

Complex **170** catalyzes the amination of primary alcohols with ammonia to selectively form primary amines, as well as the reverse reaction, deamination of primary amines by water to form alcohols.[135] Dehydrogenation of alcohols catalyzed by **170** under neutral conditions generates acetals, while esters are formed in the presence of catalytic base.[136] However, the role of long-range MLC in these reactions was not studied.

Recently, Hofmann et al. synthesized an analogous complex **172** with PCy$_2$-substituted AcrPNP^{Cy} ligand which also shows catalytic activity in amination of alcohols with ammo-

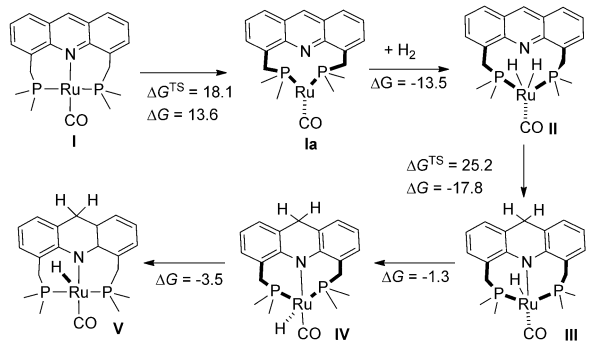

Scheme 88. Proposed mechanism of dearomatization of **170** in a reaction with H_2. Calculated free energies are given in kcal mol^{-1}.

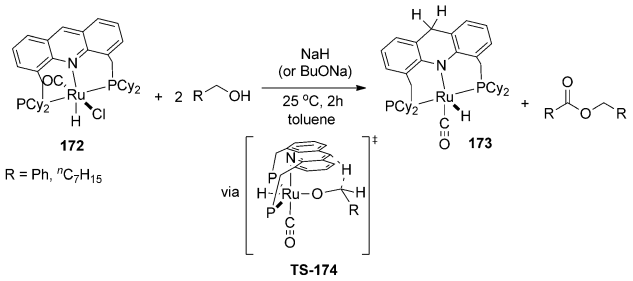

Scheme 89. Formation of **173** by alcohol dehydrogenation by **172**.

nia.[137] The stoichiometric reaction of **172** with an alcohol in the presence of a base leads to the reduction of the central acridine ring and generation of **173** (Scheme 89). DFT analysis of the reaction with MeOH as a model substrate showed that a plausible mechanism involves formation of an alkoxide complex followed by hydride transfer from the CH_2 group of the alcohol to the C9 position of the central acridine ring (Scheme 89).[137]

Our group has recently found that complex **170** in the presence of a catalytic amount of NaOH catalyzes unusual lactam formation from cyclic amines using water as the only reagent (Scheme 90).[138] This reaction is accompanied by

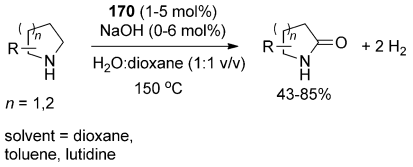

Scheme 90. Lactam formation from cyclic amines and water catalyzed by **170**/NaOH.

liberation of 2 equiv of H_2 gas and it does not require any oxidants apart from water. This represents a highly atom-economical way of lactam synthesis that avoids the use of strong stoichiometric oxidants that are typically required for such reaction, for example, PhIO, RuO_2/$NaIO_4$, peroxides, or O_2/Au catalyst.[139]

Further mechanistic investigation into this unprecedented reaction showed that the catalytically competent species is the

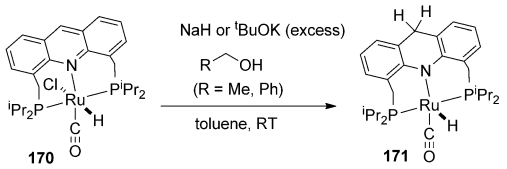

Scheme 91. Synthesis of **171** by reaction of **170** with alcohols.

dearomatized complex **171**, which can be synthesized independently by a reaction of **170** with benzyl alcohol or ethanol in the presence of NaH or ^{t}BuOK (Scheme 91).[140] Notably, complex **171** catalyzed 2-pyrrolidone formation from pyrrolidine even in the absence of a base in neutral H_2O/dioxane solution at 135 °C.

The reduction of the central acridine ring after reaction with alcohols is unambiguously confirmed by the X-ray structure of **171** (Figure 2a).[140] The short Ru–N distance

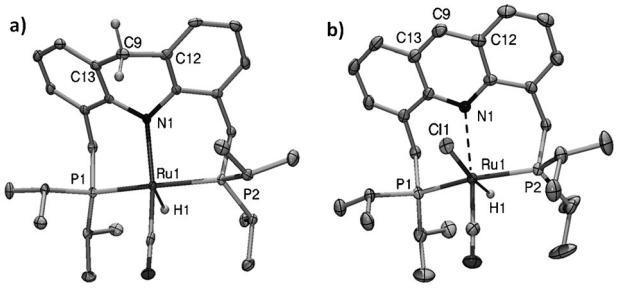

Figure 2. ORTEP representations of a) **171** and b) **170** (50% probability ellipsoids) and selected bond distances [Å] and angles [°]. a) Complex **171**: Ru1–N1 2.124, C9–C12 1.502, C9–C13 1.502; C12-C9-C13 108.1. b) Complex **170**: Ru1–N1 2.479, C9–C12 1.381, C9–C13 1.381; C12-C9-C13 120.6.

(2.124 Å) suggests that there is a strong interaction between the Ru center and a negatively charged N-atom. By comparison, the Ru–N distance in the parent complex **170** is (2.479 Å), suggesting only weak interaction with a remote aromatized acridine N-atom (Figure 2b).[136]

Possible mechanisms for the formation of **171** in the presence of alcohols, or under lactam formation conditions were investigated by DFT.[140] Under lactam formation conditions, β-hydride transfer could occur from the coordinated deprotonated pyrrolidine with a low calculated activation barrier via **TS-175** (Scheme 92).[140]

A DFT study of the possible mechanisms of pyrrolidone formation showed that the conformational flexibility of the reduced AcrPNP^{iPr} and its ability to coordinate both in *mer*- and *fac*-fashion plays an important role both in β-hydride elimination and in H_2 liberation steps.[140] At the same time, the central aromatic ring remains dearomatized throughout the course of the catalytic cycle. An alternative pathway via aromatization/dearomatization of the acridine ring and formation of a Ru^0 intermediate is characterized by high calculated activation barriers and is unlikely to be operative.

Overall, Ru complexes with acridine-based pincer ligands show unusual reactivity in H_2, alcohol and amine activation

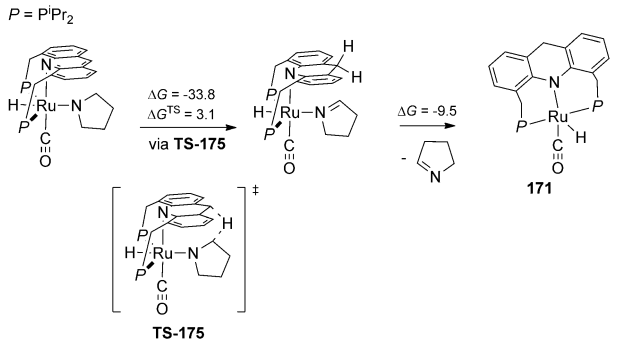

Scheme 92. Formation of **180** in the presence of pyrrolidine under catalytic conditions. Calculated ΔG and ΔG^{TS} are in kcal mol^{-1}.

leading to a hydride transfer to the acridine ring. This generates a conformationally flexible, dearomatized system with a reduced central ring that can coordinate in both *mer*- and *fac*-fashion, the latter likely playing an important role in catalytic reactions. Notably, the hydride transfer from alcohols to the acridine ring leading to their dehydrogenation is reminiscent of alcohol dehydrogenase reactivity that leads to NAD^+ reduction to NADH.[141] At the same time, it is unlikely that the acridine ring aromatization/dearomatization occurs reversibly under the catalytic conditions studied so far for these systems.

3.5. MLC by Aromatization/Dearomatization in Other N-Heterocycles: Phenanthroline, Quinoline, Pyrrole, Diazafluorene

The concept of MLC by aromatization/dearomatization can also be extended to complexes of other N-heterocyclic ligands. Some of these ligands demonstrate reversible aromatization/dearomatization of the heterocyclic system, which enables some catalytic transformations.

For example, our group reported that the Ru complex **176**, supported by a tetradentate phenanthroline-based ligand exhibits stepwise MLC reactivity in double H_2 activation through a reversible aromatization/deconjugation sequence (Scheme 93).[142] First, the dearomatized complex **177** is generated by benzylic arm deprotonation of **176** with

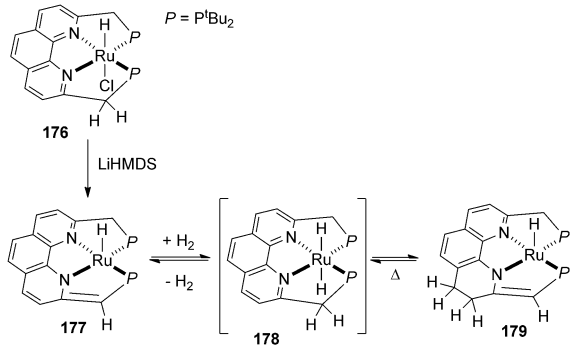

Scheme 93. Reversible stepwise H_2 activation by **177**.

1 equiv of $LiN(SiMe_3)_2$. Complex **177** then reacts with 1 equiv of H_2 to generate an unstable rearomatized dihydride **178**, which was detected by NMR spectroscopy and synthesized independently. Further reaction with H_2 leads to hydrogenation of one of the double bonds of the phenanthroline backbone to give **179** with a partially deconjugated phenanthroline fragment. Importantly, these transformations are reversible and heating of **179** in refluxing toluene under argon regenerates **177**. The formation of **179** was also observed when **177** reacted with alcohols via intermediate formation of **178**.

This reactivity was employed in catalytic alcohol dehydrogenative coupling to form esters catalyzed by complexes **177** or **179**, and coupling of alcohols with amines to give imines catalyzed by **177**. Although complex **179** is probably not directly involved in the proposed catalytic cycle, its ability to reversibly liberate H_2 enables catalytic reactivity in acceptorless alcohol dehydrogenation.[142]

Another type of long-range cooperativity in heterolytic H_2 activation was reported by Song et al. for a Ru complex supported by 4,5-diazafluorenide ligand.[143] Complex **180** heterolytically splits H_2, leading to dearomatization of the central ring by proton migration to the 9-position and formation of a new Ru–H bond (Scheme 94). The reaction

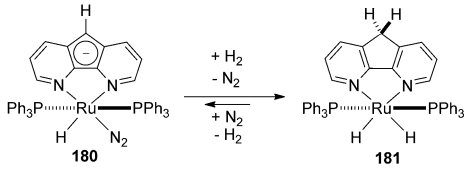

Scheme 94. H_2 activation by Ru 4,5-diazafluorenide complex.

with D_2 leads to incorporation of D into the 9-position of the ligand, formation of Ru–D as well as D-incorporation into the *ortho*-CH of PPh_3 ligand due to concomitant reversible cyclometalation. Exposure of a partially deuterated **181** to H_2 leads to protium incorporation in the 9-position, Ru center and *ortho*-H of PPh_3 indicating that the reaction is reversible.

Quinoline can also be employed for the design of pincer ligands capable of MLC by benzylic arm deprotonation, similar to systems described in Section 3.1. For example, Vigalok et al. reported that the palladium complex **182** with a PNF-type pincer ligand is a catalyst for Sonogashira-type cross-coupling that operates through metal–ligand cooperative alkyne activation (Scheme 95).[144] This was confirmed by the generation of the dearomatized complex **183** in the presence of a base and its reaction with a D-labeled phenylacetylene in the presence of aryl iodide that leads to D-label incorporation into the ligand benzylic arm and the formation of a C–C coupled product (Scheme 95). Aryl iodide was used in this process to trap the Pd^0 species resulting from C–C reductive elimination from Pd^{II}. Other examples of E–H bond functionalization (E = O, N, S) using quinoline-based pincer ligands were also reported by Vigalok et al..[145]

Another example of bond activation by dearomatization under oxidative conditions was reported by Goldberg et al.

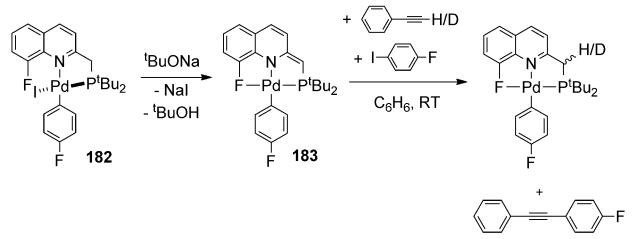

Scheme 95. C–C coupling mediated by **182**.

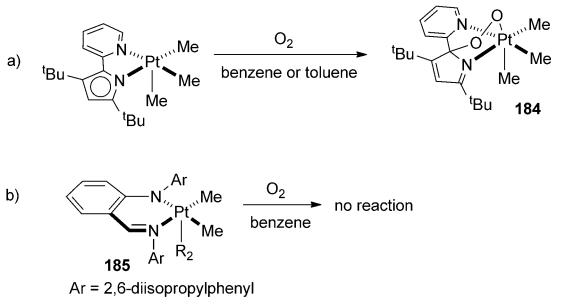

Scheme 96. Reactivity of five-coordinate Pt^{IV} complexes with O_2.

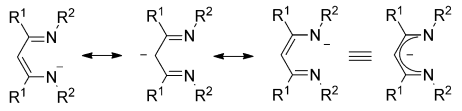

Scheme 97. Resonance forms of nacnac$^-$ ligand.

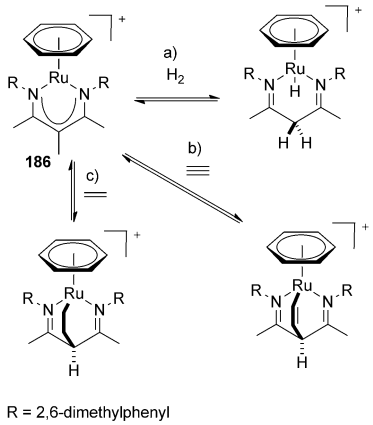

Scheme 98. Reactivity of **186** in heterolytic H_2 splitting and cycloaddition reactions.

and involves O_2 reaction with a five-coordinate Pt^{IV} complex supported by an anionic pyridyl-pyrrolide ligand to afford a peroxo species **184** (Scheme 96a).[146] The Pt center does not change its formal oxidation state and acts as an electrophilic site in this reaction, while the ligand undergoes dearomatization with the formation of a new C(sp^3)–O bond at the Lewis-basic carbon atom. The presence of the electrophilic Pt^{IV} center as well as the nucleophilic carbon center are both important for promoting such reactivity. For example, the five-coordinate complex **185** with an anionic imino-arylamide ligand did not react with O_2, as such reaction would require unfavorable dearomatization of a stable six-membered arene ring (Scheme 96b). The discussion of cooperative O_2 activation in Pt^{IV} complexes leading to C–O bond formation will continue in Section 3.6.

3.6. 1,3-Diketiminate Ligands

MLC reactivity through conjugation/deconjugation can also be observed in complexes with acyclic ligands such as anionic bidentate 1,3-diketiminates (referred to as "nacnac$^-$" ligands). The combination of strong electron-donating ability and steric bulkiness of the nacnac ligands enable preparation of well defined coordinatively unsaturated metal complexes and their reactivity studies. The MLC-type reactivity in these systems is usually due to partial negative charge delocalization at the central carbon atom as can be seen from resonance structures of the nacnac$^-$ ligand (Scheme 97).

For example, the Ru arene complex **186** was shown to heterolytically split H_2 in a reversible fashion that breaks the π-delocalized system of 1,3-diketiminate and leads to sp^2-to-sp^3 rehybridization of the central β-carbon supported by X-ray crystallographic characterization of the product (Scheme 98a).[147] Reversible cycloaddition reactivity was observed in the reaction with ethylene and acetylene (Scheme 98b,c).[147] Complex **186** is catalytically active in styrene hydrogenation at 40 bar H_2, however, it is not clear if MLC plays a role in the catalytic reaction.

The reactivity of CO_2 with a cationic Sc methyl complex **187** reported by Piers et al. results in CO_2 insertion into Sc–Me to form acetates followed by further sequential CO_2 reaction that leads to the formation of a new C–C bond at the α-carbon of the nacnac ligand (Scheme 99).[148] This parallels the reactivity of dearomatized lutidine-based pincer complexes of Ru and Re described in Section 3.1. However, the products of CO_2 reaction with [(nacnac)Sc] complex are unstable and eventually decompose by ligand displacement, preventing their potential catalytic applications.[148]

The reactivity of coordinatively unsaturated [(nacnac)-Pt^{IV}] complexes with O_2 was studied by Goldberg et al. The reaction of complex **188** with O_2 affords a peroxo species **189**, which then decomposes with O–O bond splitting leading to oxygenation of a C–H bond at the ligand backbone (Scheme 100a).[146,149] To stabilize the peroxo intermediate, a Me-substituted nacnac ligand was used to give a more stable peroxo complex **190** (Scheme 100b).[146] In both cases, O_2 insertion leads to sp^2-to-sp^3 rehybridization of the central carbon atom at the nacnac ligand, similar to the reaction shown in Scheme 100a. Complex **190** participates in the stoichiometric O-atom transfer reactions with sulfides, PPh_3 and CO that leads to the formation of **191** bearing a monooxygenated nacnac ligand (Scheme 100c).[146]

Overall, although MLC-reactivity is known for coordinatively unsaturated complexes, there is currently no evidence that such reactivity plays a role in catalytic reactions. The reactivity of the nacnac ligand (e.g. lability or irreversible

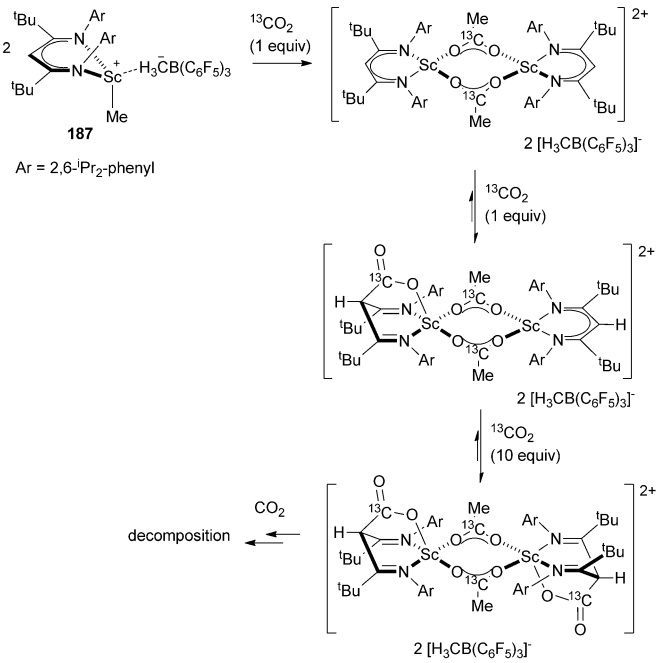

Scheme 99. CO_2 activation by [(nacnac)Sc] cationic complex.

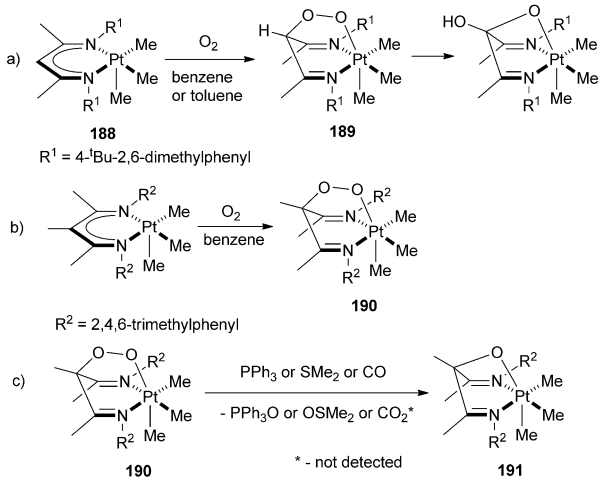

Scheme 100. Reactivity of five-coordinated [(nacnac)Pt^{IV}] complexes with O_2.

oxygenation) is an important drawback for potential catalytic application of the derived complexes in catalysis.

3.7. Imidazole and Pyridine-based NHCs and Pyrazole-based Ligands

The reactivity of imidazole- and pyridine-based NHC ligands containing a NH group and pyrazole-based ligands will be briefly discussed in this section to illustrate another mode of MLC and to draw parallels with the reactivity of other systems described above. The detailed reactivity of these ligands and their applications in catalysis were recently

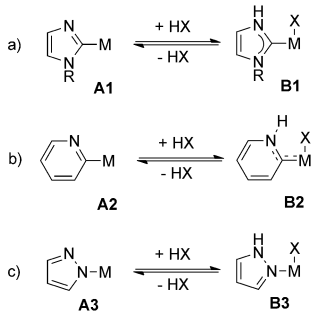

Scheme 101. General representation of bond activation in a) NH-protic imidazole-based NHC complexes, b) pyridine-based NHC complexes, and c) pyrazole complexes.

covered in a comprehensive review by Kuwata and Ikariya.[150]

The common motifs in these three ligand types is the presence of an acidic NH group in the β-position to the metal (Scheme 101). Metal–ligand cooperation in H_2 and HX activation reactions involves protonation/deprotonation of a β-NH group thus resembling MLC in amide/amine complexes and 2-aminopyridine-based pincer complexes described in Sections 2.1 and 3.1, respectively. Although the β-NH group remains non-coordinated to the metal center, its protonation/deprotonation affects the 1st coordination sphere of the metal due to conjugation via the π-electron system (Scheme 101).

For example, the reversible protonation/deprotonation shown in Scheme 102 involves interconversion between imidazol-2-yl complex **192** and an NH-protic NHC complex

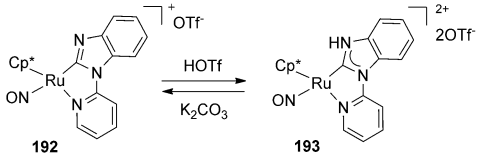

Scheme 102. Reversible protonation of imidazol-2-yl Ru complex to generate the NHC complex **193**.

193 with different properties of a Ru–C bond.[151] The ^{13}C NMR spectrum of **193** exhibits a Ru–C signal at δ_C 182.2, absent from the spectrum of **192** and consistent with the formation of a NHC species. In turn, X-ray structures of **192** and **193** are also consistent with their assignment as imidazol-2-yl and NHC complexes, respectively. This reactivity was proposed to play a role in catalytic dehydrative coupling of allyl alcohol with *N*-(2-pyridyl)benzimidazole.[151]

Reaction of the Ir imidazol-2-yl complex **194** with H_2 in the presence of $KB(C_6F_5)_4$ as a chloride-abstracting agent leads to H_2 heterolysis to give the Ir hydride **195** with a protic NHC ligand (Scheme 103). Activation of acetylene by **194** affords an Ir acetylide complex with a protic NHC ligand.

An interesting example of MLC was observed by Carmona et al. in the pyridine-derived NHC complexes (2-

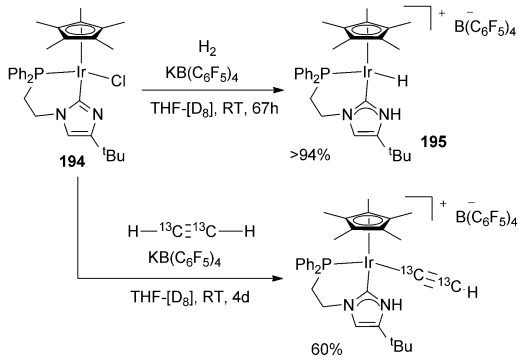

Scheme 103. Activation of H_2 and alkynes by imidazol-2-yl Ir complex.

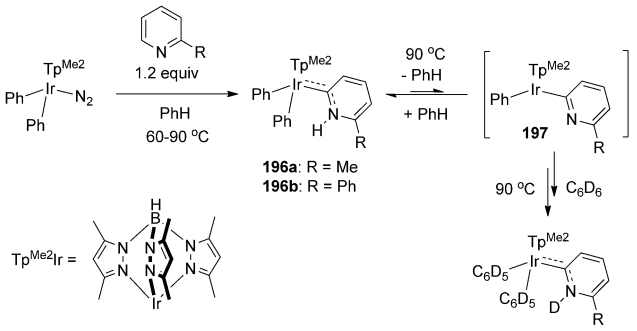

Scheme 104. Synthesis of **196** and its reactivity in benzene activation.

pyridylidenes) of Ir^{III}, **196a,b** (Scheme 104).[152–154] The coordination of the pyridylidene ligand can be seen as resulting from tautomerization of the 2-substituted pyridine induced by the metal center. For free pyridines, three possible tautomers can be considered, resulting from the proton shift to an N-atom (Scheme 105). Although tautomer **II** has a much higher energy compared to the aromatic structure **I**, it can be stabilized by contribution of a carbene resonance structure **IIb** and through coordination to a metal center.[152] Complex **196** synthesized by 2-substituted pyridine activation by Ir diphenyl precursor activates a C–H/C–D bond of benzene/C_6D_6 as evident from the exchange reaction with C_6D_6, which could occur via an unsaturated 2-pyridyl complex **197** as a transient intermediate (Scheme 104).[152]

Similarly, heterolytic splitting of H_2 likely involves the intermediate **197** formed by elimination of benzene from **196**

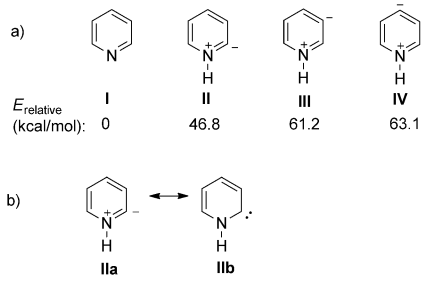

Scheme 105. a) Tautomers of pyridine and their relative calculated energies. b) Resonance structures of **II**.

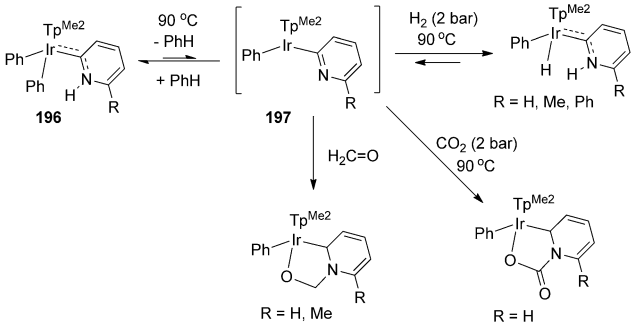

Scheme 106. Activation of H_2, CO_2 and formaldehyde by **196**.

(Scheme 106).[153] Activation of the C=O bonds in CO_2 and formaldehyde was also proposed to occur through initial formation of **197** followed by coordination of aldehyde or CO_2 to an unsaturated Ir center and then a nucleophilic attack of the pyridyl nitrogen onto the coordinated C=O group (Scheme 106).[153]

A pronounced effect of the presence of β-NH groups on catalytic activity was observed in Fe-catalyzed hydrazine disproportionation to form NH_3 and N_2 (Scheme 107).[155] The

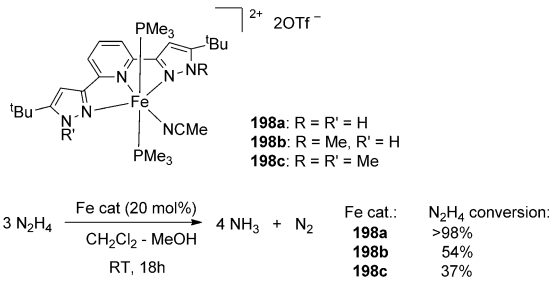

Scheme 107. Fe-catalyzed hydrazine disproportionation.

catalyst, supported by a NNN pincer ligand containing two NH groups in both pyrazole arms, showed the highest activity, while the complexes with one or both NH groups replaced by NMe were less active. The proposed mechanism involves bidirectional proton-coupled electron transfer (PCET) between the Fe complex and the hydrazine ligand, facilitated by participation of NH groups at the pyrazoles (Scheme 108). In addition, NH groups at the pyrazole can participate in stabilization of diazene intermediate through multiple hydrogen bonds.

3.8. Carbocyclic Ligands

In this section, MLC reactivity will be discussed for carbocycle-based ligands in which it is based on conjugation/deconjugation in a carbon-only fragment. Examples of such ligands are less abundant compared to N-heterocyclic systems and the mechanisms of bond activation are generally less studied.

The reactivity of complex **53**, supported by an indene-based ligand that can potentially form a conjugated indenide

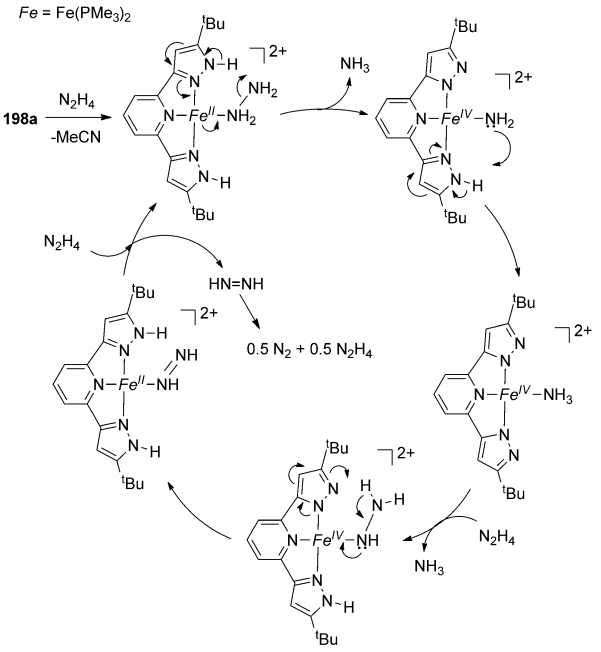

Scheme 108. Proposed mechanism of hydrazine disproportionation.

backbone upon deprotonation, was discussed in Section 2.3 in the context of M–S cooperativity. However, a different mode of bond activation via C-atoms of the indenide backbone can also be operative in this system. In particular, complex **53** reacts with acetonitrile in the presence of a base to give a ketimide complex **200** (Scheme 109), resembling nitrile

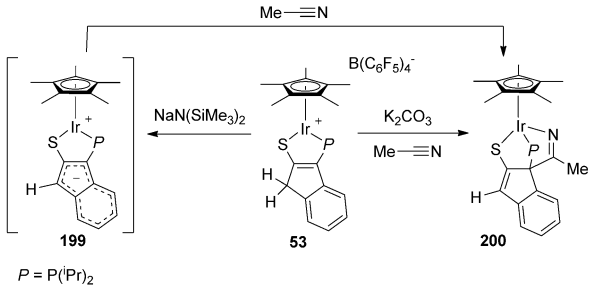

Scheme 109. Acetonitrile activation by **53** by M–indenide cooperation.

activation in lutidine-based systems (Section 3.1).[59] This reaction likely occurs through formation of a zwitterionic intermediate **199** by deprotonation of **53**. However, no data on the potential reversibility of nitrile activation or reactivity of ketimide complexes were reported.

The net N–H activation by Ru complexes with indenide-based ligands was also reported by Stradiotto et al.; however, the mechanism was not studied and could involve non-MLC pathways.[156]

Reversible protonation/deprotonation of an indenediide backbone in SCS Pd pincer complexes was proposed to play an active role in catalytic cyclization of alkynoic acids (Scheme 110).[157]

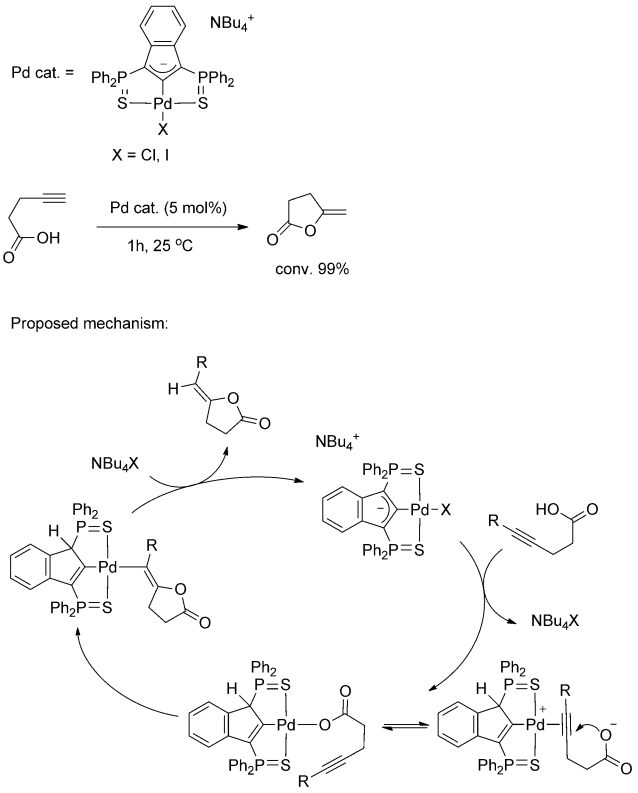

Scheme 110. Indenediide Pd pincer complexes used for catalytic cyclization of alkynoic acids and proposed mechanism.

Heterolytic cleavage of H_2, as well as H_2 liberation induced by addition of CO, were reported for Ru complexes supported by metallocene-based pincer PCP ligands.[158] First, the (PCP)Ru complexes **201a**,**b** heterolytically split H_2, leading to partial deconjugation of the Cp ring of the metallocene backbone as evident from C–C bond length alternations in the X-ray structure of **202a** (Scheme 111).[158] Although the products **202a**,**b** contain Cp–H and Ru–H hydrogen atoms present in mutual transoid position, this could result from the follow up rearrangement after initial H_2 activation. Then, facile reaction of **202a**,**b** with CO gas generates complexes **203a**,**b** which were characterized by X-ray crystallography.

Complex **203a** reacts further in a CD_2Cl_2 solution at room temperature to first rearrange to isomer **204a**, in which a mutual cisoid arrangement of Cp–H and Ru–H was deduced from NMR data. Further reaction leads to H_2 liberation and formation of complex **205a**, which is eventually converted to an agostic complex **206** as the major product (80%), in which aromaticity of the cyclopentadienyl ring is essentially restored (no significant C–C bond length alternations in the Cp ring are present in the X-ray structure of **206**).[159] Facile H_2 liberation is likely enabled by the cisoid orientation of the Ru-hydride and the Cp-ring proton in isomer **205a**.

The ruthenocene analog **203b** also liberates H_2, presumably by a similar isomerization process to form **204b**, which turned out to be less stable compared to **204a** and was not fully characterized (Scheme 111). The final product of

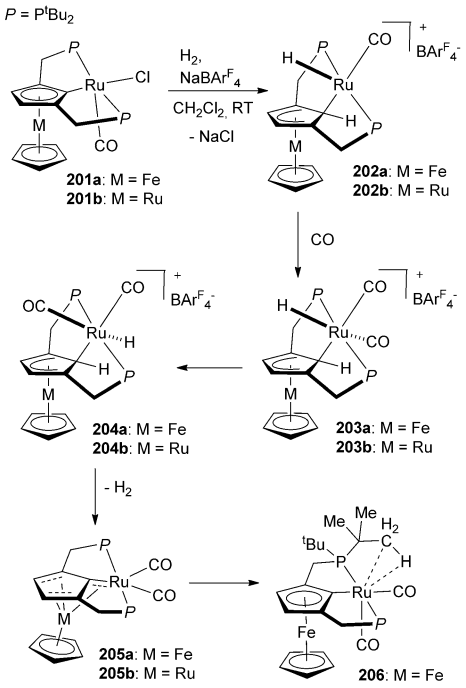

Scheme 111. H_2 splitting and liberation reactivity of Ru complexes with metallocene-derived pincer ligands.

reaction, complex **205b**, was sufficiently stable to allow for isolation and full characterization. Analysis of the X-ray structure of **205b** allows to suggest carbene-like binding of the central atom of a PCP ligand.

Thus, the reactivity of metallocene-derived complexes in Scheme 111 is reminiscent of H_2 elimination/addition reactivity of aliphatic PCP complexes described in Section 2.5, however, in the case of metallocene-derived complexes H_2 splitting and liberation leads to various degrees of conjugation in the cyclopentadienyl ring of the metallocene.

3.9. Shvo Catalyst and Analogous Systems

The Shvo complex **207** is a dinuclear Ru complex supported by a tetraphenyl-substituted hydroxycyclopentadienyl ligand (Scheme 112). This complex serves as a stable

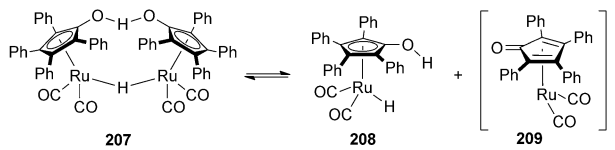

Scheme 112. The Shvo complex and its dissociation in solution.

pre-catalyst for a wide variety of reactions involving hydrogen transfer, such as transfer hydrogenation of carbonyl compounds and imines, direct hydrogenation, alcohol and amine oxidation etc.[160] Complex **207** and its analogs were discovered by Shvo in 1984–1985 during studies of Ru-catalyzed alcohol transfer dehydrogenation to esters. It was first shown that if diphenylacetylene was present as a hydrogen acceptor during alcohol dehydrogenation catalyzed by $[Ru_3(CO)_{12}]$, a new catalytically active species formed spontaneously supported by a cyclopentadienone ligand, which formed under these conditions through Ru-catalyzed [2+2+1] cycloaddition of two diphenylacetylene molecules and a CO ligand.[161] Complex **207** was then prepared independently and was shown to be a pre-catalyst for efficient Ru-catalyzed hydrogenation of alkenes, alkynes, ketones, aldehydes etc.[162]

The Shvo complex **207** has a dimeric structure in the solid state, however, its catalytic reactivity is determined by dissociation into the catalytically active monomeric complexes **208** and the coordinatively unsaturated **209** in solution (Scheme 112).[160] This system is one of the earliest examples of hydrogen transfer catalysts that operate through the MLC pathway (Scheme 113). For example, in the proposed outer-

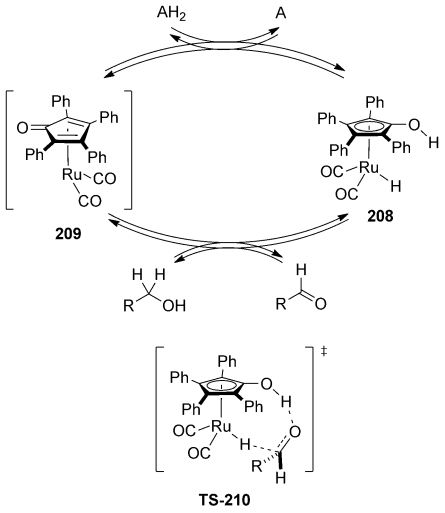

Scheme 113. Proposed mechanism of hydrogen transfer involving alcohols in Shvo complex (A: hydrogen acceptor).

sphere mechanism for carbonyl group hydrogenation, hydrogen transfer to a carbonyl group occurs from the $18e^-$ complex **208** by a simultaneous transfer of a hydride and a proton from the Ru^{II} center and the OH group at the hydroxycyclopentadienyl ligand, respectively.[163] This mechanism was supported by KIE studies by Casey et al. based on measurements of individual and combined KIE's for complexes with selectively deuterated RuH and OH positions.[163] The reverse reaction, dehydrogenation of alcohols, also occurs through an outer-sphere pathway as is evident from KIE studies by Backvall et al.[164] The dehydrogenation reaction involves the reactive species **209**, which can be described as a formal Ru^0 species supported by an η^4-coordinated cyclopentadienone ligand. While **209** is a reactive coordinatively unsaturated species and could not be directly observed, trapping with additional CO led to isolation of a tricarbonyl complex characterized by X-ray crystallography, and its geometry was consistent with η^4-coordination of a formally neutral cyclopentadienone ligand. Thus, the bond

activation by MLC in Shvo's system involves interconversion between Ru complexes with the η^5-bound hydroxycyclopentadienyl ligand and the η^4-bound cyclopentadienone.

Shvo's catalyst is also capable of direct hydrogenation which should involve H_2 activation by unsaturated species **209**. The possible mechanisms of H_2 activation in Shvo-type systems were elucidated through mechanistic studies of the reverse reaction, H_2 elimination, using tolyl-substituted analog **208-Tol** (Scheme 114).[165] Elimination of H_2 in the

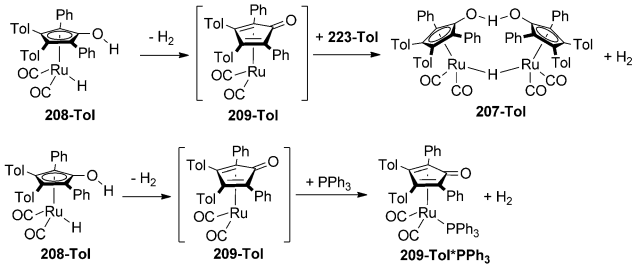

Scheme 114. H_2 elimination from **208-Tol**.

absence of additives produces a dimeric product **207-Tol**, while trapping with PPh_3 affords mononuclear **209-Tol-PPh$_3$**. The calculated activation barrier for the direct H_2 elimination in a model system, 43.2 kcal mol^{-1} (**TS-211** in Scheme 115 a) was found to be significantly higher than the experimentally determined enthalpy of activation (26.1 kcal mol^{-1}), which led to the proposal of proton shuttle mechanisms. In particular, a protic solvent-assisted pathway is likely operative in the presence of alcohols (**TS-212** in Scheme 115 b), and H_2 elimination in aprotic solvents such as toluene may be assisted by the hydroxy group of the hydroxycyclopentadienyl ligand of another molecule of **208-Tol** (**TS-213** in Scheme 115 c). Accordingly, dimerization of complex **208-Tol** in aprotic solvents was confirmed through NMR studies.[165]

The acidity of the ionizable group at the Cp ligand plays a large role in determining the accessibility of an outer-sphere pathway. For instance, the amino-analog of Shvo's complex, **214**, with a less acidic PhNH group reacted slowly with benzaldehyde at 75 °C to give benzyl alcohol.[166] At the same time, protonation of this complex with triflic acid leads to the formation of a more acidic **214-H$^+$**, which reacts with benzaldehyde even at −80 °C (Scheme 116).[166]

Although the iron analog of Shvo's catalyst **215** showed low catalytic activity, complex **216** was found to be catalytically active for hydrogenation of aldehydes, ketones and aldimines (Scheme 117).[167] Complex **216** was first synthesized by Knölker et al.[168] and its catalytic activity was later investigated by Casey and Guan.[167] An outer-sphere mechanism of aldehyde hydrogenation analogous to that in Shvo's system was proposed for iron-catalyzed reduction of carbonyl compounds.[169]

Iridium complexes supported by hydroxycyclopentadienyl ligand were recently reported by Nozaki et al. to catalyze acceptorless dehydrogenation of C–C bonds (Scheme 118).[170] Among several tested Ir complexes, the complexes **217 a,b** containing an OH group in the Cp ligand

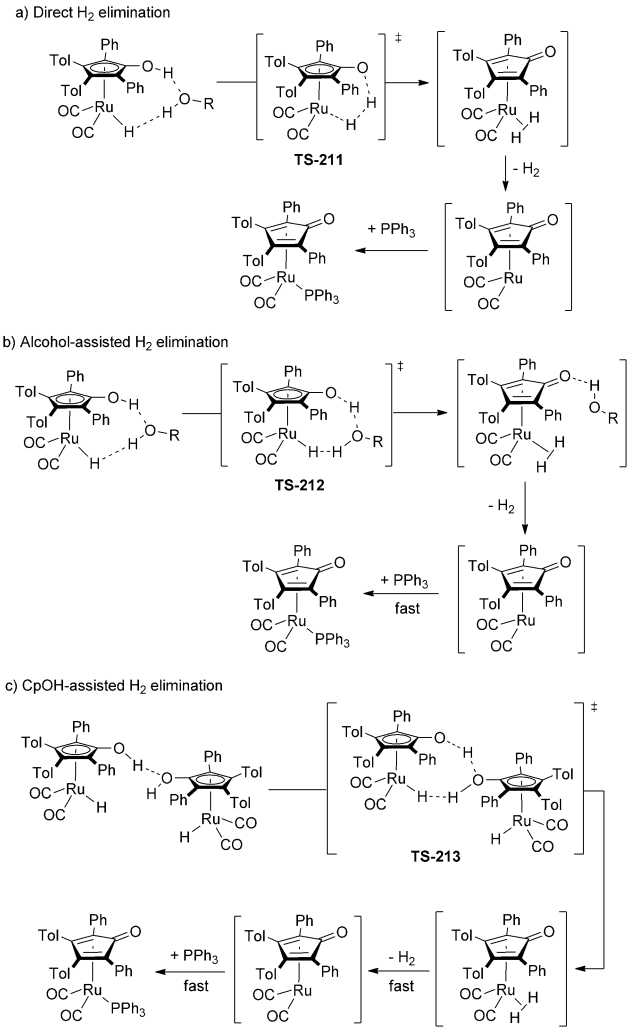

Scheme 115. Possible mechanisms of H_2 elimination from **208-Tol**.

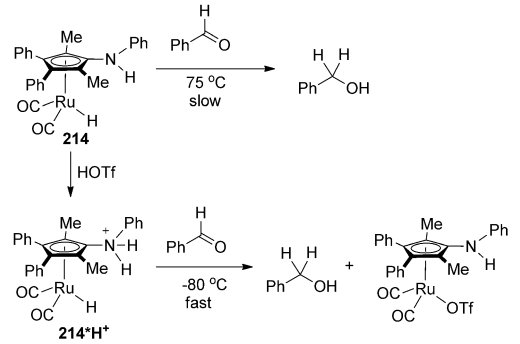

Scheme 116. Reaction of aminocyclopentadienyl Ru complexes with benzaldehyde.

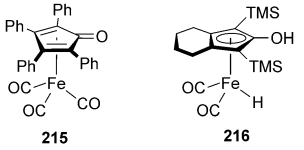

Scheme 117. Iron complexes analogous to Shvo's catalyst.

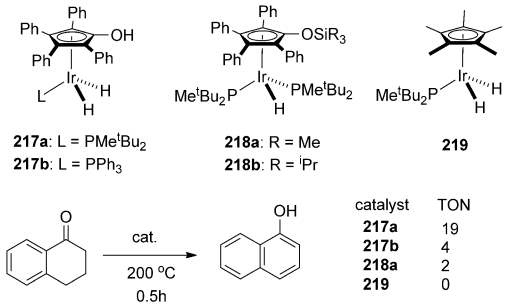

Scheme 118. Comparison of catalytic activity of Ir complexes in acceptorless C–C bond dehydrogenation.

generally showed higher catalytic activity in C–C bond dehydrogenation compared to silyl-protected complexes **218a,b** and Cp* complex **219** (Scheme 118).[170] Although metal–ligand cooperation could potentially play a role enabling H_2 elimination, further mechanistic studies will be required to elucidate the role of the CpOH ligand in this reaction.

In summary, the Shvo complex is one of the earliest examples of catalytic systems for hydrogen transfer reactions that operates by metal–ligand cooperation. Hydrogen transfer reactions result in interconversion between a Ru^{II} hydride complex with η^5-bound hydroxycyclopentadienyl ligand and a formal Ru^0 complex with η^4-bound, formally neutral cyclopentadienone ligand. The initial discovery of Shvo's system inspired further studies of the potential of such system in catalysis by other metals including Fe and Ir that show catalytic reactivity in hydrogenation and dehydrogenation reactions.

4. Summary and Outlook

As shown in this Review, the modes of metal–ligand cooperative bond activation are highly diverse, depending on the nature of the metal and ligand structures, and they occur both in biological and chemical catalytic systems. Examples of bond activation discussed in this Review include not only the more common H_2 and HX activation by bifunctional catalysts, but also rare examples of cooperative reactivity under oxidative conditions, for example, reactivity with O_2 or N_2O. Another very recent development is MLC involving substrates with multiply bonded functionalities, including carbonyl compounds, CO_2 and nitriles, already forming the basis for new catalytic reactions based on nitriles. Several cases described here illustrate that it is not always an easy task to distinguish between metal-mediated reactivity and MLC pathways, and detailed experimental and theoretical studies are required to elucidate the role of the ligand in bond breaking and formation.

It is also worth noticing that careful experimental and theoretical examination of MLC reactivity involving H_2 or HX activation revealed that several of these reactions operate through pathways assisted by solvents capable of hydrogen bonding (such as alcohols or water), or adventitious water, by forming transition states with bridging hydrogen bonded molecules.

We have shown that ligand tautomerization plays an important role in MLC reactivity. In particular, even if the reactive center is located remote from the metal center (formally in 2nd coordination sphere), bond activation through such "long-range" MLC may lead to immediate changes in the 1st coordination sphere of the metal by ligand tautomerization or aromatization/dearomatization of a heterocyclic structure. These cases include ligands that are based on lutidine, 2-aminopyridine or 2-hydroxypyridine backbones, as well as ligands containing acridine, pyrazole or imidazole donors.

While in many cases described here small-molecule activation by MLC enables catalytic transformations, there are also examples where MLC-type reactivity leads to catalyst deactivation.

Some future developments in the field of MLC reactivity could involve increasing the diversity of ligand motifs that are known to participate in bond activation. The most studied systems showing MLC are based on N-donor ligands, although some recent examples demonstrate that other donor atoms such as carbon, sulfur or boron also have a great potential for MLC reactivity. The vast majority of examples for MLC reactivity by aromatization/dearomatization involve pyridine-based ligands (i.e. ligands based on lutidine, 2-aminopyridine or 2-hydroxypyridine framework), and systems based on other heterocycles are somewhat less studied, although some recent examples show that they may also demonstrate interesting catalytic reactivity.

Although we have also discussed several examples of O_2 activation by MLC, utilization of such reactions for catalytic transformations remains a challenge, and an irreversible ligand decomposition is a significant problem.

Overall, harnessing metal–ligand cooperation for bond breaking or formation offers an important tool in the design of well-defined transition metal complexes that catalyze selective transformations under mild conditions. MLC has already significantly expanded the scope of catalytic reactions that can be achieved by using transition metal complexes as compared to previously developed systems in which ligands play a spectator role only, while most of the reactivity occurs at the metal center. This has already led to several sustainable environmentally benign catalytic reactions, such as new hydrogenation reactions of polar bonds under unprecedented mild conditions, and new acceptorless dehydrogenation systems, of importance both for organic synthesis and for the development of alternative energy resources. Cooperative action of the metal center and a carbon or a heteroatom reactive center at the ligand may offer a suitable spatial and electronic arrangement for mild and selective bond activation processes, resembling highly selective bond activation reactions that occur in enzymes under mild conditions.

Acknowledgements

We thank our co-workers and collaborators, whose names appear in the cited references, for their valuable contribu-

tions. This research was supported by the European Research Council under the FP7 framework (ERC No 246837), by the Israel Science Foundation, by the MINERVA Foundation, and by the Kimmel Center for Molecular Design. D.M. is the holder of the Israel Matz Professorial Chair of Organic Chemistry.

How to cite: *Angew. Chem. Int. Ed.* **2015**, *54*, 12236–12273
Angew. Chem. **2015**, *127*, 12406–12445

[1] a) J. C. Gordon, G. J. Kubas, *Organometallics* **2010**, *29*, 4682; b) J. I. van der Vlugt, *Eur. J. Inorg. Chem.* **2012**, 363; c) V. T. Annibale, D. Song, *RSC Adv.* **2013**, *3*, 11432; d) D. L. DuBois, *Inorg. Chem.* **2014**, *53*, 3935.
[2] B. Zhao, Z. Han, K. Ding, *Angew. Chem. Int. Ed.* **2013**, *52*, 4744; *Angew. Chem.* **2013**, *125*, 4844.
[3] R. H. Crabtree, *New J. Chem.* **2011**, *35*, 18.
[4] R. Noyori, S. Hashiguchi, *Acc. Chem. Res.* **1997**, *30*, 97.
[5] R. Noyori, T. Okhuma, *Angew. Chem. Int. Ed.* **2001**, *40*, 40; *Angew. Chem.* **2001**, *113*, 40.
[6] a) R. Noyori, M. Koizumi, D. Ishii, T. Ohkuma, *Pure Appl. Chem.* **2001**, *73*, 227; b) R. Noyori, M. Kitamura, T. Ohkuma, *Proc. Natl. Acad. Sci. USA* **2004**, *101*, 5356.
[7] a) T. Ikariya, A. J. Blacker, *Acc. Chem. Res.* **2007**, *40*, 1300; b) T. Ikariya, I. D. Gridnev, *Top. Catal.* **2010**, *53*, 894; c) T. Ikariya, *Bull. Chem. Soc. Jpn.* **2011**, *84*, 1.
[8] a) P. A. Dub, T. Ikariya, *ACS Catal.* **2012**, *2*, 1718; b) H. Li, M. B. Hall, *ACS Catal.* **2015**, *5*, 1895; c) O. Eisenstein, R. H. Crabtree, *New J. Chem.* **2013**, *37*, 21; d) P. E. Sues, K. Z. Demmans, R. H. Morris, *Dalton Trans.* **2014**, *43*, 7650; e) R. H. Morris, *Acc. Chem. Res.* **2015**, *48*, 1494; f) L. A. Berben, *Chem. Eur. J.* **2015**, *21*, 2734; g) H. Grützmacher, *Angew. Chem. Int. Ed.* **2008**, *47*, 1814; *Angew. Chem.* **2008**, *120*, 1838.
[9] T. Ohkuma, H. Ooka, S. Hashiguchi, T. Ikariya, R. Noyori, *J. Am. Chem. Soc.* **1995**, *117*, 2675.
[10] C. A. Sandoval, T. Ohkuma, K. Muniz, R. Noyori, *J. Am. Chem. Soc.* **2003**, *125*, 13490.
[11] a) D. Di Tommaso, S. A. French, A. Zanotti-Gerosa, F. Hancock, E. J. Palin, C. R. A. Catlow, *Inorg. Chem.* **2008**, *47*, 2674; b) T. Leyssens, D. Peeters, J. N. Harvey, *Organometallics* **2008**, *27*, 1514.
[12] S. Takebayashi, N. Dabral, M. Miskolzie, S. H. Bergens, *J. Am. Chem. Soc.* **2011**, *133*, 9666.
[13] a) K. Abdur-Rashid, S. E. Clapham, A. Hadzovic, J. N. Harvey, A. J. Lough, R. H. Morris, *J. Am. Chem. Soc.* **2002**, *124*, 15104; b) M. Z.-D. Iuliis, R. H. Morris, *J. Am. Chem. Soc.* **2009**, *131*, 11263.
[14] K. Muniz, *Angew. Chem. Int. Ed.* **2005**, *44*, 6622; *Angew. Chem.* **2005**, *117*, 6780.
[15] J. Takehara, S. Hashiguchi, A. Fujii, S.-i. Inoue, T. Ikariya, R. Noyori, *Chem. Commun.* **1996**, 233.
[16] M. Yamakawa, H. Ito, R. Noyori, *J. Am. Chem. Soc.* **2000**, *122*, 1466.
[17] C. P. Casey, J. B. Johnson, *J. Org. Chem.* **2003**, *68*, 1998.
[18] a) C. Hedberg, K. Källström, P. I. Arvidsson, P. Brandt, P. G. Andersson, *J. Am. Chem. Soc.* **2005**, *127*, 15083; b) J.-W. Handgraaf, E. J. Meijer, *J. Am. Chem. Soc.* **2007**, *129*, 3099.
[19] W. W. N. O, A. J. Lough, R. H. Morris, *Organometallics* **2012**, *31*, 2137.
[20] W. W. N. O, R. H. Morris, *ACS Catal.* **2013**, *3*, 32.
[21] W. W. N. O, A. J. Lough, R. H. Morris, *Organometallics* **2011**, *30*, 1236.
[22] P. Maire, T. Büttner, F. Breher, P. Le Floch, H. Grützmacher, *Angew. Chem. Int. Ed.* **2005**, *44*, 6318; *Angew. Chem.* **2005**, *117*, 6477.
[23] a) T. Zweifel, J.-V. Naubron, H. Grützmacher, *Angew. Chem. Int. Ed.* **2009**, *48*, 559; *Angew. Chem.* **2009**, *121*, 567; b) T. Zweifel, J.-V. Naubron, T. Büttner, T. Ott, H. Grützmacher, *Angew. Chem. Int. Ed.* **2008**, *47*, 3245; *Angew. Chem.* **2008**, *120*, 3289; c) S. P. Annen, V. Bambagioni, M. Bevilacqua, J. Filippi, A. Marchionni, W. Oberhauser, H. Schönberg, F. Vizza, C. Bianchini, H. Grützmacher, *Angew. Chem. Int. Ed.* **2010**, *49*, 7229; *Angew. Chem.* **2010**, *122*, 7387; d) M. Trincado, H. Grützmacher, F. Vizza, C. Bianchini, *Chem. Eur. J.* **2010**, *16*, 2751; e) R. E. Rodríguez-Lugo, M. Trincado, M. Vogt, F. Tewes, G. Santiso-Quinones, H. Grützmacher, *Nat. Chem.* **2013**, *5*, 342; f) N. Donati, M. Koenigsmann, D. Stein, L. Udino, H. Grützmacher, *C. R. Chim.* **2007**, *10*, 721.
[24] T. Li, I. Bergner, F. N. Haque, M. Z.-D. Iuliis, D. Song, R. H. Morris, *Organometallics* **2007**, *26*, 5940.
[25] a) W. Zuo, A. J. Lough, Y. F. Li, R. H. Morris, *Science* **2013**, *342*, 1080; b) W. Zuo, S. Tauer, D. E. Prokopchuk, R. H. Morris, *Organometallics* **2014**, *33*, 5791; c) A. A. Mikhailine, M. I. Maishan, A. J. Lough, R. H. Morris, *J. Am. Chem. Soc.* **2012**, *134*, 12266.
[26] N. Blaquiere, S. Diallo-Garcia, S. I. Gorelsky, D. A. Black, K. Fagnou, *J. Am. Chem. Soc.* **2008**, *130*, 14034.
[27] a) M. D. Fryzuk, C. D. Montgomery, S. J. Rettig, *Organometallics* **1991**, *10*, 467; b) M. D. Fryzuk, P. A. MacNeil, *Organometallics* **1983**, *2*, 682; c) M. D. Fryzuk, P. A. MacNeil, S. J. Rettig, *Organometallics* **1985**, *4*, 1145; d) M. D. Fryzuk, P. A. MacNeil, S. J. Rettig, *J. Am. Chem. Soc.* **1987**, *109*, 2803.
[28] B. Askevold, H. W. Roesky, S. Schneider, *ChemCatChem* **2012**, *4*, 307.
[29] a) S. Schneider, J. Meiners, B. Askevold, *Eur. J. Inorg. Chem.* **2012**, 412; b) S. Chakraborty, W. W. Brennessel, W. D. Jones, *J. Am. Chem. Soc.* **2014**, *136*, 8564; c) S. Chakraborty, H. Dai, P. Bhattacharya, N. T. Fairweather, M. S. Gibson, J. A. Krause, H. Guan, *J. Am. Chem. Soc.* **2014**, *136*, 7869.
[30] S. Werkmeister, K. Junge, B. Wendt, E. Alberico, H. Jiao, W. Baumann, H. Junge, F. Gallou, M. Beller, *Angew. Chem. Int. Ed.* **2014**, *53*, 8722; *Angew. Chem.* **2014**, *126*, 8867.
[31] a) Z. E. Clarke, P. T. Maragh, T. P. Dasgupta, D. G. Gusev, A. J. Lough, K. Abdur-Rashid, *Organometallics* **2006**, *25*, 4113; b) X. Chen, W. Jia, R. Guo, T. W. Graham, M. A. Gullons, K. Abdur-Rashid, *Dalton Trans.* **2009**, 1407; c) T. J. Schmeier, G. E. Dobereiner, R. H. Crabtree, N. Hazari, *J. Am. Chem. Soc.* **2011**, *133*, 9274.
[32] M. Bertoli, A. Choualeb, A. J. Lough, B. Moore, D. Spasyuk, D. G. Gusev, *Organometallics* **2011**, *30*, 3479.
[33] W. Kuriyama, T. Matsumoto, Y. Ino, O. Ogata, (Takasago Int.), WO 2011048727, **2011**.
[34] B. Askevold, J. T. Nieto, S. Tussupbayev, M. Diefenbach, E. Herdtweck, M. C. Holthausen, S. Schneider, *Nat. Chem.* **2011**, *3*, 532.
[35] M. Nielsen, A. Kammer, D. Cozzula, H. Junge, S. Gladiali, M. Beller, *Angew. Chem. Int. Ed.* **2011**, *50*, 9593; *Angew. Chem.* **2011**, *123*, 9767.
[36] a) M. Käß, A. Friedrich, M. Drees, S. Schneider, *Angew. Chem. Int. Ed.* **2009**, *48*, 905; *Angew. Chem.* **2009**, *121*, 922; b) A. N. Marziale, A. Friedrich, I. Klopsch, M. Drees, V. R. Celinski, J. Schmedt auf der Guenne, S. Schneider, *J. Am. Chem. Soc.* **2013**, *135*, 13342.
[37] a) A. Choualeb, A. J. Lough, D. G. Gusev, *Organometallics* **2007**, *26*, 5224; b) S. Bi, Q. Xie, X. Zhao, Y. Zhao, X. Kong, *J. Organomet. Chem.* **2008**, *693*, 633.
[38] D. Spasyuk, S. Smith, D. G. Gusev, *Angew. Chem. Int. Ed.* **2012**, *51*, 2772; *Angew. Chem.* **2012**, *124*, 2826.
[39] A. Friedrich, M. Drees, M. Kaess, E. Herdtweck, S. Schneider, *Inorg. Chem.* **2010**, *49*, 5482.

[40] S. Chakraborty, P. O. Lagaditis, M. Forster, E. A. Bielinski, N. Hazari, M. C. Holthausen, W. D. Jones, S. Schneider, *ACS Catal.* **2014**, *4*, 3994.
[41] E. Alberico, P. Sponholz, C. Cordes, M. Nielsen, H.-J. Drexler, W. Baumann, H. Junge, M. Beller, *Angew. Chem. Int. Ed.* **2013**, *52*, 14162; *Angew. Chem.* **2013**, *125*, 14412.
[42] E. A. Bielinski, M. Forster, Y. Zhang, W. H. Bernskoetter, N. Hazari, M. C. Holthausen, *ACS Catal.* **2015**, *5*, 2404.
[43] L. C. Gregor, C.-H. Chen, C. M. Fafard, L. Fan, C. Guo, B. M. Foxman, D. G. Gusev, O. V. Ozerov, *Dalton Trans.* **2010**, *39*, 3195.
[44] Y. Zhu, C.-H. Chen, C. M. Fafard, B. M. Foxman, O. V. Ozerov, *Inorg. Chem.* **2011**, *50*, 7980.
[45] a) C. C. Cummins, S. M. Baxter, P. T. Wolczanski, *J. Am. Chem. Soc.* **1988**, *110*, 8731; b) P. J. Walsh, F. J. Hollander, R. G. Bergman, *J. Am. Chem. Soc.* **1988**, *110*, 8729.
[46] J. R. Webb, S. A. Burgess, T. R. Cundari, T. B. Gunnoe, *Dalton Trans.* **2013**, *42*, 16646.
[47] S. Kuwata, T. Ikariya, *Dalton Trans.* **2010**, *39*, 2984.
[48] T. Kimura, N. Koiso, K. Ishiwata, S. Kuwata, T. Ikariya, *J. Am. Chem. Soc.* **2011**, *133*, 8880.
[49] K. Ishiwata, S. Kuwata, T. Ikariya, *J. Am. Chem. Soc.* **2009**, *131*, 5001.
[50] a) S. Musa, I. Shaposhnikov, S. Cohen, D. Gelman, *Angew. Chem. Int. Ed.* **2011**, *50*, 3533; *Angew. Chem.* **2011**, *123*, 3595; b) G. A. Silantyev, O. A. Filippov, S. Musa, D. Gelman, N. V. Belkova, K. Weisz, L. M. Epstein, E. S. Shubina, *Organometallics* **2014**, *33*, 5964.
[51] S. Musa, S. Fronton, L. Vaccaro, D. Gelman, *Organometallics* **2013**, *32*, 3069.
[52] B. Saha, S. M. W. Rahaman, P. Daw, G. Sengupta, J. K. Bera, *Chem. Eur. J.* **2014**, *20*, 6542.
[53] A. Bartoszewicz, R. Marcos, S. Sahoo, A. K. Inge, X. Zou, B. Martin-Matute, *Chem. Eur. J.* **2012**, *18*, 14510.
[54] W.-Y. Chu, X. Zhou, T. B. Rauchfuss, *Organometallics* **2015**, *34*, 1619.
[55] Z. K. Sweeney, J. L. Polse, R. G. Bergman, R. A. Andersen, *Organometallics* **1999**, *18*, 5502.
[56] T. I. Gountchev, T. D. Tilley, *J. Am. Chem. Soc.* **1997**, *119*, 12831.
[57] R. C. Linck, R. J. Pafford, T. B. Rauchfuss, *J. Am. Chem. Soc.* **2001**, *123*, 8856.
[58] A. Ienco, M. J. Calhorda, J. Reinhold, F. Reineri, C. Bianchini, M. Peruzzini, F. Vizza, C. Mealli, *J. Am. Chem. Soc.* **2004**, *126*, 11954.
[59] K. D. Hesp, R. McDonald, M. J. Ferguson, M. Stradiotto, *J. Am. Chem. Soc.* **2008**, *130*, 16394.
[60] Y. Ohki, M. Sakamoto, K. Tatsumi, *J. Am. Chem. Soc.* **2008**, *130*, 11610.
[61] M. Sakamoto, Y. Ohki, G. Kehr, G. Erker, K. Tatsumi, *J. Organomet. Chem.* **2009**, *694*, 2820.
[62] J. Tao, S. Li, *Dalton Trans.* **2010**, *39*, 857.
[63] Y. Ohki, Y. Takikawa, H. Sadohara, C. Kesenheimer, B. Engendahl, E. Kapatina, K. Tatsumi, *Chem. Asian J.* **2008**, *3*, 1625.
[64] T. Stahl, K. Müther, Y. Ohki, K. Tatsumi, M. Oestreich, *J. Am. Chem. Soc.* **2013**, *135*, 10978.
[65] H. F. T. Klare, M. Oestreich, J.-i. Ito, H. Nishiyama, Y. Ohki, K. Tatsumi, *J. Am. Chem. Soc.* **2011**, *133*, 3312.
[66] H. Kameo, H. Nakazawa, *Chem. Asian J.* **2013**, *8*, 1720.
[67] J. B. Bonanno, T. P. Henry, P. T. Wolczanski, A. W. Pierpont, T. R. Cundari, *Inorg. Chem.* **2007**, *46*, 1222.
[68] N. Tsoureas, Y.-Y. Kuo, M. F. Haddow, G. R. Owen, *Chem. Commun.* **2011**, *47*, 484.
[69] W. H. Harman, J. C. Peters, *J. Am. Chem. Soc.* **2012**, *134*, 5080.
[70] H. Fong, M.-E. Moret, Y. Lee, J. C. Peters, *Organometallics* **2013**, *32*, 3053.
[71] B. R. Barnett, C. E. Moore, A. L. Rheingold, J. S. Figueroa, *J. Am. Chem. Soc.* **2014**, *136*, 10262.
[72] B. E. Cowie, D. J. H. Emslie, *Chem. Eur. J.* **2014**, *20*, 16899.
[73] N. Curado, C. Maya, J. Lopez-Serrano, A. Rodriguez, *Chem. Commun.* **2014**, *50*, 15718.
[74] a) H. D. Empsall, E. M. Hyde, R. Markham, W. S. McDonald, M. C. Norton, B. L. Shaw, B. Weeks, *J. Chem. Soc. Chem. Commun.* **1977**, 589; b) C. Crocker, R. J. Errington, R. Markham, C. J. Moulton, K. J. Odell, B. L. Shaw, *J. Am. Chem. Soc.* **1980**, *102*, 4373; c) C. Crocker, R. J. Errington, R. Markham, C. J. Moulton, B. L. Shaw, *J. Chem. Soc. Dalton Trans.* **1982**, 387; d) C. Crocker, H. D. Empsall, R. J. Errington, E. M. Hyde, W. S. McDonald, R. Markham, M. C. Norton, B. L. Shaw, B. Weeks, *J. Chem. Soc. Dalton Trans.* **1982**, 1217; e) C. Crocker, R. J. Errington, W. S. McDonald, K. J. Odell, B. L. Shaw, R. J. Goodfellow, *J. Chem. Soc. Chem. Commun.* **1979**, 498.
[75] D. Gelman, S. Musa, *ACS Catal.* **2012**, *2*, 2456.
[76] D. G. Gusev, A. J. Lough, *Organometallics* **2002**, *21*, 2601.
[77] R. J. Burford, W. E. Piers, M. Parvez, *Organometallics* **2012**, *31*, 2949.
[78] D. V. Gutsulyak, W. E. Piers, J. Borau-Garcia, M. Parvez, *J. Am. Chem. Soc.* **2013**, *135*, 11776.
[79] C. C. Comanescu, V. M. Iluc, *Organometallics* **2014**, *33*, 6059.
[80] L. E. Doyle, W. E. Piers, J. Borau-Garcia, *J. Am. Chem. Soc.* **2015**, *137*, 2187.
[81] A. M. Winter, K. Eichele, H.-G. Mack, W. C. Kaska, H. A. Mayer, *Dalton Trans.* **2008**, 527.
[82] C. Gunanathan, D. Milstein, *Acc. Chem. Res.* **2011**, *44*, 588.
[83] E. Ben-Ari, G. Leitus, L. J. W. Shimon, D. Milstein, *J. Am. Chem. Soc.* **2006**, *128*, 15390.
[84] a) M. Feller, A. Karton, G. Leitus, J. M. L. Martin, D. Milstein, *J. Am. Chem. Soc.* **2006**, *128*, 12400; b) L. Schwartsburd, M. A. Iron, L. Konstantinovski, Y. Diskin-Posner, G. Leitus, L. J. W. Shimon, D. Milstein, *Organometallics* **2010**, *29*, 3817.
[85] M. A. Iron, E. Ben-Ari, R. Cohen, D. Milstein, *Dalton Trans.* **2009**, 9433.
[86] G. Zeng, Y. Guo, S. Li, *Inorg. Chem.* **2009**, *48*, 10257.
[87] a) C. Gunanathan, D. Milstein, *Chem. Rev.* **2014**, *114*, 12024; b) C. Gunanathan, D. Milstein, *Science* **2013**, *341*, 1229712; c) C. Gunanathan, D. Milstein in *Pincer and Pincer-type Complexes*, *Applications in Organic Synthesis and Catalysis* (Eds.: K. J. Szabo, O. F. Wendt), Wiley, New York, pp. 1 – 30, **2014**; d) C. Gunanathan, D. Milstein, *Top. Organomet. Chem.* **2011**, *37*, 55; e) D. Milstein, *Top. Catal.* **2010**, *53*, 915.
[88] T. Zell, D. Milstein, *Acc. Chem. Res.* **2015**, DOI: 10.1021/acs.accounts.5b00027.
[89] J. Zhang, G. Leitus, Y. Ben-David, D. Milstein, *Angew. Chem. Int. Ed.* **2006**, *45*, 1113; *Angew. Chem.* **2006**, *118*, 1131.
[90] J. Zhang, G. Leitus, Y. Ben-David, D. Milstein, *J. Am. Chem. Soc.* **2005**, *127*, 10840.
[91] C. Gunanathan, Y. Ben-David, D. Milstein, *Science* **2007**, *317*, 790.
[92] X. Yang, M. B. Hall, *J. Am. Chem. Soc.* **2010**, *132*, 120.
[93] Y. Sun, C. Koehler, R. Tan, V. T. Annibale, D. Song, *Chem. Commun.* **2011**, *47*, 8349.
[94] S. W. Kohl, L. Weiner, L. Schwartsburd, L. Konstantinovski, L. J. W. Shimon, Y. Ben-David, M. A. Iron, D. Milstein, *Science* **2009**, *324*, 74.
[95] a) J. Li, Y. Shiota, K. Yoshizawa, *J. Am. Chem. Soc.* **2009**, *131*, 13584; b) K. S. Sandhya, C. H. Suresh, *Organometallics* **2011**, *30*, 3888.
[96] D. Milstein, *Philos. Trans. R. Soc. A* **2015**, *373*, 20140189.
[97] D. E. Prokopchuk, B. T. H. Tsui, A. J. Lough, R. H. Morris, *Chem. Eur. J.* **2014**, *20*, 16960.
[98] E. Balaraman, C. Gunanathan, J. Zhang, L. J. W. Shimon, D. Milstein, *Nat. Chem.* **2011**, *3*, 609.

[99] E. Balaraman, Y. Ben-David, D. Milstein, *Angew. Chem. Int. Ed.* **2011**, *50*, 11702; *Angew. Chem.* **2011**, *123*, 11906.
[100] J. R. Khusnutdinova, J. A. Garg, D. Milstein, *ACS Catal.* **2015**, *5*, 2416.
[101] E. Balaraman, E. Khaskin, G. Leitus, D. Milstein, *Nat. Chem.* **2013**, *5*, 122.
[102] E. Fogler, J. A. Garg, P. Hu, G. Leitus, L. J. W. Shimon, D. Milstein, *Chem. Eur. J.* **2014**, *20*, 15727.
[103] M. Vogt, A. Nerush, Y. Diskin-Posner, Y. Ben-David, D. Milstein, *Chem. Sci.* **2014**, *5*, 2043.
[104] E. Khaskin, M. A. Iron, L. J. W. Shimon, J. Zhang, D. Milstein, *J. Am. Chem. Soc.* **2010**, *132*, 8542.
[105] M. Feller, Y. Diskin-Posner, L. J. W. Shimon, E. Ben-Ari, D. Milstein, *Organometallics* **2012**, *31*, 4083.
[106] M. Montag, J. Zhang, D. Milstein, *J. Am. Chem. Soc.* **2012**, *134*, 10325.
[107] C. A. Huff, J. W. Kampf, M. S. Sanford, *Chem. Commun.* **2013**, *49*, 7147.
[108] M. Vogt, M. Gargir, M. A. Iron, Y. Diskin-Posner, Y. Ben-David, D. Milstein, *Chem. Eur. J.* **2012**, *18*, 9194.
[109] C. A. Huff, J. W. Kampf, M. S. Sanford, *Organometallics* **2012**, *31*, 4643.
[110] M. Vogt, A. Nerush, M. A. Iron, G. Leitus, Y. Diskin-Posner, L. J. W. Shimon, Y. Ben-David, D. Milstein, *J. Am. Chem. Soc.* **2013**, *135*, 17004.
[111] G. A. Filonenko, E. Cosimi, L. Lefort, M. P. Conley, C. Copéret, M. Lutz, E. J. M. Hensen, E. A. Pidko, *ACS Catal.* **2014**, *4*, 2667.
[112] G. A. Filonenko, D. Smykowski, B. M. Szyja, G. Li, J. Szczygiel, E. J. M. Hensen, E. A. Pidko, *ACS Catal.* **2015**, *5*, 1145.
[113] S. Perdriau, D. S. Zijlstra, H. J. Heeres, J. G. de Vries, E. Otten, *Angew. Chem. Int. Ed.* **2015**, *54*, 4236; *Angew. Chem.* **2015**, *127*, 4310.
[114] A. Anaby, B. Butschke, Y. Ben-David, L. J. W. Shimon, G. Leitus, M. Feller, D. Milstein, *Organometallics* **2014**, *33*, 3716.
[115] M. Feller, E. Ben-Ari, Y. Diskin-Posner, R. Carmieli, L. Weiner, D. Milstein, *J. Am. Chem. Soc.* **2015**, *137*, 4634.
[116] H. Li, B. Zheng, K.-W. Huang, *Coord. Chem. Rev.* **2014**, *293 – 294*, 116.
[117] D. Benito-Garagorri, K. Mereiter, K. Kirchner, *Eur. J. Inorg. Chem.* **2006**, 4374.
[118] B. Bichler, C. Holzhacker, B. Stoeger, M. Puchberger, L. F. Veiros, K. Kirchner, *Organometallics* **2013**, *32*, 4114.
[119] N. Gorgas, B. Stoeger, L. F. Veiros, E. Pittenauer, G. Allmaier, K. Kirchner, *Organometallics* **2014**, *33*, 6905.
[120] S. Qu, Y. Dang, C. Song, M. Wen, K.-W. Huang, Z.-X. Wang, *J. Am. Chem. Soc.* **2014**, *136*, 4974.
[121] T. Chen, H. Li, S. Qu, B. Zheng, L. He, Z. Lai, Z.-X. Wang, K.-W. Huang, *Organometallics* **2014**, *33*, 4152.
[122] D. Srimani, Y. Ben-David, D. Milstein, *Angew. Chem. Int. Ed.* **2013**, *52*, 4012; *Angew. Chem.* **2013**, *125*, 4104; S. Michlik, R. Kempe, *Nat. Chem.* **2013**, *5*, 140.
[123] a) J. Frank, A. R. Katritzky, *J. Chem. Soc. Perkin Trans. 2* **1976**, 1428; b) L. Forlani, G. Cristoni, C. Boga, P. E. Todesco, E. Del Vecchio, S. Selva, M. Monari, *ARKIVOC* **2002**, 198; c) H. W. Yang, B. M. Craven, *Acta Crystallogr. Sect. B* **1998**, *54*, 912.
[124] W. Lubitz, H. Ogata, O. Rüdiger, E. Reijerse, *Chem. Rev.* **2014**, *114*, 4081; C. d. Tard, C. J. Pickett, *Chem. Rev.* **2009**, *109*, 2245.
[125] C. M. Moore, E. W. Dahl, N. K. Szymczak, *Curr. Opin. Chem. Biol.* **2015**, *25*, 9.
[126] a) S. Shima, O. Pilak, S. Vogt, M. Schick, M. S. Stagni, W. Meyer-Klaucke, E. Warkentin, R. K. Thauer, U. Ermler, *Science* **2008**, *321*, 572; b) T. Hiromoto, K. Ataka, O. Pilak, S. Vogt, M. S. Stagni, W. Meyer-Klaucke, E. Warkentin, R. K. Thauer, S. Shima, U. Ermler, *FEBS Lett.* **2009**, *583*, 585.
[127] X. Yang, M. B. Hall, *J. Am. Chem. Soc.* **2009**, *131*, 10901.
[128] A. M. Royer, T. B. Rauchfuss, D. L. Gray, *Organometallics* **2010**, *29*, 6763.
[129] A. J. Lough, S. Park, R. Ramachandran, R. H. Morris, *J. Am. Chem. Soc.* **1994**, *116*, 8356.
[130] J. F. Hull, Y. Himeda, W.-H. Wang, B. Hashiguchi, R. Periana, D. J. Szalda, J. T. Muckerman, E. Fujita, *Nat. Chem.* **2012**, *4*, 383.
[131] Y. Suna, M. Z. Ertem, W.-H. Wang, H. Kambayashi, Y. Manaka, J. T. Muckerman, E. Fujita, Y. Himeda, *Organometallics* **2014**, *33*, 6519.
[132] W.-H. Wang, J. T. Muckerman, E. Fujita, Y. Himeda, *ACS Catal.* **2013**, *3*, 856.
[133] G. Zeng, S. Sakaki, K.-i. Fujita, H. Sano, R. Yamaguchi, *ACS Catal.* **2014**, *4*, 1010.
[134] C. Gunanathan, B. Gnanaprakasam, M. A. Iron, L. J. W. Shimon, D. Milstein, *J. Am. Chem. Soc.* **2010**, *132*, 14763.
[135] a) C. Gunanathan, D. Milstein, *Angew. Chem. Int. Ed.* **2008**, *47*, 8661; *Angew. Chem.* **2008**, *120*, 8789; b) J. R. Khusnutdinova, Y. Ben-David, D. Milstein, *Angew. Chem. Int. Ed.* **2013**, *52*, 6269; *Angew. Chem.* **2013**, *125*, 6389.
[136] C. Gunanathan, L. J. W. Shimon, D. Milstein, *J. Am. Chem. Soc.* **2009**, *131*, 3146.
[137] X. Ye, P. N. Plessow, M. K. Brinks, M. Schelwies, T. Schaub, F. Rominger, R. Paciello, M. Limbach, P. Hofmann, *J. Am. Chem. Soc.* **2014**, *136*, 5923.
[138] J. R. Khusnutdinova, Y. Ben-David, D. Milstein, *J. Am. Chem. Soc.* **2014**, *136*, 2998.
[139] a) R. M. Moriarty, R. K. Vaid, M. P. Duncan, M. Ochiai, M. Inenaga, Y. Nagao, *Tetrahedron Lett.* **1988**, *29*, 6913; b) X.-F. Wu, M. Sharif, A. Pews-Davtyan, P. Langer, K. Ayub, M. Beller, *Eur. J. Org. Chem.* **2013**, 2783; c) X.-F. Wu, M. Sharif, J.-B. Feng, H. Neumann, A. Pews-Davtyan, P. Langer, M. Beller, *Green Chem.* **2013**, *15*, 1956; d) X.-F. Wu, C. B. Bheeter, H. Neumann, P. H. Dixneuf, M. Beller, *Chem. Commun.* **2012**, *48*, 12237; e) Y. Wang, H. Kobayashi, K. Yamaguchi, N. Mizuno, *Chem. Commun.* **2012**, *48*, 2642; f) W. Xu, Y. Jiang, H. Fu, *Synlett* **2012**, *23*, 801; g) E. R. Klobukowski, M. L. Mueller, R. J. Angelici, L. K. Woo, *ACS Catal.* **2011**, *1*, 703; h) K. Tanaka, S. Yoshifuji, Y. Nitta, *Chem. Pharm. Bull.* **1988**, *36*, 3125; i) A. Nishinaga, T. Shimizu, T. Matsuura, *J. Chem. Soc. Chem. Commun.* **1979**, 970.
[140] U. Gellrich, J. R. Khusnutdinova, G. M. Leitus, D. Milstein, *J. Am. Chem. Soc.* **2015**, *137*, 4851.
[141] J. G. Salway, *Metabolism at a Glance*, *3rd ed.*, Wiley, New York, **2013**.
[142] R. Langer, I. Fuchs, M. Vogt, E. Balaraman, Y. Diskin-Posner, L. J. W. Shimon, Y. Ben-David, D. Milstein, *Chem. Eur. J.* **2013**, *19*, 3407.
[143] E. Stepowska, H. Jiang, D. Song, *Chem. Commun.* **2010**, *46*, 556.
[144] A. Scharf, I. Goldberg, A. Vigalok, *J. Am. Chem. Soc.* **2013**, *135*, 967.
[145] A. Scharf, I. Goldberg, A. Vigalok, *Inorg. Chem.* **2014**, *53*, 12.
[146] M. L. Scheuermann, A. T. Luedtke, S. K. Hanson, U. Fekl, W. Kaminsky, K. I. Goldberg, *Organometallics* **2013**, *32*, 4752.
[147] A. D. Phillips, G. b. Laurenczy, R. Scopelliti, P. J. Dyson, *Organometallics* **2007**, *26*, 1120.
[148] F. A. LeBlanc, A. Berkefeld, W. E. Piers, M. Parvez, *Organometallics* **2012**, *31*, 810.
[149] M. L. Scheuermann, U. Fekl, W. Kaminsky, K. I. Goldberg, *Organometallics* **2010**, *29*, 4749.
[150] S. Kuwata, T. Ikariya, *Chem. Commun.* **2014**, *50*, 14290.
[151] K. Araki, S. Kuwata, T. Ikariya, *Organometallics* **2008**, *27*, 2176.
[152] S. Conejero, J. López-Serrano, M. Paneque, A. Petronilho, M. L. Poveda, F. Vattier, E. Álvarez, E. Carmona, *Chem. Eur. J.* **2012**, *18*, 4644.

[153] C. Cristóbal, Y. A. Hernández, J. López-Serrano, M. Paneque, A. Petronilho, M. L. Poveda, V. Salazar, F. Vattier, E. Álvarez, C. Maya, E. Carmona, *Chem. Eur. J.* **2013**, *19*, 4003.
[154] E. Álvarez, Y. A. Hernández, J. López-Serrano, C. Maya, M. Paneque, A. Petronilho, M. L. Poveda, V. Salazar, F. Vattier, E. Carmona, *Angew. Chem. Int. Ed.* **2010**, *49*, 3496; *Angew. Chem.* **2010**, *122*, 3574.
[155] K. Umehara, S. Kuwata, T. Ikariya, *J. Am. Chem. Soc.* **2013**, *135*, 6754.
[156] M. A. Rankin, G. Schatte, R. McDonald, M. Stradiotto, *Organometallics* **2008**, *27*, 6286.
[157] N. Nebra, J. Monot, R. Shaw, B. Martin-Vaca, D. Bourissou, *ACS Catal.* **2013**, *3*, 2930.
[158] A. A. Koridze, A. V. Polezhaev, S. V. Safronov, A. M. Sheloumov, F. M. Dolgushin, M. G. Ezernitskaya, B. V. Lokshin, P. V. Petrovskii, A. S. Peregudov, *Organometallics* **2010**, *29*, 4360.
[159] A. M. Sheloumov, F. M. Dolgushin, M. V. Kondrashov, P. V. Petrovskii, K. A. Barbakadze, O. I. Lekashvili, A. A. Koridze, *Russ. Chem. Bull.* **2007**, *56*, 1757.
[160] a) R. Karvembu, R. Prabhakaran, K. Natarajan, *Coord. Chem. Rev.* **2005**, *249*, 911; b) J. S. M. Samec, J.-E. Backvall, P. G. Andersson, P. Brandt, *Chem. Soc. Rev.* **2006**, *35*, 237; c) B. L. Conley, M. K. Pennington-Boggio, E. Boz, T. J. Williams, *Chem. Rev.* **2010**, *110*, 2294.
[161] Y. Blum, Y. Shvo, *Isr. J. Chem.* **1984**, *24*, 144.
[162] Y. Blum, D. Czarkie, Y. Rahamim, Y. Shvo, *Organometallics* **1985**, *4*, 1459.
[163] a) C. P. Casey, S. W. Singer, D. R. Powell, R. K. Hayashi, M. Kavana, *J. Am. Chem. Soc.* **2001**, *123*, 1090; b) C. P. Casey, J. B. Johnson, *Can. J. Chem.* **2005**, *83*, 1339.
[164] J. B. Johnson, J.-E. Bäckvall, *J. Org. Chem.* **2003**, *68*, 7681.
[165] C. P. Casey, J. B. Johnson, S. W. Singer, Q. Cui, *J. Am. Chem. Soc.* **2005**, *127*, 3100.
[166] C. P. Casey, T. E. Vos, S. W. Singer, I. A. Guzei, *Organometallics* **2002**, *21*, 5038.
[167] C. P. Casey, H. Guan, *J. Am. Chem. Soc.* **2007**, *129*, 5816.
[168] H.-J. Knölker, E. Baum, H. Goesmann, R. Klauss, *Angew. Chem. Int. Ed.* **1999**, *38*, 2064; *Angew. Chem.* **1999**, *111*, 2196.
[169] C. P. Casey, H. Guan, *J. Am. Chem. Soc.* **2009**, *131*, 2499.
[170] S. Kusumoto, M. Akiyama, K. Nozaki, *J. Am. Chem. Soc.* **2013**, *135*, 18726.

Received: April 28, 2015
Published online: September 7, 2015

